SAN DIEGO STATE UNIVERSITY AND

UNIVERSITY OF CALIFORNIA

Santa Barbara

Spatially Explicit Uncertainty and Sensitivity Analysis Methods for Land-Use Models

A dissertation submitted in partial satisfaction of the

requirements for the degree Doctor of Philosophy

in Geography

by

Seda Salap-Ayca

Committee in charge:

Professor Piotr Jankowski, Chair

Professor Keith C. Clarke

Professor Atsushi Nara

Professor Phaedon C. Kyriakidis

September 2018

The dissertation of Seda Salap-Ayca is approved.

Keith C. Clarke

Phaedon C. Kyriakidis

Atsushi Nara

Piotr Jankowski, Committee Chair

August 2018

Spatially Explicit Uncertainty and Sensitivity Analysis Methods for Land-Use Models

ACKNOWLEDGEMENTS

VITA OF SEDA SALAP-AYCA

August 2018

(Last name changed from ŞALAP to ŞALAP-AYÇA in August 2014)

EDUCATION

B.S in *Mining Engineering*, Middle East Technical University (METU), June 2005, (Graduation rank 4th among 59) (Junior/Senior GPA:3.31/4.00)

Double Minor on *Geographic Information Systems and Remote Sensing* in Faculty of Engineering, METU, June 2005, (GPA:3.00 Honor Degree/4.00)

M.Sc. in *Geodetic and Geographic Information Technologies(*GGIT), METU, Ankara, Turkey, September 2008 (GPA:3.56 Honor Degree/ 4.00)

Ph.D. Candidate in *GGIT*, METU, Ankara, Turkey, August 2013 (not completed)

Ph.D. in *Geography*, San Diego State University (SDSU) – University of California Santa Barbara (UCSB) (Joint Doctoral Program), August 2018

PROFESSIONAL APPOINTMENTS

Spring 2018 – Instructor, Geography Department, SDSU, San Diego, USA

2016-2017 – Teaching Assistant, Geography Department, SDSU, San Diego, USA

2013-2018 – Research Assistant, Geography Department, SDSU, San Diego, USA

2012-2013 – GIS Project Coordinator – Senior GIS Analyst, ELTEMTEK, Electric Facilities Engineering Services

2005-2011 – Research and Teaching Assistant, Civil Engineering Department, METU, Ankara, Turkey

Spring 2011 – Instructor for Turkish Electricity Transmission Company, METU, Continuous Education Center, Ankara, Turkey

Fall 2008 – Instructor for Turkish Electricity Transmission Company, METU, Continuous Education Center, Ankara, Turkey

2003-2005 – Student Assistant, METU, Mining Engineering Department, Ankara, Turkey

ACADEMIC PUBLICATIONS

Referred Journal Articles

Şalap-Ayça, S., Jankowski, P., Clarke, K.C., and Nara, A (2018) (under review) Assessing the Effectiveness of Visualization Techniques for Spatial Sensitivity Analysis. *Cartography and Geographic Information Science.*

Şalap-Ayça, S., Jankowski, P. (2018). Analysis of the Influence of Parameter and Scale Uncertainties on a Local Multi-Criteria Land Use Evaluation Model. *Stochastic Environmental Research and Risk Assessment*. DOI: https://doi.org/10.1007/s00477-018-1535-z

Şalap-Ayça, S., Jankowski, P., Clarke, K. C., Kyriakidis, P.C., and Nara, A. (2018) A meta-modeling approach for spatio-temporal uncertainty and sensitivity analysis: an application for a cellular automata-based urban growth and land-use change model. *International Journal of Geographic Information Science*. 32 (4). 637-662 DOI: https://doi.org/10.1080/13658816.2017.1406944

Şalap-Ayça, S. and Jankowski, P. (2016) Integrating Local Multi-Criteria Evaluation with Spatially Explicit Uncertainty-Sensitivity Analysis. *Spatial Cognition and Computation*. 16(2),106-132, DOI: 10.1080/13875868.2015.1137578

Şalap, S., Karslıoğlu, M.O., Demirel, N. (2009) "Development of a GIS-based monitoring and management system for underground coal mining safety" *International Journal of Coal Geology*. 80 (2009) 105-112. DOI: i: 10.1016/j.coal.2009.08.008

Conference Proceedings

Şalap-Ayça, S., Jankowski, P. (2017) A Meta-Modeling Based Tool for Spatially Explicit Uncertainty and Sensitivity Analysis. Geocomputation 2017, Leeds, UK. Pages 1-7

Şalap-Ayça, S., Jankowski, P. (2017) Mirror, mirror on the wall, which one is the best decision of all? An Assessment of Visualization Techniques for Displaying Spatially Explicit Quantification of Model Uncertainty, on Spatio-Temporal Uncertainty and Sensitivity Analysis: Methods, Applications, and Challenges Session, American Association of Geographers, Annual Conference, 2017, Boston, the U.S.A

Şalap-Ayça, S., Jankowski, P. (2016) Investigating the Scale Effect of Watershed Delineation on Local Multi-Criteria Method for Land Use Evaluation. Proceedings in

International Conference on Sensitivity Analysis of Model Output (SAMO),p 81-82 November 30th- December 3rd, 2016, Reunion Island

Erlacher, C., Jankowski, P., **Şalap-Ayça, S.,** Anders, K.H., Paulus, G. (2016) Development of a High-Performance Capabilities for Supporting Spatially-Explicit Uncertainty- and Sensitivity Analysis in Multi-Criteria Decision Making. Proceedings in International Conference on Sensitivity Analysis of Model Output (SAMO), p 38-39, November 30th- December 3rd, 2016, Reunion Island

Erlacher, C., **Şalap-Ayça, S.,** Jankowski, P., Anders, K.H., Paulus, G. (2016) "A GPU-based Solution for Accelerating Spatially-Explicit Uncertainty- and Sensitivity Analysis in Multi-Criteria Decision Making". Spatial Accuracy Assessment in Natural Resources and Environmental Sciences ,2016, Montpellier, France, p305-312.

Şalap-Ayça S. and Jankowski, P. (2016) Investigating the Effects of Neighborhood Schemes on Local Multi-Criteria Evaluation. Spatial Analysis and Modeling Specialty Group, Student Paper Competition, American Association of Geographers, Annual Conference, 2016, San Francisco.

Erlacher, C., **Şalap-Ayça, S.,** Jankowski, P, Anders, K.H., Paulus, G. (2016) Parallel Concept of Spatially Explicit Uncertainty and Sensitivity Analysis. Association of Geographers, Annual Conference, 2016, San Francisco.

Ligmann-Zielinska, A., Liu, W., Kramer, D. B, Cheruvelil, K. S., Soranno, P. A, Jankowski, P., and **Salap S.** (2014).Multiscale Spatial Sensitivity Analysis for Agent-Based Modelling of Coupled Landscape and Aquatic Systems. International Environmental Modelling and Software Society (iEMSs), San Diego, USA.

Şalap, S (2012) The Development of a Solar Energy Site Planning System based on Multi Criteria Decision Analysis in GIS, A Case Study in Karaman and Icel Cities in Turkey. ESRI Energy and Gas Utilities User Conference 2012, October 07-10, 2012, Salt Lake City, UTAH, the USA.

Şalap,S., Ayça A., Akyürek Z.,Yalçıner,A.C.(2011).Tsunami Risk Analysis and Disaster Management by Using GIS: A Case Study in Southwest Turkey, Göcek Bay Area. 14th AGILE International Conference on Geographic Information Science, April 18-22,2011, Utrecht, The Netherlands.

Şalap, S.,Karslıoğlu, M.O., Demirel, N.(2009).Development of GIS-based emergency management system for underground coal mine safety. 11th International Symposium on Environmental Issues and Waste Management in Energy and Mineral Production, SWEMP 16-19 November 2009, Banff, Alberta, Canada. Pages 388-395.

BOOKS AND LECTURE NOTES

Şalap, S., Karslıoğlu, M.O., Demirel, N. "A GIS-based Management System for Underground Mining Safety, A Practical Approach" Lambert Academic Publishing, Saarbrücken,2009. 77 pages.

Karslioglu, M.O, **Şalap, S**., Bolat K. (as the Geomatics Division Members of METU Civil Engineering Department). "Surveying Summer Practice Guide (as a part of CE 300)", METU-CE Press, 2011. 68 pages.

AWARDS AND HONORS

Spring 2018 – Cotton-Beland Associates Award for Environmental GIS Award, SDSU, Department of Geography

Spring 2017 – Cotton- Beland Associates Award for GIS Techniques Award, SDSU, Department of Geography

Spring 2016 – ESRI EDC Student of the Year Award, SDSU, Department of Geography

Spring 2016 – Jack and Laura Dangermond Geography Travel Scholarship from U.C.S.B, Geography

Summer 2015 – Marshall Plan Scholarship holder for three months in Carinthia University of Applied Science, Austria

June 2014 – Attendee on Summer School on Sensitivity Analysis – SAMO 2014, Ranco (Italy) - June 24-27, 2014

April 2011 – Travel Grant from ESRI for 14th AGILE Conference in Utrecht, Netherlands

November 2009 – Travel grant from The Scientific and Technological Research Council of Turkey "2224 – Support Program for Participation of Scientific Activities Abroad" for 11th International Symposium on Environmental Issues and Waste Management in Energy and Mineral Production, SWEMP.

2000-2005 – Prime Ministry Education Scholarship

Spring 2005 – High Honor Student in Senior Year in Mining Engineering Department, METU

Fall 2005 – High Honor Student in Senior Year in Mining Engineering Department, METU

Fall 2005 – Taylan Bozdağ Prize for being the first successful student in Senior Year in the Mining Engineering Department, METU

Spring 2004 – Taylan Bozdağ Prize for being the third successful student in Junior Year in the Mining Engineering Department, METU.

SERVICE FOR SCIENTIFIC JOURNALS

Reviewer – Land Use Policy - Elsevier

Reviewer – International Journal of Coal Geology -Elsevier

Reviewer - Süleyman Demirel University Journal of Natural and Applied Sciences

ABSTRACT

Spatially Explicit Uncertainty and Sensitivity Analysis Methods for Land-Use Models

by

Seda Salap-Ayca

Descriptive and predictive models of land use are potentially an important tool in aiding land use decision making, providing that the reliability of their results including model output uncertainty is accounted for, explained, and properly communicated to model users.

This study aims to contribute to spatial analysis of land use through an integrated, spatially-explicit approach to uncertainty and sensitivity analysis (iU-SA) for temporal and non-temporal land-use models employed in evaluation and simulation tasks. Two land-use models representative of land management practices and the transition of natural landscapes to urban land use have been tested in conjunction with the proposed iU-SA methodology. More explicitly, this research follows a three-step procedure to investigate the applicability of iU-SA for (1) land-use evaluation models, (2) land-use forecasting models, and (3) methods of visualizing the result of iU-SA.

In the first part, a methodology for local multi-criteria evaluation (LMCE) extended with iU-SA has been developed to focus on the effects of local criteria weights and modeling scale on the variability of model output. The results show that LMCE provides more heterogeneity compared to global approach, however, raising the question of scale dependency. This question has been addressed in a scale sensitivity analysis, which showed

that both scale and criteria weights play an important role in the results and in the ranking of the final decision of the decision-making process.

In the second part, using the example of an urban growth model, a meta-modeling approach has been developed for spatially explicit U-SA. The quality of results obtained with the meta-modeling approach is comparable to the full-order modeling approach, which is computationally costly. The study shows that the meta-modeling approach can significantly reduce the computational effort of carrying out spatially explicit iU-SA in the application of spatio-temporal models.

The overarching rationale of this dissertation has been to develop methods for better decision making. Therefore, in the final step, the effectiveness of the different visualization techniques for SA outputs is examined as a communication tool for decision making. The visualization of SA and user confidence dependency has been examined based on an empirical study of a web-designed survey applied for participants coming from different levels of expertise. Although the results did not show a statistically significant difference between compared visual representations, the dominant maps representation improved the correct answer rate for the expert users. The findings are insightful for the future works on improving the proposed techniques for SA visualization.

TABLE OF CONTENTS

LIST OF FIGURES

LIST OF TABLES

I.   Introduction

A. *Motivation*

"Man is part of the ecology of the earth: a system of relationships between the earth, its atmosphere, its climates, its vegetation, and its inhabitants of all kinds, which is of great and beautiful complexity, and which is yet an everyday experience for all men."(Chadwick 1971, p.2)

Humankind has been utilizing land since the very beginning of its existence. With changes in physical conditions and social needs, people have developed various ways of using land to meet these needs. Over the course of its terrestrial existence, humankind not only benefited from the environment, but also made efforts to understand it. Starting in the modern era with Copernicus and Galileo, and continuing with Newton and Maxwell, scientific world has evolved around the logical reasoning based on verifiable facts and data. As part of the scientific approach to understand the world, models have been developed to disentangle the mystery of cause and effect, therefore, enable both the description and predication of conditions in our physical world.

Today, we still need models to understand the environment. They are the abstract representations of systems or processes and indispensable tools for evaluation and predication. Models are expected to be accurate in their representation and prediction of processes and phenomena and at the same time easy to understand. This premise is supported by Occam's razor, which tells us other things being equal, simpler explanations are generally better than more complex ones.

Therefore, given two models with equal explanatory power, the simpler one is always preferred. However, one should also consider Albert Einstein's quote on simplicity:

"everything should be made as simple as possible, but not simpler". Especially, as stated by Clarke (2004), *"When **critical decisions, such as those affecting human safety**, depend on models, the model must be sufficient for the task, yet can become impossible for all but the modeler to understand holistically."* (Clarke 2004, p.215)

According to statistics given by the World Health Organization (WHO), the urban population, which currently accounts for 54% of the total world population, is expected to grow at an average rate of 1.6 % annually until 2030 (WHO 2016). The increase in global population has been accompanied by large-scale changes, and land use is one of them (Berg 2018). In 2018, the landcover has been stated to be more than one-half urban for the first time in its history (The Demographia 2015).

As the global population increases, the available land undergoes land use change pressures over time with inevitable consequences for the environment. Therefore, each and every decision made over land use change becomes critical. The obvious consequences of urban expansion worldwide are diminishing forest and agricultural lands and this land use transition becomes an issue of concern at both local and global scales. Therefore, descriptive and predictive models of land use are potentially an important tool in aiding land use decision making, providing that the reliability of their results including model output uncertainty is accounted for, explained, and properly communicated to model users.

B. Research Context

"Understanding patterns and the origin of the regularities (phenomena), and relating them to one another, offers our best hope of comprehending emergent phenomena in complex systems. The crucial step is to extract the regularities from incidental and irrelevant details. This process is called modelling." (Holland, 1999, p.4)

Land-use is a dynamic activity resulting in changes on the surface features that humans and the ecology of the earth depend on. Hence, land-use processes have both local and global impacts on the overall environmental systems including but not limited to forests, farmlands, waters and air systems (Foley et al. 2005). Therefore, comprehending the land-use practices and dynamics, and understanding the outcomes are quintessential for sustainable use of our environment – and this process can be assisted with land-use modeling.

Similar to other modeling practices, land-use modeling is also aiming to mimic the complex phenomena by approximating the abstract representation of land-use processes. Furthermore, the land-use models are also expected to be simple, accurate, transparent, and capable of simulating complex phenomena. Model simplification can be accomplished through model approximation. Although a system can be treated as the sum of its parts, this assumption fails in the case of land-use systems where parts interact with each other. Therefore, the accuracy and transparency become more critical and can be achieved, among others, by providing a confidence level to the model output. Since many process representations in models are subjected to uncertainty, which imposes a limit on the confidence of the model output, land-use models reliability can be increased by quantifying and representing the uncertainty.

This study aims to contribute to spatial analysis of land use through an integrated, spatially-explicit approach to uncertainty and sensitivity analysis (iU-SA) for temporal and non-temporal land-use models employed in evaluation and simulation tasks. The major impact of land-use practices is due to either land management practices or the transition of natural landscapes to urban land use. Therefore, two land-use models representative of these processes have been tested in conjunction with the proposed iU-SA methodology. More

3

explicitly, this research follows a three-step procedure to investigate the applicability of an iU-SA for (1) land-use evaluation models, (2) land-use forecasting models, and (3) methods of visualizing the result of iU-SA.

In the first part of the research, the focus is on conservation-driven land management requiring land allocation decisions. By investigating the role of scale on the result of a multi-criteria land-use evaluation model, I developed a robust approach to identify land conservation suitable areas together with exploring the uncertainty associated with their selection and finding the sensitive areas to variation in criteria preferences. As a result of this research step, I expected to find out whether or not there is a relationship between spatial heterogeneity (as one of the characteristics of spatial structure), data representation scale, and the level of uncertainty in results of a spatial multi-criteria land-use evaluation model.

In the second part of the research, the iU-SA framework is extended to accommodate higher, than in the multi-criteria land use evaluation model, computational requirements of a dynamic, urban growth land-use model. The framework is extended to address not only spatial but also temporal sensitivity of the model in a computationally more efficient manner necessitated by a larger than in the case of multi-criteria evaluation model input dataset and model complexity. The size of input dataset, number of model input factors, and structural model complexity highlight the problem of computational cost. Therefore, for the urban growth model, a new, computationally efficient approach is proposed. The approach that relies on meta-model representation is computationally efficient for high dimensional models with a relatively large number of input parameters that can interact and hence, contribute to the overall model variability. Of particular interest in this part of the research is investigating

a trade-off between higher computational efficiency in implementing iU-SA analysis and the quality of sensitivity analysis results.

In the final stage of research, the question of effective methods for displaying the results of the sensitivity analysis is examined. The investigation focuses on whether or not the sensitivity maps are effective in communicating the meaning of uncertainty and sensitivity of model results to target audiences (i.e., decision makers, analysts, engineers). To this end, the usability of different types of maps including adjacent visualization and coincident dominance maps is examined. The map usability is tested with two groups of participants using a web surveying approach. One group (the base group) is asked to interpret sensitivity analysis results represented by adjacent visualization technique. The other group (test group) is given the same interpretation task but with coincident representation. The survey results are analyzed to determine which map type (adjacent versus coincident) is more effective in gaining user's confidence to discern influential model inputs form non-influential ones, and correctly interpret sensitive locations in a model's study area.

C. Broader Significance and Scientific Merit

Understanding the drivers of model output uncertainty is important not only from a purely scientific but also from a practical standpoint of supporting decision making in real-world situations. By analyzing and visually representing the underlying causes of model output variability (uncertainty), the proposed research is expected to promote model transparency, inform the decision-making in land-use problems, and offer a systematic approach to tracing uncertainty in spatio-temporal models simulating different human-environment systems.

The broader impacts of this research lie in its potential for testing the applicability of spatially explicit uncertainty and sensitivity analysis to various types of spatial models informing decision making affecting different human-environment systems. The intellectual merit of the proposed research is its expected contribution to the methodology for spatially explicit uncertainty and sensitivity analysis achieved by analyzing the influence of model parameters on model output variability in two different types of spatial models.

D. Outline

The remainder of this dissertation is outlined in the paragraphs below.

First chapter focuses on the integrating local multi-criteria evaluation with spatially explicit uncertainty and sensitivity analysis. First Section (II.A) investigates the effect of uncertainty in local criteria weights by comparing global weights for a multi-criteria evaluation in the decision-making problem of land-use evaluation. This section is an Accepted Manuscript of an article published by Taylor & Francis in *Journal of Spatial Cognition& Computation* on 22nd of February,2016, available online at https://doi.org/10.1080/13875868.2015.1137578

Based on Section (II.A) findings, the following Section (II.B), extends the research by identifying key criteria weights at different scales and different sample distribution, and providing a complete robust spatial information set for decision makers. This section is an Accepted Manuscript of an article published by Springer-Verlag in *Journal of Stochastic Environmental Research and Risk Assessment* on 23rd of March 2018, available online at https://doi.org/10.1007/s00477-018-1535-z.

Chapter III introduces a new approach for a computationally efficient meta-modeling approach for spatially explicit U-SA on the example of a land-use forecasting model. This

chapter is an Accepted Manuscript of an article published by Taylor & Francis in *Journal of International Journal of Geographic Information Science* on 29th of November 2017, available online at https://doi.org/10.1080/13658816.2017.1406944.

Chapter IV, examines the effectiveness of two different visualization techniques depicting the results of sensitivity analysis. In a case study applied to a widely used spatio-temporal model of urban growth, the efficacy of both types of maps is tested for expert and novice end-users. This chapter is comprised of a submitted manuscript to *Cartography and Geographic Information Science* journal published by Taylor & Francis.

Finally, Chapter V presents a general conclusion on the findings of the presented dissertation research. This chapter also highlights the contribution and limitations of the presented research. Closing remarks are made for the directions for the future research and studies.

II.   An Integrated Spatially Explicit Uncertainty and Sensitivity Analysis for Land-Use Evaluation Models

Land use evaluation involves careful consideration of several environmental factors and their relative importance quantified by factor weights. The conventional methods of Multi-Criteria Evaluation (MCE) fail to account for local variability in criteria values and criteria preferences, disregarding local influence in spatial decision making. Local multi-criteria evaluation provides a mechanism for computing factor (criteria) weights within local neighborhoods that capture spatial heterogeneity and contribute to more accurate evaluation results. The accuracy of results, however, is tempered by the potential uncertainty of criteria weights.

In the first part of this chapter, a methodology for local multi-criteria evaluation extended by an integrated uncertainty-sensitivity analysis is presented and second part of this chapter focuses on the local criteria weights and modeling scale on the variability of model output. The efficacy of the approach is presented on the example of Environmental Benefit Index (EBI) model used by the U.S. Department of Agriculture Conservation Reserve Program (CRP) to select environmentally sensitive agricultural areas for conservation. The uncertainty analysis resulted in identifying robust areas for CRP selection characterized by high suitability and low uncertainty. The sensitivity analysis focused on the next-best group of candidates characterized by high suitability and high uncertainty. A potential practical value of this approach is the improved analytical support for land suitability evaluation requiring a consideration of sub-optimal land units (high suitability/high uncertainty). Also, this approach can guide modelling effort by allowing the analyst to visualize spatial distribution

and patterns of model output uncertainty and focus data collection on influential model input factors.

A.   *Integrating Local Multi-Criteria Evaluation with Spatially Explicit Uncertainty and Sensitivity Analysis*

1. **Introduction**

For more than twenty years, multi-criteria evaluation (MCE) has been widely used as a decision aiding approach in cases where a single evaluation measure becomes necessary for screening multiple decision alternatives. A number of MCE methods including weighted linear combination (WLC) (Malczewski 2000), analytical hierarchy process (AHP) (Saaty 1980), reference point methods (Hwang and Yoon 1981), and outranking methods (Roy 1996) have been proposed to solve spatial problems in a wide variety of areas such as socio-economic applications, land allocation, land suitability, and environmental management (e.g., Joerin et al. 2001; Store and Kangas 2001; Malczewski 2004; Malczewski and Rinner 2005; Chen et al. 2013).

In MCE methods, the feasible decision alternatives represented numerically by evaluation (performance) criteria, their relative preferences (criteria weights), and criterion values measuring the performance of alternatives on evaluation criteria are screened using a decision rule(s) to find the most suitable alternative. Criterion weight in MCE is assumed to be a constant expressing numerically the relative importance of the corresponding criterion compared with other criteria under consideration. Conventionally, in MCE methods criteria preferences are assumed to be stationary in geographical space and hence, the criteria weights do not spatially vary. Put differently, criteria weights are assumed to be homogenous within a study area. Moreover, each decision alternative is standardized ignoring the fact that

standardization procedure depends on a local context. Therefore, the conventional methods are regarded as global MCE methods since they do not explicitly account for local variability in criteria values and criteria preferences (Malczewski 2011).

Global MCE approach works fine under two assumptions when: (1) there is little variability in criteria values across the alternatives under evaluation, (2) the existing variability is deemed non-influential for criteria preferences. In spatial global MCE, where the number of location-based alternatives can be potentially large, both assumptions may be difficult to uphold. In such case a relationship between a criterion and its weight cannot be independent from location unless the attribute characteristics of geographic space under analysis are uniform. The recognition of conceptual disconnection between the global approach to spatial MCE and the heterogeneity of criteria values and weights has been noted in the research contributions made by Feick & Hall (2004); Ligmann-Zielinska & Jankowski (2008, 2012); and most prominently by Malczewski (2011). Feick and Hall (2004) contributed by providing a methodology for generating and visualizing criteria weight sensitivity through multivariate maps. Ligmann-Zielinska and Jankowski (2008) proposed a framework for spatial MCE by examining spatial relations within neighborhood space and then advanced the spatially explicit MCE by proposing the idea of proximity-adjusted preferences (Ligmann-Zielinska and Jankowski 2012). Malczewski (2011) introduced a local approach to MCE by developing local version of Weighted Linear Combination (WLC) technique. The main theoretical argument for the local MCE is that criteria weights should be correlated with criteria value ranges. This relationship can be modeled with local weights by relying on *weight range sensitivity* principle (Stewart and Ely; Nitzsch and Weber 1993; Fischer 1995; Monat 2009; Malczewski 2011). This study contributes to spatial MCE methodology by articulating the presence of uncertainty included

10

in criteria weights and extending a local MCE technique with integrated, spatially-explicit uncertainty-sensitivity analysis of criteria weights.

Uncertainty is an inextricable part of representing complex real-world phenomena in spatial decision models. The uncertainty in decision making potentially comes from multiple sources including original data, model structure, and/or assumptions (Zhang and Goodchild 2002; Chu-Agor et al. 2011; Chen et al. 2013). Nevertheless, evaluation criteria weights are usually considered the foremost source of controversy and uncertainty in MCE. An uncertainty analysis compares the importance of input uncertainties with relative contribution to uncertainty in the outputs. Following uncertainty analysis, sensitivity analysis accounts for the variation in the output of a model and its dependence on input by defining it quantitatively and/or qualitatively. Therefore, unlike uncertainty analysis, which measures the uncertainty in model's results (*forward-looking*), sensitivity analysis backtracks the relationship between inputs and outputs of the model (*backward-looking*). In this sense, the integrated uncertainty and sensitivity analysis (iUSA) of criteria weights potentially increases the level of confidence in the model output by helping analysts to understand the interaction between model input and output and consequently explain the influence of input values on uncertainty of the model output (Alexander 1989; Chu-Agor et al. 2011). This is particularly critical when model output is used for making predictions or drives the decision making.

In the literature, there are several application examples of sensitivity analysis (SA) used for justifying recommendations based on MCE results (Alexander 1989; Butler et al. 1997; Jankowski et al. 1997; Butler and Olson 1999; Tarantola et al. 2002; Feick and Hall 2004; Gómez-Delgado and Bosque-Sendra 2004; Feizizadeh et al. 2014). Common to these

applications is the use of SA in testing theoretical structure of complex decision models including the choice of variables, parameters, and model functions.

Following the emergence of Global SA (GSA) (Homma and Saltelli 1996; Saltelli et al. 1999b; Sobol' 2001), where the influence of the variation of model components (called model factors) on the model output is studied, its adoption in GIS and MCE came quickly. Especially in recent years, the investigations of variance-based GSA approaches in the MCE context have been on the rise due to the multiparametric nature of MCE. Saltelli and his co-authors (1999a) recommended in their study GSA methods for spatial problem analysis. They proposed Fourier Amplitude Sensitivity Test (FAST) as a model independent method effective for both monotonic and non-monotonic models (Saltelli et al. 1999a). Tarantola and his co-authors (2002) advanced GSA by using Extended-FAST method and tested it in an environmental assessment case study. This new technique is an extension of FAST by introducing a resampling technique. It also introduces the computation of first-order (S) and total sensitivity (S_T) indices, which are instrumental to understand the influence of model's factors on model output variability. Saisana, Saltelli and Tarantola (2005) argued that composite indicators (similar to aggregation functions in MCDA models), commonly used in many policy studies, could be the massive source of uncertainty due to the large amount of data used in deriving index values. Research conducted by Saisana and her colleagues has been aimed at increasing robustness and quality of composite indicators by using GSA methods. Gómez-Delgado and Tarantola (2006) proposed an integrated approach for Extended-FAST method in conjunction with GIS –MCE. In 2010, Saltelli and his co-authors presented another GSA approach, which is superior to FAST and Extended-FAST by easing the computational cost of higher-order model factor interactions. This method of Sobol' decomposes the output variance into fractions

so that the fractional composition of each input can be traced with first order and total effects (Saltelli et al. 2010).

Despite a relatively high number of GSA studies published in recent years, there have been only a handful studies on spatially explicit iUSA of model input factors. Feick and Hall (2004) proposed an approach, which enables decision participants to examine weight sensitivity in both criteria and geographic space. Research by Ligmann-Zielinska and Jankowski (2014) offers not only an application example of GSA but it also contributes to GSA methods by developing a spatially-explicit approach to GSA. Feizizadeh and his co-authors (2014) used the approach developed by Ligmann-Zielinska and Jankowski and applied it to model the uncertainty and sensitivity of landslide suitability maps.

This section (II-A) integrates statistical and spatial analysis methods to investigate the effect of uncertainty inherent in criteria weights on MCE model output. It does it on the example of Environmental Benefit Index (EBI), introduced by United States Department of Agriculture (USDA) Crop Reserve Program (CRP), to prioritize agricultural land units submitted by agricultural producers to be set aside for conservation (USDA 2011). The EBI is a decision-making model belonging to the class of multiple criteria composite index models. In land allocation/prioritization problems requiring a consideration of spatially-explicit land allocation alternatives, eliciting land allocation criteria weights is as important as criteria selection. The majority of MCE methods applicable to operationalizing and solving multiple criteria composite index models are based on an implicit assumption that criteria preferences are stationary in space. In this section (II-A), the concept of MCE based on local weights and originally proposed by Malczewski (Malczewski 2011) is extended through visualization and spatial analysis of uncertainty and sensitivity of model output due to criteria weights.

13

Consequently, the results of local MCE model substantiated by spatially explicit iUSA can help to prioritize land units for conservation with more insight and understanding of model results than global or local MCE without comprehensive iUSA.

The reminder of the section (II-A) proceeds as follows. Methodology (II-A-2) describes the integrating local MCE (i.e. MCE method with spatially-variable criteria weights) with spatially explicit iUSA framework, proposed by Ligmann-Zielinska and Jankowski (2014). Then, in application (II-A-3), the case study illustrating the application of the iUSA framework for EBI model is described. Results and discussion section (II-A-4) presents the outcomes of the iUSA by comparing global and local MCE results, discusses how the obtained information can be used in reducing the decision-making uncertainty. After discussing limitations with a brief account of future research directions at the end of section II-A-4, the section is closed by a summary in II-A-5.

2. **Methodology**

a) **Overview**

The iUSA framework has been implemented in this research to extend both global and local MCE. The implementation written in Python consists of three sequential steps applicable to both global and local MCE (Figure II-1). In first step, Monte Carlo (MC) simulations are executed to generate criteria weight samples. Next, in the second step comprising uncertainty analysis, the multiple outputs of MC simulations are summarized into average suitability and uncertainty maps. For the third and final step, GSA is performed by employing the variance-decomposition of suitability map. By performing the variance decomposition, the variability of the output suitability map is apportioned to each input criterion weight and results are depicted in the form of S and S_T sensitivity index maps. In this study, global and local MCE

14

methods are implemented separately to compare the effects of spatial heterogeneity in the criteria weights.
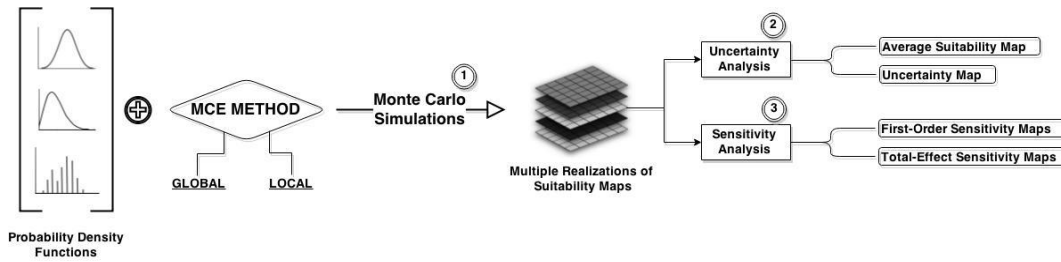
Figure II-1 Overview for Integrated Uncertainty- Sensitivity Analysis for Global and Local MCE

b) Sampling

Since criteria weights are regarded as the main uncertainty source under the investigation, in the first step, the input uncertainty is investigated through relative preferences of the alternatives. Weight samples are generated with quasi-random radial sampling by using Sobol's experimental design implemented in Simlab software tool developed by the European Joint Research Center (Simlab can be freely accessed from simlab.jrc.ec.europa.eu/) (Sobol' 2001; Lilburne and Tarantola 2009; Saltelli et al. 2010). The quasi-random sampling method produces arbitrary samples, which are equivalent to samples obtained from random sampling, but has the advantage of covering the sampling domain more uniformly than random sampling(Saltelli et al. 2010; Ligmann-Zielinska and Jankowski 2014).

In quasi-random radial sampling, two weight sample lists (N_a and N_b respectively) are generated using the probability density functions of each criterion weight, where the weight values are independently drawn. Following Sobol's experimental design, MCE model is run for $(k+2)*N$ times, where k is the number of uncertain model factors (here: the criteria weights) and N is the number of factor samples. For each run (R), the model calculates a suitability score for each land unit and produces a suitability surface.

15

c) Global Ideal Point Method

In this section (II-A), Ideal Point Method (IPM) is used to calculate suitability surfaces. IPM is one of MCE techniques belonging to the family of reference point techniques (Hwang and Yoon 1981) and used by various researchers in integrations of GIS with MCE (Jankowski 1995; Jankowski et al. 2001; Malczewski 2006; Ligmann-Zielinska et al. 2012; Qin 2013; Ligmann-Zielinska and Jankowski 2014). The implementation of IPM in this research follows the steps of Technique for Order of Preference by Similarity to Ideal Solution (TOPSIS) originally proposed by Hwang and Yoon (1981). In the first step, a feasible alternative set is determined and then the alternatives (a_{ik}) are standardized to achieve unitless criteria values (v_{ik}: i-th alternative for k-th criterion). In the global IPM, standardized criteria values vary depending on their distance from the two (global) extreme reference points: Ideal (v_k^*) and Nadir (v_{k*}). For the selected areal unit of interest (polygon/raster cell), distances to ideal ($v_k^* - v_{ik}$) and nadir point ($v_{ik} - v_{k*}$) are calculated to compute suitability scores. The areal unit (i.e. decision alternative), which is closest in the multi-criterion space to the ideal point and at the same time farthest from the nadir point, is assigned the highest suitability score. The suitability score is determined on the bases of separation from ideal (Eq. II-1) and separation from nadir (Eq. II-2) and calculated as follows:

$$s_i^p = \left\{ \sum_{k=1}^{n} \left(w_k (v_k^* - v_{ik}) \right)^p \right\}^{1/p} \qquad \textbf{Eq. II-1}$$

$$d_i^p = \left\{ \sum_{k=1}^{n} \left(w_k (v_{ik} - v_{k*}) \right)^p \right\}^{1/p}$$

Eq. II-2

Where: w_k is the global weight for k-th criterion and p is the TOPSIS parameter. The suitability score is then computed for every areal unit i (Eq. II-3).

$$f_i^p = \frac{d_i^p}{s_i^p + d_i^p}$$

Eq. II-3

IPM is an advantageous method for spatial evaluation problems since it does not assume the preference independence of attributes, which is not always the case in spatial problems (Hwang and Yoon 1981; Ligmann-Zielinska and Jankowski 2014; Malczewski and Rinner 2015). One important aspect of IPM is the selection of p parameter scaling the separation from the ideal point. Values between 1 and infinity can be selected, with 1 representing the compensatory decision strategy, in which the overall deviation from the ideal point is minimized, and infinity representing the non-compensatory strategy, in which the maximum deviation from the ideal is minimized (Malczewski and Rinner 2015).

d) Local Ideal Point Method

In the local version of IPM standardized criteria values are based on local extreme reference points (Ideal and Nadir) thus capturing local variation in criterion values (Qin 2013). In the local IPM, the geographic space under consideration is delimited by constructing neighborhoods defined for each areal unit (polygon/raster cell), in which local variations in criterion values are noted. In raster based datasets, equally sized neighborhoods can be defined by a moving window. For vector based representation of space, the neighborhood can be defined by contiguity, distance-based or k-nearest neighbors (Carter and Rinner 2014).The decision on the selection of suitable model to define neighborhoods is guided by the decision

17

problem itself. Structural characteristics of the problem at hand, its spatial distribution, and expected direction of change in spatial pattern can be guidelines for the choice of neighborhood definition (Carter and Rinner 2014). After defining neighborhoods, within each neighborhood a local range (r_k^q) is determined by the maximum and minimum criterion scores (a_{ik}) in a given neighborhood (q) for each areal unit (k) (Eq. II-4).

$$r_k^q = \max_k^q\{a_{ik}\} - \min_k^q\{a_{ik}\}$$ **Eq. II-4**

Given the local ranges, the local standardized criteria values are calculated based on the local range for each respective neighborhood. In Malczewski's 2011 study, the value function used for criteria standardization in global MCE was modified in local MCE by introducing a local range for each neighborhood. Hence, the raw criteria values are standardized by considering the local range values as follows (Eq. II-5):

$$v_k^q = \frac{a_{ik} - \min_k{}^q(a_{ik})}{r_k^q}$$ **Eq. II-5**

Similar to local standardized criteria values, the local ideal and nadir points for each neighborhood are determined within the neighborhood. Since the best and worst values in the neighborhood do not necessarily equal to global ideal and nadir values, these values can be different from 0 and 1. However, global ideal and nadir values are always 1 and 0 respectively, regardless of where the basic areal unit of analysis is located.

The definition of local criteria weights is based on the range sensitivity principle - similarly to defining other parameters in local MCE. It is determined as follows (Eq. II-6):

$$w_k^q = \frac{\dfrac{w_k r_k^q}{r_k}}{\sum_{k=1}^n \dfrac{w_k r_k^q}{r_k}} \quad 0 \le w_k^q \le 1 \text{ and } \sum_{k=1}^n w_k^q = 1$$ **Eq. II-6**

A local weight is a function of global weight (w_k), global range (r_k) and local range (r_k^q). Therefore, it is determined largely based on the relationship between local and global criterion value variability and the overall (global) importance of a given criterion.

Finally, to calculate the overall scores; weighted distances (($s^{p,q}$) , ($d^{p,q}$)) between ideal $v(a_{ik})^{q*}$ and nadir reference points $v(a_{ik})_*^q$ (Eq. II-7 and Eq. II-8) and relative closeness ($f^{p,q}$)(Eq. II-9) values are calculated.

$$s^{p,q} = \left\{ \sum_{k=1}^{n} \left(w_k^q \frac{(v(a_{ik})^{q*}) - v_k^q}{v(a_{ik})^{q*} - v(a_{ik})_*^q} \right)^p \right\}^{1/p} \qquad \textbf{Eq. II-7}$$

$$d^{p,q} = \left\{ \sum_{k=1}^{n} \left(w_k^q \frac{(v_k^q - v(a_{ik})_*^q)}{v(a_{ik})^{q*} - v(a_{ik})_*^q} \right)^p \right\}^{1/p} \qquad \textbf{Eq. II-8}$$

$$f_i^{p,q} = \frac{d_i^{p,q}}{s_i^{p,q} + d_i^{p,q}} \qquad \textbf{Eq. II-9}$$

e) Spatially Explicit iUSA

For the spatially explicit uncertainty analysis, multiple realizations of the suitability map are computed from all weight vectors obtained from quasi-random sampling. These sensitivity maps are summarized with minimum (MIN), maximum (MAX), average (AVG) and standard deviation (STD) maps. The two extreme value maps (MAX and MIN) help to understand the repeating high and low suitability locations whereas AVG and STD maps are the key surfaces to explain the distribution of suitability values in the study area and the accompanying uncertainty.

Following the MC simulation, the variance decomposition method is applied to quantify the influence of each criteria weight on the variability (i.e. uncertainty) of the suitability map, expressed by S and S_T sensitivity indices. The S_i is described as the direct contribution of the

19

i-th criterion weight to the variance of the output suitability. The S_i values are computed for each spatial unit in the study area. The resulting map of S_i can guide the analyst in identifying the most influential input parameter; however, the overall weight contribution (including higher order interactions with other weights) is measured by S_T. The S_T index is the sum of first-order and higher order effects for the given input factor (for details on the index formulas refer to (Saltelli et al. 2008). In the result of spatially explicit global sensitivity analysis, S_i and S_T maps are produced for each criterion weight.

3. **Application**

The methodology presented in section 2, was applied for EBI model with the goal of improving land prioritization/selection problem for CRP in Southwest Michigan. The study area includes six counties; Allegan, Barry, Cass, Kalamazoo, St Joseph and Van Burren where the CRP has been ongoing (Figure II-2).
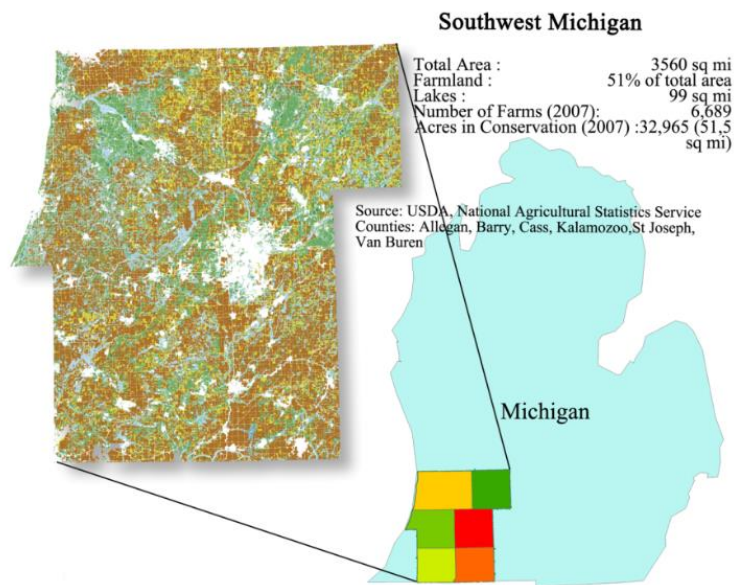
Figure II-2 Study Site, Southwest Michigan

20

EBI consists of five different factors (criteria) including N1 (wildlife), N2 (water quality), N3 (erosion), N4 (enduring benefits), and N5 (air quality). Conventionally, the EBI index value is determined as non-weighted sum of five index factors (Eq.10).

$$EBI = \sum_{i=1}^{5} Ni \qquad \text{Eq. II-10}$$

In Eq. II-9, each factor has equal influence on the index value. However, it is conceivable that the index factors can be assigned different levels of importance expressed by weights. In addition, these preferences can affect the overall score of EBI, which is a decision parameter for CRP. Therefore, an integrated MCE – iUSA has been performed to: (1) identify high suitability areas for land conservation and crop reserve characterized by low uncertainty, (2) identify candidate areas characterized by high suitability but limited by high uncertainty and (3) find criteria weights contributing the most to high uncertainty of suitable areas and pinpoint the locations in the study area where the influence of these weights is the strongest.

a) Neighborhood Selection and Criteria Standardization

Local IPM starts with defining the first-order contiguity neighborhood scheme, in which each neighborhood is considered more homogenous when compared with the rest of the study area. The neighborhoods should be defined before implementing local IPM. In this study, neighborhoods were determined based on the boundaries of 10-digit watersheds in the study area. The choice of 10-digit watershed as the areal unit of analysis is dictated by processes governing five EBI factors (criteria), for which watershed boundaries act as physical separation lines. As stated in Carter and Rinner's (2014) study, neighborhoods comprised of small number of units can fail to capture local variability and produce zero ranges of criteria values, which results in division by zero errors in (Eq. II-5) and (Eq. II-6). Therefore, each neighborhood is

21

checked to yield non-zero ranges for all attributes. Hence, one can expect to find higher inter-watershed variability in criteria values than intra-watershed variability.

The factors of EBI come with different measurement scales and require standardization as the first step of MCE procedure. For this purpose, the criteria values representing each factor are transformed into a common unitless scale using global and local standardization formulas. For the global IPM, the five criteria factors of EBI are standardized using linear transformation. For the local IPM, each criterion value is standardized using (Eq. II-5). All input factors are to be maximized - they are valued as benefit criteria. The standardized criteria maps for global and local versions of IPM are depicted in Figure II-3 and Figure II-4 .
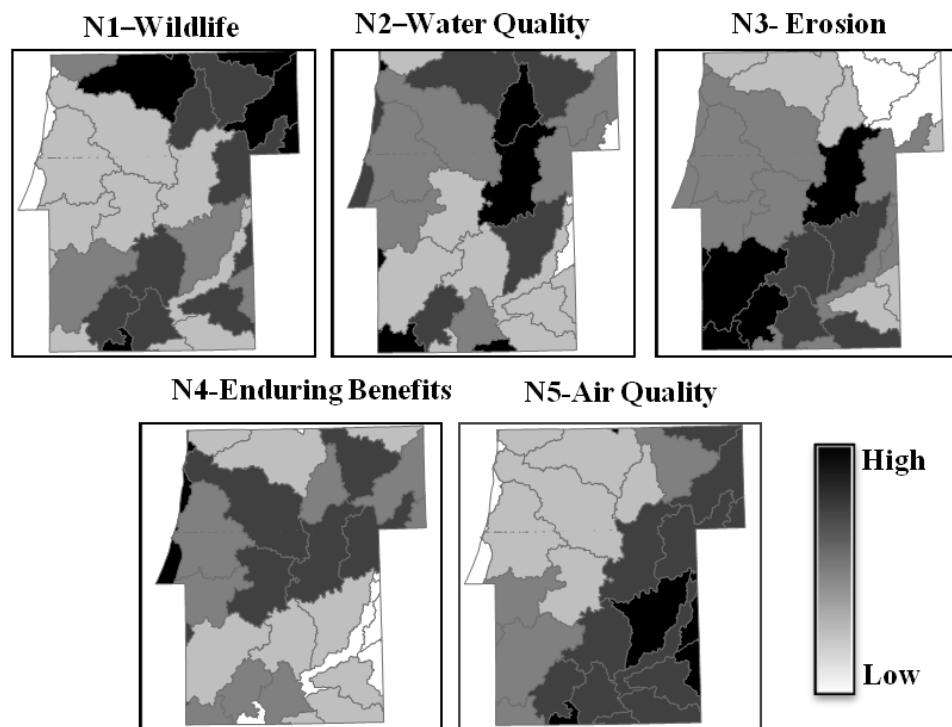
Figure II-3. Standardized Criteria Maps for Global IPM – (Zoned by 10 digit Watersheds Units)
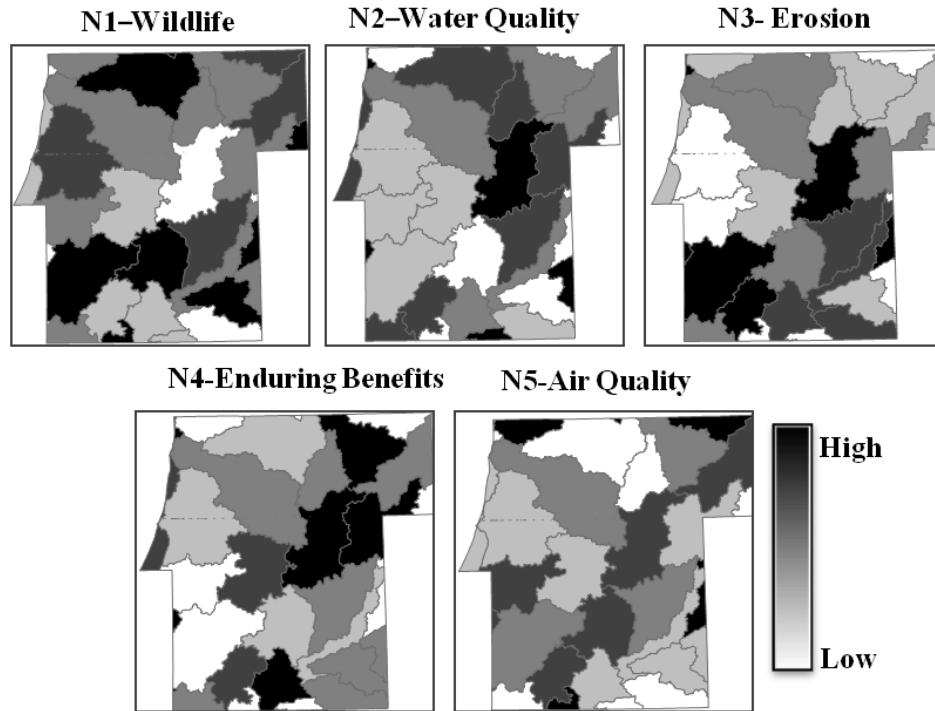
Figure II-4 Standardized Criteria Maps for Local IPM – (Zoned by 10 digit Watersheds Units)

b) Simulation Setup

Each criterion weight in the EBI model is sampled from a uniform distribution with an equal chance of being selected. The choice of uniform distribution for sampling the criteria weights is dictated by the scarcity of information about weight value distributions. After producing the weight sample using quasi-random sampling, the weight values are normalized to sum up to 1.0 so that they can be used as input in MC simulation.

With five factors (k=5) and 352 weight samples (N=352) the EBI model was run 2464 times (N*(k+2)). Although the results of MC simulation are unbiased for any number of model runs, using larger number of runs gives more reliable results of uncertainty analysis. Moreover, with small N, large negative numbers for the sensitivity indices S and S_T could result, thus violating the [0–1] value range of both indices. However, choosing a larger sample requires

23

more processing memory and computational power. Therefore, a compromise should be made between a sufficiently high N and reliable output values. For this implementation, due to computational resource limitations, N was set to 352 (the elapsed computation time for 31 polygons was 47 h and 49 min), which still allowed obtaining reliable S and S_T values (yielding 36.8% negative values for the S index for global model and 40.6 % negative values for the S index for local model).

In local IPM, parameters are calculated for each sample of weights depending on the number of neighbors surrounding each of the polygons, which varies between 2 and 9. Although the number of runs (N) is the same for both global and local models, in the local IPM the model is run for each neighborhood for each weight sample resulting in longer simulation time.

The uncertainty analysis of global and local suitability scores was run using MC and sample weights yielding average suitability (AVG) and standard deviation (STD) maps for global and local versions of the model. For every input factor in both global and local model versions, one S and one S_T index values were computed. As explained in Section 2.5, the sensitivity indices are derived based on variance decomposition method (Saltelli et al. 2010), in which the variability of suitability maps is apportioned to each criterion weight.

4. **Results and Discussion**

a) **Spatial Uncertainty Analysis for Global IPM**

The results of MC simulations, in which the global IPM was solved N times, were summarized as average suitability map (Figure II-5, left) and standard deviation of average suitability (STD) map (Figure II-5, right). The average map is produced by computing the

mean of all IP scores calculated in MC runs. The computed suitability scores have an average value ranging from 36% to 73% for the entire study area. By examining Figure II-5 (left), one can see the watersheds, which are highly suitable land conservation and crop reserve candidates (darker colors in lower left and center polygons). However, the level of confidence for these watersheds can be only ascertained by comparing the AVG map with the STD map. A relative high uncertainty is associated with high standard deviation, therefore in order to select the priority regions with confidence, AVG map should be examined in concert with STD map. To help examine the relationship between suitability and uncertainty, the study area was partitioned into four quadrants, which are High AVG – High STD, High AVG - Low STD, Low AVG – High STD, and Low AVG – Low STD (Figure II-6). The value threshold for High average suitability is greater than 55% (Figure II-7 – top) and the value threshold for High STD (uncertainty) is greater than 6 % (Figure II-7 - bottom). The thresholds are based on the distributions of AVG and STD values (Figure II-7), however, the ultimate selection of thresholds is an arbitrary choice made by the analyst.

Average Suitability Score (AVG)   Standard Deviation of AVG (STD)
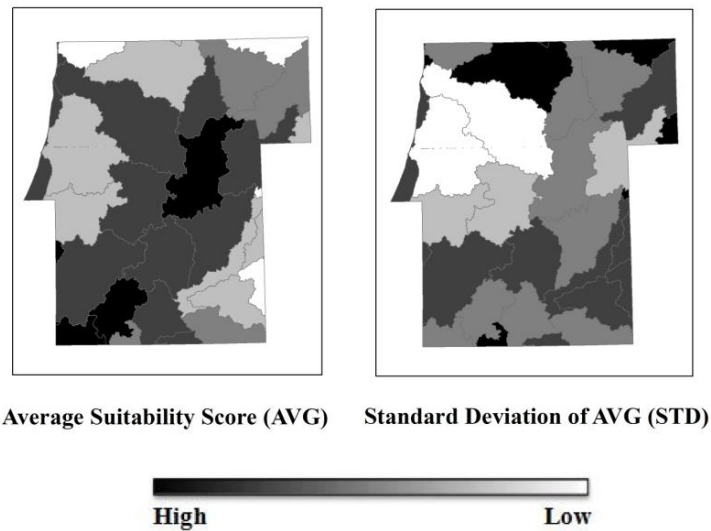
High   Low

Figure II-5 Average Suitability (AVG) and Uncertainty (STD) Maps for Global IPM
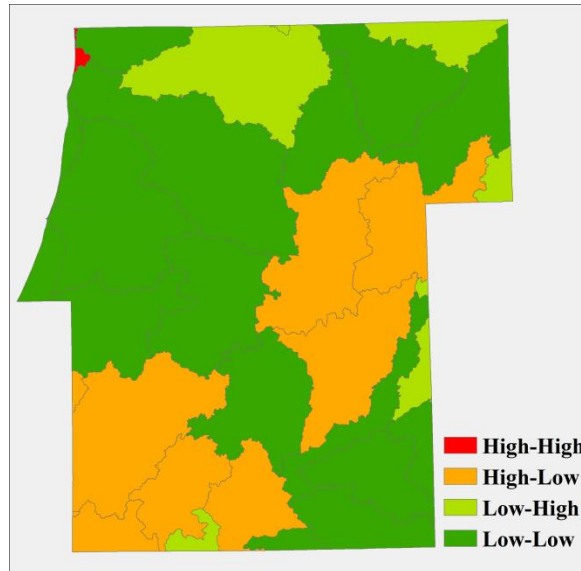
Figure II-6 EBI Priority Zones for Global IPM representing High-High as Candidate and High-Low as Robust Regions

According to this partition schema, the robust areas are selected based on AVG≥55 % and STD<6% (High-Low or HL), whereas candidate areas are selected based on AVG≥55% and STD≥6 % (High-High or HH). The remaining areas with AVG<55% are discarded as being less productive categories (Figure II-6).

After examining both AVG and STD maps, the pattern is clear. The robust areas with high mean IP scores and with low standard deviation can be found in the central-eastern and in the south-western regions of the study area (Figure II-6). These are the obvious watersheds to be selected for conservation as part of the CRP. There is only one small watershed, in the north-western corner of the study area that falls into the candidate area category (High–High).
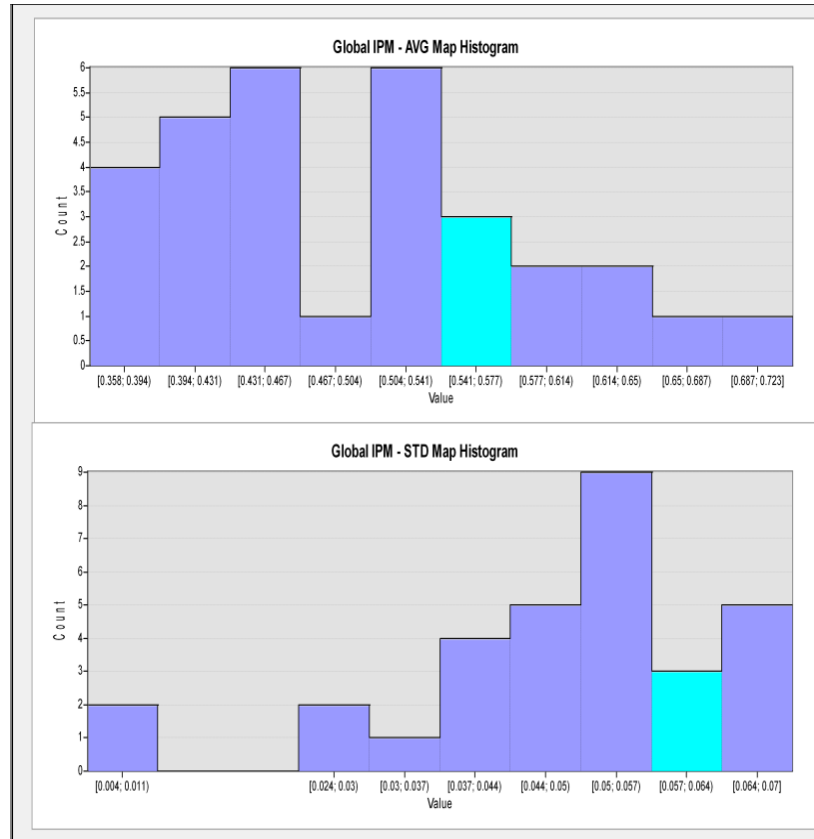
Figure II-7 AVG (top) and STD (bottom) Map Histograms for Global IPM

b) **Spatial Uncertainty Analysis for Local IPM**

The outputs of local IPM based on MC simulations comprise EBI suitability maps and their aggregate results are depicted on Average Suitability (AVG) and standard deviation (STD) maps (Figure II-8).

For local IPM model, the average suitability scores range from 21% to 72%. However, similarly to the global case, this average suitability map should be interpreted in concert with the uncertainty (STD) map in order to locate robust and candidate areas with confidence.

Again, like in the global model case, the study area was divided into four groups (Figure II-9) by selecting threshold values based on the statistical distributions of AVG and STD: 55% for high average suitability, and 8% for high uncertainty (Figure II-10).

27
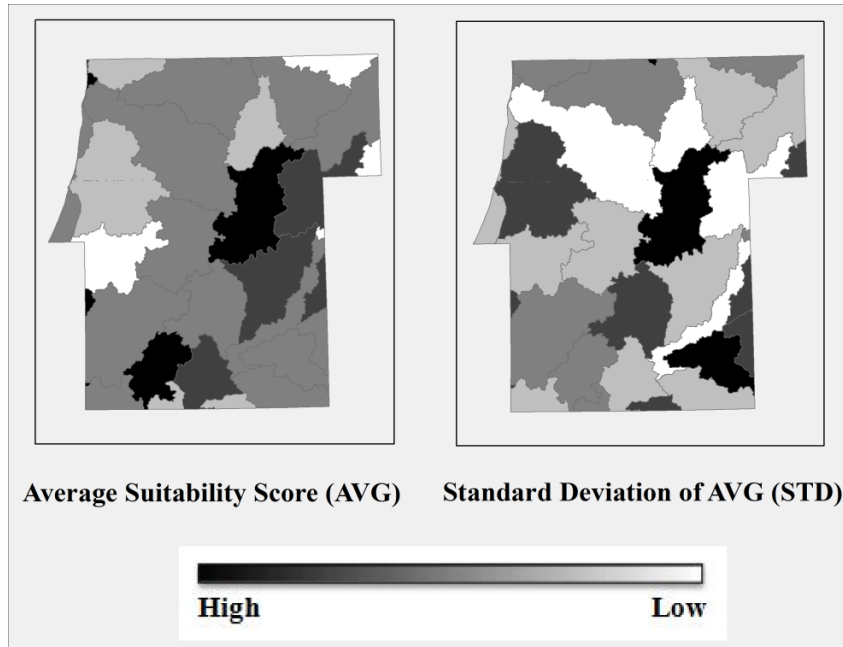
Figure II-8 Average Suitability (AVG) and Uncertainty (STD) Maps for Local IPM
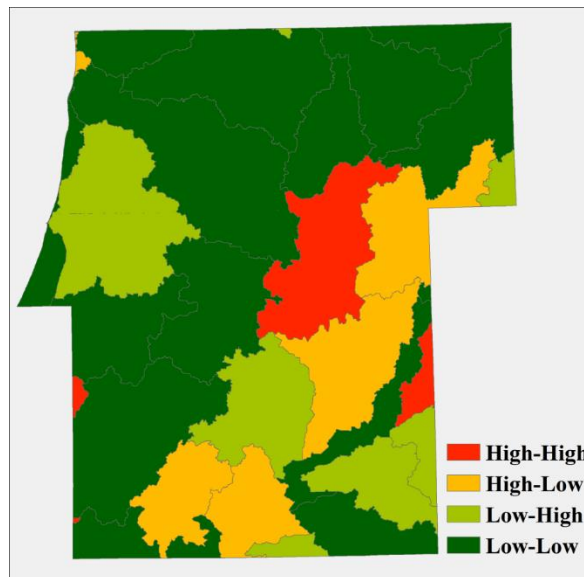
**Figure II-9 EBI Priority Zones for Local IPM - High-High as Candidate Regions
and High-Low as Robust Regions**

Based on these thresholds, robust areas are characterized by AVG≥55% and STD<8%

(High-Low or HL) values and candidate areas are characterized by AVG≥55% and STD≥8 %

(High-High or HH). The remaining areas with AVG<55% are discarded as being less productive categories (Figure II-9).

The pattern of robust and candidate areas for the local model is perceivably different from the global model. The robust areas (High-Low) form two prominent clusters - one in the central-eastern and another in the southern part of the study area. There are three candidate areas (High-High) located near the center and long the western and eastern boundaries of the study area. This difference in pattern/number of robust/candidate areas between the global and local models can be attributed to the effect of local variations in preferences and factor values. However, in order to better explain the reasons behind the observed differences one needs to perform global sensitivity analysis with criteria weights as model input factors.
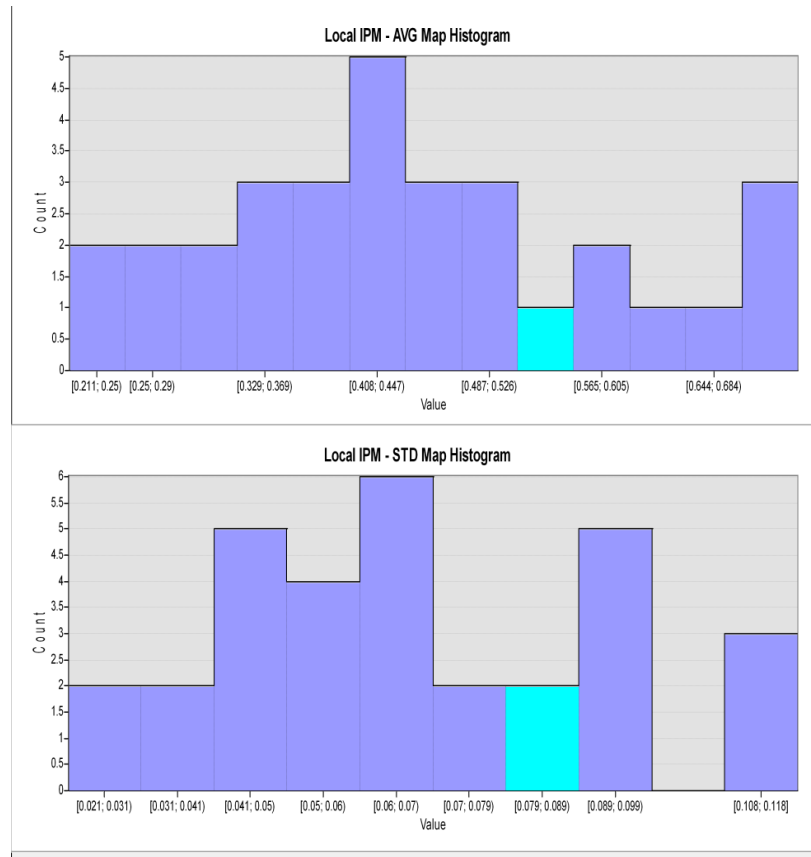
Figure II-10 AVG (top) and STD (bottom) Map Histograms for Local IPM

29

c) Spatial Sensitivity Analysis for Global IPM

The spatial distribution of the S sensitivity indices for weights in global IPM is depicted in Figure II-11. Most of the five factors have relatively high index values in the central-western part of the study area. Especially, for *water quality* -N2, *erosion* - N3 and *air quality* - N5 factors, the S index exceeds 1.0, which poses difficulties in interpretation. Conventionally, the S index value equal to 1.0 means that all of the observed variability in the suitability score, at a given location, is due to the given criterion weight. According to Saltelli and his co-authors (2000), very small sample sizes (small N) are likely to produce values exceeding 1.0 for S indices (Saltelli et al. 2000). Therefore, a relatively small sample size used in this study for MC simulation could have resulted in S values exceeding 1.0. Although there are similarities among some watersheds, their S_T sensitivity index values do not follow the pattern of S sensitivity index and show more variability, which indicates higher order interactions between criteria weights (Figure II-12). As stated in Section 2.5, S_T represents the fractional contribution of a particular weight, including its interactions with other weights, to model output variability. The level of interaction among criteria weights may depend on the source of criteria values. For example, most of the factors forming EBI depend on land cover data. Moreover, soil characteristics of the region effect both soil erosion (included in the factor N3) and air quality (N5). Put differently, correlations among factors can influence the total order output sensitivity.

To better understand the weights and their effects, five S maps representing N1-N5 factors were combined by means of an overlay operation selecting for each unit of analysis (i.e. watershed) the criterion that had the maximum S sensitivity value. The result is a dominance map (Figure II-11, bottom-right). The majority of the study area is dominated by the *air quality*

30

factor (N5). Hence, the weight of N5 is the most influential, when considered in isolation from other weights, in affecting the uncertainty of suitability scores. For the candidate small watershed, located in the north—western part of the study area, *water quality* (N2) is the dominating factor. One can investigate higher order interactions to understand this sensitivity (Figure II-12). Although S_T indices do not fully explain the uncertainty of model output, it is more reliable to investigate the overall (S_T) effect of each single factor than individual (S) effect (Saltelli et al. 2000). In the S_T dominance map (Figure II-12, bottom-right), N5 is dominating factor for the candidate watershed. This can be interpreted that the single input weight (N5), which seems insignificant in S-dominance map for the candidate watershed, is more influential than N2 weight when interacting with other factor weights. Therefore, its influence on the output variance is greater when its interactions are considered.

N1 - Wildlife
(min 0.00, max 0.60)

N2 - Water Quality
(min 0.00 , max 21.76)

N3 - Erosion
(min 0.00 , max 21.45)

N4 - Enduring Benefits
(min 0.00 , max 4.48)

N5 -Air Quality
(min 0.00 , max 66.6)

Dominance Map

Dominant Type
N2
N5
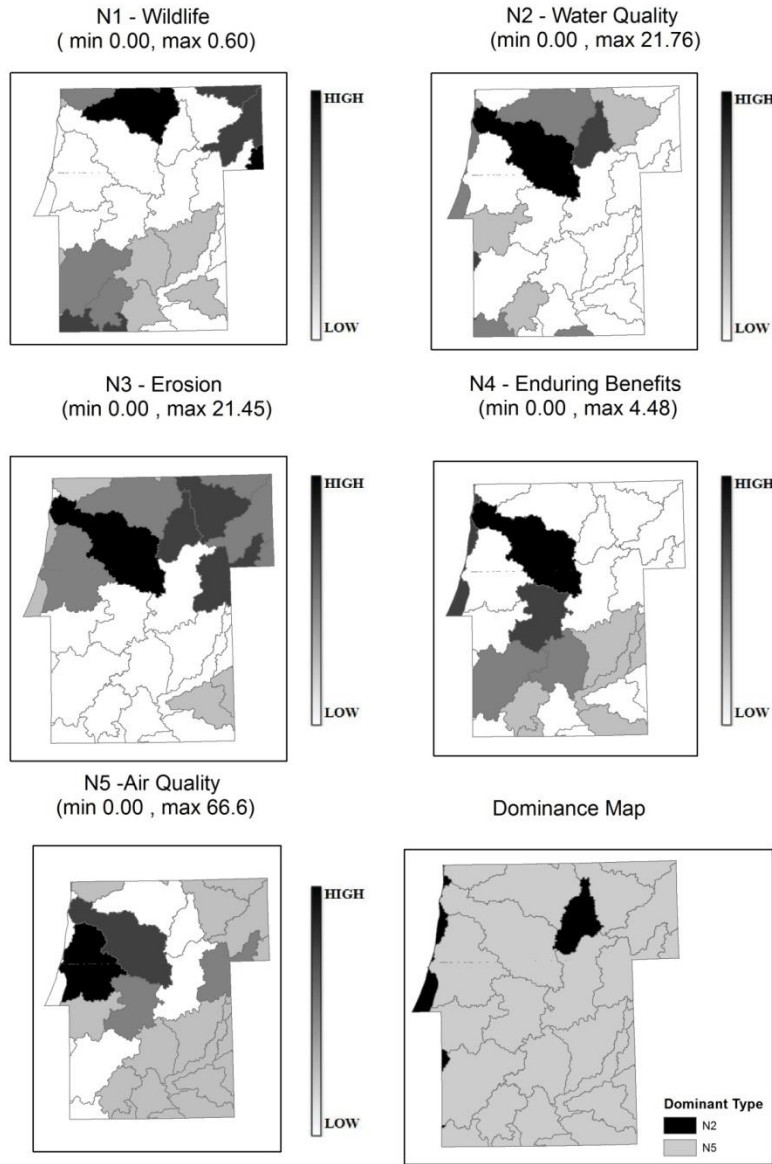
Figure II-11 First –Order Sensitivity Indices and Dominance Map for Criteria Weights for Global IPM
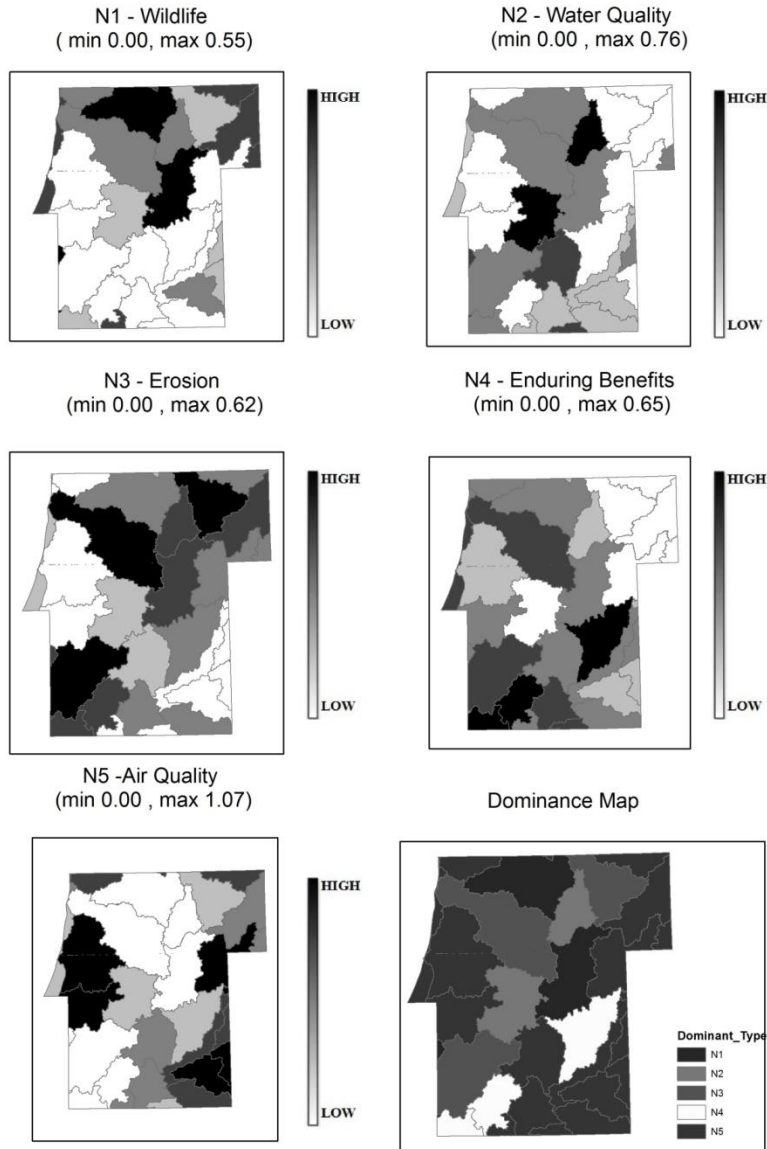
Figure II-12 Total–Effect Sensitivity Indices and Dominance Map for Criteria Weights for Global IPM

d) Spatial Sensitivity Analysis for Local IPM

Interpreting a similar map overlay of local S-index maps (Figure II-13), again the most dominant factor is *air quality* – N5 (Figure II-13 – right bottom). However, for the locally-calculated S-index map, the second dominant criterion is *water quality* – N2 criterion. Interestingly, one can also observe the criterion *enduring benefit* – N4 dominating some of the

watersheds located in middle and south-eastern parts of the area. This shows that the local variation of weights results in higher number of criteria weights contributing to uncertainty of the model output. Therefore, one can argue that investigating spatial heterogeneity in sensitivity analysis is important for revealing the influence input factors, which under the global model appear to have little influence on uncertainty of the model output.

After examining the S and S_T dominance maps (Figure II-13 and Figure II-14) for candidate regions in local IPM, one can see that *water quality* - N2 and *air quality* -N5 are influential for first-order sensitivity effect, whereas *wildlife* - N1 and N2 are dominant when the interactions are considered. Interestingly, N1 and N2 represent two very different and uncorrelated input factors, yet their weights appear to contribute to the output variance. In aggregate, for both global and local models, N2 and N5 appear to drive the output uncertainty of the models. Moreover, since the S and S_T maps reveal a spatially variable pattern characterized by high S and S_T values in high STD (high uncertainty) areas, it is difficult to cast a particular criterion weight as non-influential and set it to a constant value.

N1 - Wildlife
(min 0.00 , max 0.95)

N2 - Water Quality
(min 0.00 , max 3.72)

N3 - Erosion
(min 0.00 , max 3.36)

N4 - Enduring Benefits
(min 0.00 , max 2.29)

N5 -Air Quality
(min 0.00 , max 15.38)
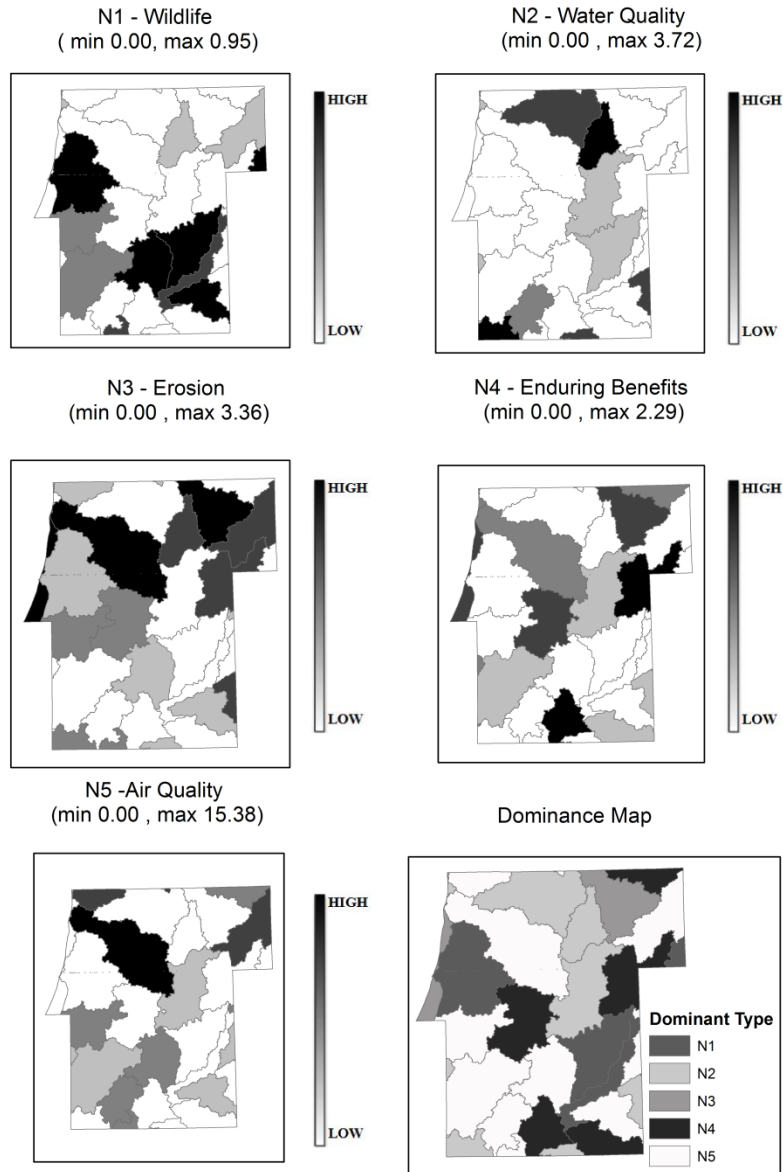
Dominance Map

Figure II-13 First –Order Sensitivity Indices and Dominance Map for Criteria Weights for Local IPM

N1 - Wildlife
(min 0.00, max 0.92)

N2 - Water Quality
(min 0.00 , max 0.94)

N3 - Erosion
(min 0.00 , max 0.66)

N4 - Enduring Benefits
(min 0.00 , max 0.74)

N5 -Air Quality
(min 0.00 , max 1.12)
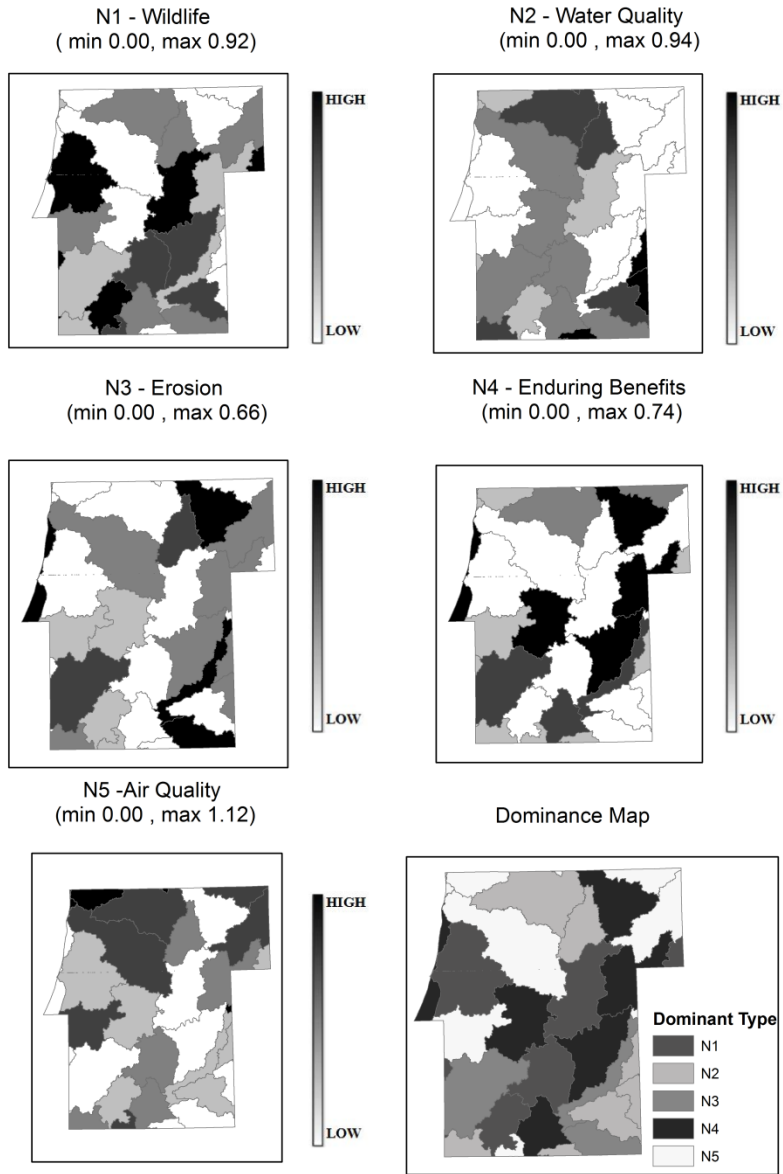
Dominance Map

Figure II-14 Total –Effect Sensitivity Indices and Dominance Map for Criteria Weights for Local IPM

e) Comparison of Results of iUSA for Global and Local Multi-Criteria Evaluation Models

There are two categories of watersheds resulting from the multi-criteria evaluation integrated with uncertainty-sensitivity analysis and of interest for decision recommendation; the high suitability/low uncertainty (High-Low) category, and the high suitability/high uncertainty (High-High) category. The former comprises robust watersheds, which are an obvious choice for land conservation. The latter represents candidate watersheds worthy of further investigation, which was carried out by means of global sensitivity analysis. The candidate watersheds are depicted in Figure II-15 and Figure II-16 respectively. Given differing spatial distribution patterns of standardized input factors in global and local models (Figure II-3 and Figure II-4), one can expect differences between local and global models in regard to candidate watersheds.

To compare the global and local model results, we first investigated the average suitability rankings of robust and candidate watersheds for both cases. According to the rankings, 77% of the robust and candidate watersheds remained unchanged between the models. The watersheds with the most change in category designations were located in the south-western corner of the study area. Following on the observation made by Carter and Rinner (2014), different outcomes of global and local IPM in case of these watersheds could be the result of irregular neighborhood sizes. In local MCE, larger neighborhoods can hide local effects; therefore, one can expect to see more local influence in smaller neighborhoods. Not surprisingly, watersheds where the change in category designation was observed were the smallest among the preferred set (robust and candidate watersheds).

Differences in the pattern of dominant criteria weights between S to S_T can be observed not only in the global, but also in the local model. One can explain the change in the pattern of dominant criteria weights (Figure II-15 and Figure II-16) by comparing standardized criteria values (Figure II-3 and Figure II-4) and observing spatial heterogeneity in the local model (Figure II-4). An interesting difference between the local and global models is the dominance of N1 factor in the robust and candidate watersheds, which can be observed on the dominance maps of S and S_T (Figure II-13 and Figure II-14). This dominance is hidden in the dominance maps compiled for the global model (Figure II-11 and Figure II-12) This observation underscores that the influence of criteria weights on output uncertainty, unnoticed in the global model, can be detected by accounting for spatial heterogeneity of criteria values and preferences in local model.
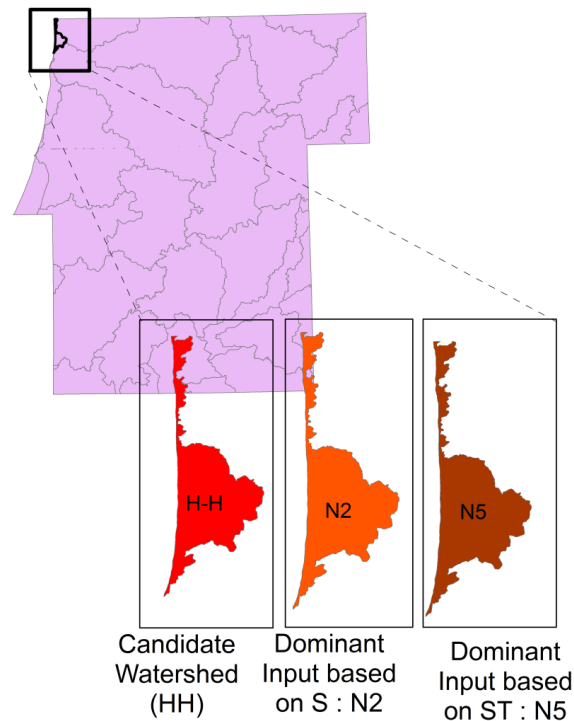
Figure II-15 Global IPM Dominant Inputs based on S and ST Maps
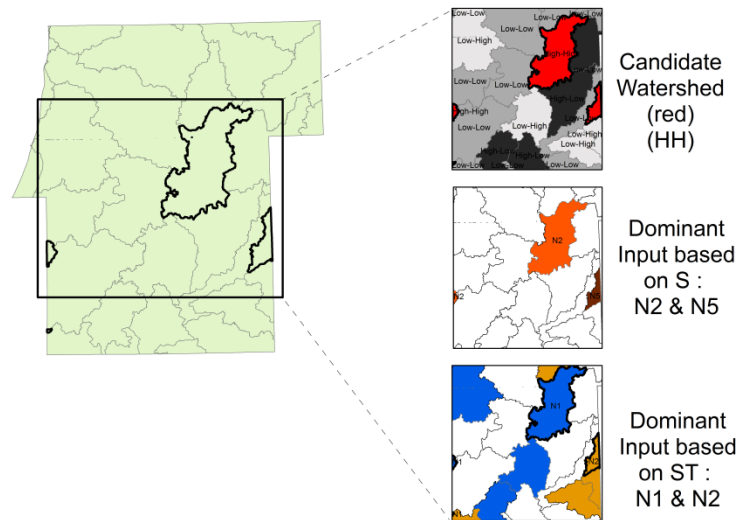
Figure II-16 Local IPM Dominant Inputs based on S and ST Maps

f) Limitations and Future Work

As discussed in the methodology section, the spatially explicit approach to uncertainty and sensitivity analysis is based on simulating many model solutions in response to variability in model parameter values, which puts high demand on computational resources. The computational cost drastically increases in the vector-based local MCE application. Potential solutions to this problem could involve screening, meta-modeling or employing a linear regression (Saltelli et al. 2008). Another approach could be to employ high performance computing. There are different boosting techniques presented in the literature such as algorithmic engineering and efficient in-memory data structures (Zhang and You 2012). Using Graphical Processing Unit (GPU) for parallel computing is another method to accelerate the computationally intensive spatial modeling problems. Its main advantage is a relatively low cost of hardware when compared with closed computing architecture counterparts such as supercomputers or other parallel computing resources.

39

Yet another potential extension of the presented here research is focusing on the effects of neighborhood selection scheme and the resulting areal unit of analysis. A question of whether or not the results of uncertainty-sensitivity analysis are stable with different analysis units is the question of scalability of the approach, and it closely relates to modifiable areal unit problem (MAUP) and edge effects (Fotheringham and Wong 1991). Since choosing the definition of a neighborhood is the key issue in local MCE, research including the effect of different neighborhood schemes on uncertainty of the output may positively contribute to improving model robustness. To this effect a mathematical optimization approach to designing different zoning schemes can be selected (Openshaw 1978; Openshaw and Rao 1995; Guo et al. 2000) and its scalability evaluated (Montello and Golledge 1998).

5. **Summary and Conclusion**

This section (II-A) presents a methodology and an application of spatially-explicit, iUSA by comparing the results of global and local approaches to solving a multi-criteria land allocation problem. The results of analysis include average suitability map accompanied by uncertainty map. Moreover, sensitivity maps are produced for each criterion weight.

In MCE, the importance of weight validation is critical if the result of evaluation is expected to be used in policy and decision making. By introducing the range sensitivity principle to decision making one aims at improving the reliability in assessing preferences expressed by criteria weights. Moreover, local MCE enables visualization and spatial analysis of criteria weights in GIS environment. Hence, the results of local IPM can help select priority areas.

Global sensitivity analysis helps to identify model input factors, which do not have a significant effect on the model output, and which consequently could be fixed as constant

40

values. Therefore, in MCE models both criteria and weight sensitivities are crucial, and in spatially explicit MCE models the geographic distribution of their input values should also be considered. Moreover, important local variations can be hidden under the assumption of stationary criteria values and weights. A thorough analysis for uncertainty and sensitivity may lead to a more rational decision process by refining the model results. The iUSA can be instrumental in visualizing locations of model output burdened by high uncertainty and thus can help uncover the sources of uncertainty through computation and visualization of input-output relationships captured by first and total order sensitivity indices.

B.   *Analysis of the Influence of Parameter and Scale Uncertainties on a Local Multi-Criteria Land-Use Evaluation Model*

1. **Introduction**

Spatial analysis has been widely used in spatial decision support systems (SDSS) in various fields such as environmental and natural resource management, land allocation, land suitability, and urban and land use planning (e.g., (Morgan and Henrion 1990; Joerin et al. 2001; Store and Kangas 2001; Malczewski 2004; Chen et al. 2013)). An important method in the context of SDSS applications has been multi-criteria evaluation (MCE), which is a structured approach for screening multiple alternatives by calculating an overall performance index value (based on criteria values and criteria weights) used to compare and rank-order the decision alternatives (Voogd 1983).

Conventionally, in MCE applications only the spatial heterogeneity of criteria values (alternatives) is accounted for, whereas criteria weights (preferences) are assumed to be spatially homogenous and fixed. This assumption ignores a potential relationship between the spatial distribution of criterion values and criterion weights. The logic of this relationship can

be expressed by the *range sensitivity principle* (Stewart and Ely; Nitzsch and Weber 1993; Fisher 1999; Monat 2009), which states that for two evaluation criteria; one with a narrow and the other with a wide range of criterion values, and given all other intrinsic properties of the criteria equal, the criterion with a wider range of values is more important than the criterion with a narrower range. This relationship between spatial heterogeneity and criteria weights has been addressed by local criteria weights and method is called local MCE (Malczewski 2011).

Providing a mechanism for representation spatial heterogeneity, local criteria weights may contribute to more accurate model results than global weights (Şalap-Ayça and Jankowski 2016). The results, however, may still be confounded by the potential uncertainty of weights, which is partially due to global weight values by way of including global extremes in the calculation of local weights. In this sense, the uncertainty of local MCE results can be accounted for with uncertainty analysis (UA), which determines the relative contribution of local criteria weights to model output variance, and can provide an insight into the spatial distribution of local MCE output values by identifying robust regions characterized by high evaluation scores and low variances (Alexander 1989; Chu-Agor et al. 2011).

Another potential source of uncertainty in local MCE is the selection of geographical analysis unit (neighborhood scheme). Understanding the role of scale in local MCE requires understanding the impact of scale on the model output and this can be achieved with a multiscale analysis approach (Samat 2006). Therefore, we have followed a multiscale approach by investigating the sensitivity of analysis unit on the model outcomes.

In this paper, a spatially-explicit approach to global uncertainty-sensitivity analysis (U-SA) based on variance decomposition has been adopted to compute and map the variability of land suitability scores (the output of local MCE model), and to account for the influence of

42

local weights and modeling scale on the model output variability. In order to present the effectiveness of the spatially explicit approach, a land use evaluation model called Environmental Benefit Index (EBI) is selected. EBI is a score-based decision support tool that has been used by the United States Department of Agriculture (USDA) for the largest ongoing agricultural conservation program, Conservation Reserve Program (CRP), to evaluate agricultural land areas (Ribaudo et al. 2001) . Since 1997, EBI has been used to weight agricultural land parcels depending on their characteristics and potential benefits for the environment (Perez 2008). Highly erodible cropland or other environmentally sensitive areas are rented from farmers and the plantation of species that will improve environmental quality is ensured (USDA 2011). However, it has been stated that the enrolled land parcels might not achieve environmental benefits at the lowest cost due to the failure of suitably addressing program variables, which the allocation decisions were based on (Reichelderfer and Boggess 1988; Babcock et al. 1997; Perez 2008). The well-constructed program instruments are expected to lend a flexibility to the decision making process and promote its influence on the distribution of program benefits (Perez 2008). As one of the program design parameters, eligibility criteria affect the extent to which potential gains in environmental performance can be achieved (Claessens et al. 2009). In this study, we aim to fill this gap by identifying key criteria weights at different scales and provide a complete robust spatial information set for CRP decision makers.

2. **Study Background**

   a) **EBI for Land Use Evaluation Model**

   The adopted land use evaluation model, EBI has been applied to evaluate and rank farmers' requests to set aside agricultural land units for conservational purposes (Womach

2005). The calculation of EBI is based on five environmental input factors including wildlife, water quality, erosion, enduring benefits, and air quality, which serve as the measures of environmental quality for an agricultural unit. Although their relative importance is not specified in the CRP manual on how to calculate the final EBI score, there are different scale ranges used for determining the input factor values. These differences in ranges can provide a justification for introducing factor weights, which express the relative importance of input factors (Keeney 1992; Fischer 1995) . In this sense, EBI can be easily operationalized with MCE techniques. The overall EBI score is calculated as the weighted sum of five factors and it expresses the environmental quality estimate of a given land parcel. The EBI scores are used to compare, rank and screen the land parcels considered for CRP funding in each enrollment period. If the overall EBI score is higher than the pre-determined threshold value for the enrollment period, a contract payment is paid to the farmer and the land unit is left uncultivated for the contract term.

Despite the environmental gains of CRP achieved for over 30 years, only the most qualified land units are selected for incentive payments due to limited program funding (NRCS 2016). Consequently, the challenge has been in identifying land areas that will maximize the conservation benefits by considering multiple criteria (factors) together with their variable levels of relative importance (weights). Given that the CRP selection decisions are based on the composite index score calculated for each land unit under consideration, it is essential to use a robust method for calculating EBI, which would give an analyst some measure of confidence in the calculated score. Since EBI is a simple additive model, a fitting solution in this case is to use multi-criteria evaluation.

b) Local Multi-Criteria Land Use Evaluation Modeling

A good practice of MCE calls for examining the robustness of model output in light of potential uncertainty in criteria weights. Yet, the interest among MCE researchers in the distributional effects of criteria weights has been relatively recent and the literature on the subject is scant. The relationship between spatial heterogeneity and criteria weights has been addressed by distance and direction-based adjustments (Rinner and Heppleston 2006; Ligmann-Zielinska and Jankowski 2008, 2012), and by measuring the unevenness of spatial distribution (entropy) within the neighborhood space (Jessop 1999; Malczewski and Rinner 2015). Moreover, Malczewski (2011) proposed a local MCE approach, in which criteria weights depend on criteria value ranges. Following the local version of Weighted Linear Combination (WLC) method (Malczewski 2011), local versions of other MCE methods including Ordered Weighted Averaging (OWA) and Ideal Point Method (IPM) (a reference point technique also used in this study) were developed and tested (Qin 2013; Carter and Rinner 2014; Malczewski and Liu 2014; Şalap-Ayça and Jankowski 2016).

In local MCE, the study area is divided into neighborhoods (comprised of analysis units), wherein the criterion values are assumed to be spatially heterogeneous. The criterion values and weights are calculated within each neighborhood based on the local extreme values, thus capturing spatial variations in the study area. The high granularity of neighborhood resulting from a geographically large scale (small area size/high level of detail) promotes the heterogeneity of criterion values whereas low granularity detracts from it.

Typically, in land use evaluation, the analysis unit is equivalent to a decision alternative (e.g. land parcel). However, in local MCE, the scale of analysis unit determines the granularity of neighborhood and by extension the values of local weights. Within a local MCE

45

neighborhood, the analysis unit is represented by a contiguous region within an evaluation area, comprised of a subset of decision alternatives. Therefore, the scale, at which the processes determining evaluation criteria values and consequently the local weights operate, may be different from the decision scale, at which decision alternatives are represented. Due to the potential mismatch between the process and decision alternative scales, the appropriate scale for the analysis unit may not be immediately obvious. The challenge here is to adopt the scale (size) of analysis unit affording sufficient variability (not too small neighborhoods) while avoiding undue homogeneity (not too large neighborhoods), in the result of which a local model solution converges to a global solution.

In this study, the decision alternative is an agricultural land parcel. However, the values of EBI environmental factors (evaluation criteria) are shaped by processes operating at a watershed scale rather than at the parcel level. This discrepancy between the scale of process unit (watershed) and the scale of decision alternative (land parcel) has been addressed by adopting watershed as the analysis unit, at which a local MCE is performed, and then reporting the results of local MCE at the parcel level (the decision alternative scale).

Watersheds range from small (a single stream without a tributary) to large drainage areas. The selection of appropriate watershed size for analysis unit depends on the scale(s) of processes governing EBI factors and the size of study area. Salap-Ayca and Jankowski (2016) have already carried out a watershed based local MCE for EBI model to compare a local approach with a global approach. However, they only considered one watershed scale and performed sensitivity analysis(SA) for only one neighboring scheme, without examining model behavior at an alternative analysis scale. Nonetheless, following up on the limitation of their work, it is reasonable to assume that for the problem at hand there is no one optimal

watershed scale and that the size of watershed may affect local MCE model results in the sense that the change of analysis unit will result in the corresponding change of parcel rank-order indicating the model sensitivity to analysis unit scale (Wong 2009). Here, we wanted to find out whether the change of watershed size would result in altering the spatial pattern of EBI scores obtained with a local MCE model.

c) Spatially Explicit Uncertainty and Global Sensitivity Analysis for Land Use Evaluation Models

The focus of U-SA is to quantitatively evaluate the variation in the output of a model and its dependence on the model input (Morgan and Henrion 1990). In the literature, the examples of SA can be grouped into two as local or global approach (Saltelli et al. 2000; Helton and Davis 2002). In a local SA, the input variations are investigated one at a time, which is computationally efficient (Crosetto and Tarantola 2001). However, this approach fails to catch the interactions among input variables, which makes global approach more popular for models with higher-order interactions are anticipated (Crosetto et al. 2000; Gómez-Delgado and Tarantola 2006; Lilburne and Tarantola 2009).

Accounting for higher order effects is especially important in models where input parameters interact with each other, since it is difficult to separate the absolute or even the relative influence of each parameter. A general procedure for variance-decomposition based global SA can be summarized in seven action steps (Saltelli et al. 2000):

1. Design the experiment by identifying the model under consideration. This step is important to understand how the information is carried from input to output of the model, and tune the internal variables where necessary before SA.

2. Quantify the sources of uncertainty by focusing on uncertain parameters.

47

3. Select the probability distribution functions of the parameters under interest. If there is insufficient knowledge about the range and distribution, a simple representation (i.e. uniform, log-uniform) can be used for exploratory analysis. There are also techniques for defining input parameter distribution.

4. Generate value samples for selected parameters from their probability distribution functions, which are defined over the sample space of the input factors and bounded by the given range for each input factor.

5. Compute multiple realizations of the model with the generated sample set to generate an output distribution for the response surface.

6. Analyze uncertainty propagation by assessing the estimated mean and conditional variance of the model output coming from model realizations covering the full range of variation for the input factors.

7. Perform SA to quantify and understand the contribution of each parameter, solely or in interaction with other parameters, to the model output.

Due to the multi-parametric and non-linear nature of many spatial decision problems including land allocation, as a global SA approach, variance-based SA is an attractive option for spatial models (Homma and Saltelli 1996; Saltelli et al. 2006; Lilburne and Tarantola 2009). The variance-based SA has been used in various application domains including environmental assessment, policy studies, chemical or radioactive decay risk assessment, hazardous waste landfill site selection, and others (Saltelli et al. 1999a; Tarantola et al. 2002; Saisana et al. 2005; Gómez-Delgado and Tarantola 2006). Ligmann-Zielinska and Jankowski (2014) proposed a spatially explicit approach to variance-based SA and demonstrated its application in land suitability assessment with a global MCE model (Ligmann-Zielinska and

Jankowski 2014). Their spatially explicit approach has been extended in this paper by addressing the scale uncertainty of analysis unit in a local MCE model in concert with the uncertainty of criteria weights. The uncertainty of scale has been analyzed by applying the variance based decomposition at two alternative scales (fine and coarse) of analysis unit.

In the following sections, we present the description of methods, the implementation of spatially explicit U-SA with a local MCE model of EBI, and the discussion of analysis results.

3. **Methodology**

The methodological approach used in the study involves the implementation of EBI model with a local MCE technique followed by the variance decomposition based global SA of weights run for two watershed scales. The Watershed Boundary Dataset (WBD), provided by the United States Geological Survey (USGS), is a hierarchical dataset covering land areas of the United States. Each hydrologic unit stored in the database is given a Hydrologic Unit Code (HUC) depending on the location and the level in the hierarchy (Seaber et al. 1987). First, a local MCE technique is applied to EBI land prioritization model at two different scales of analysis: 1) the HUC10 scale (coarser), and 2) the HUC12 scale (finer). Following that, the U-SA is run for the EBI model output. A graphical abstract of the approach is depicted in Figure II-17.
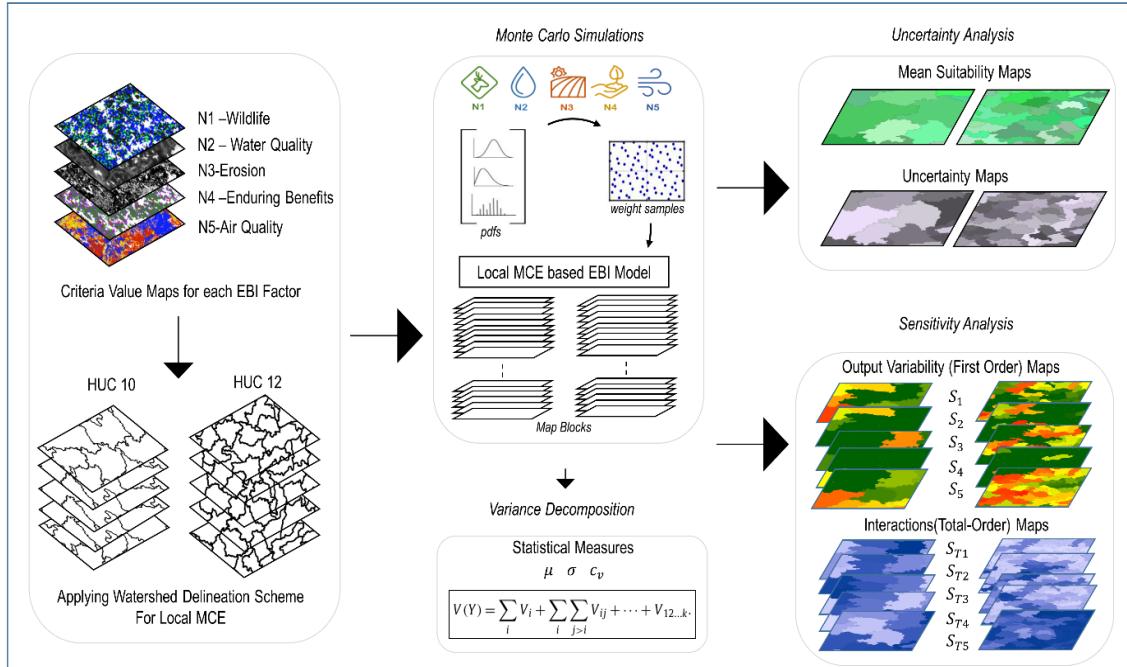
Figure II-17. Graphical abstract of the analysis approach

a) Study Area and EBI Model Overview

The CRP has been an ongoing process in Southwest Michigan, which makes it a suitable case-study area to test our methodology. The study area consists of six counties including Allegan, Barry, Cass, Kalamazoo, St Joseph and Van Burren (Figure II-18). Land cover, water and soil data for the counties were processed into five layers representing the EBI input factors following the guidelines provided by United States Department of Agriculture (USDA) (USDA 2011).
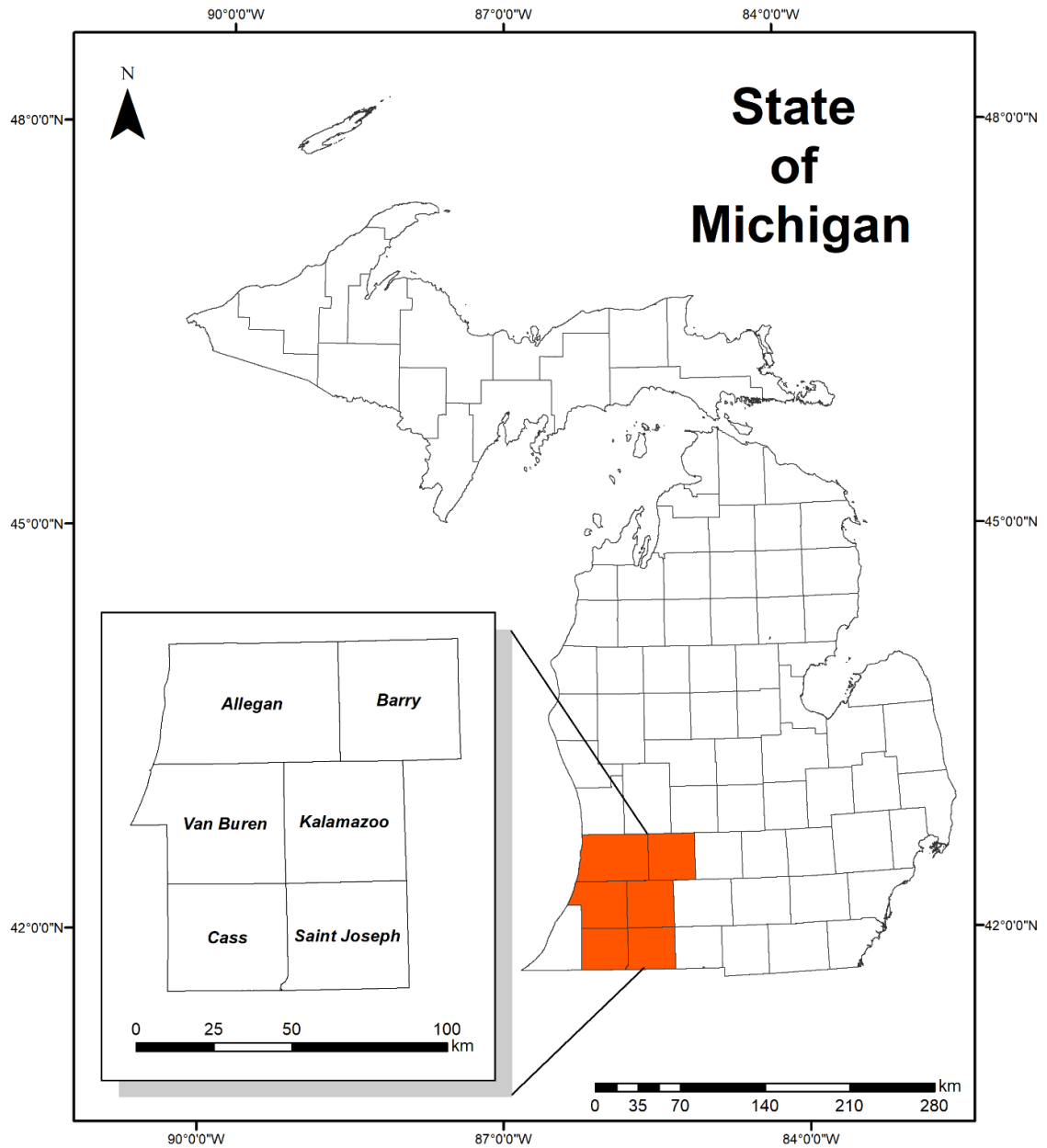
Figure II-18 Study site, Southwest Michigan

Conventionally, the EBI score is determined by taking the sum of wildlife (N1), water quality (N2), erosion (N3), enduring benefits (N4) and air quality (N5), where each factor score ranges as shown in the Table II-1. For each bidding period, a threshold value is set to determine the overall score that will maximize the conservation benefits. In MCE terms, each

51

environmental factor corresponds to a criterion and their preferences can be represented by weights. Therefore, the overall score for EBI can be calculated with a MCE technique by aggregating the factor scores with factor weights.

Table II-1. EBI Factor Score Ranges provided by USDA (USDA 2011)

EBI Factors	Minimum Score	Maximum Score	Percentage in the Overall EBI Score
N1	0	100	25.3%
N2	0	100	25.3%
N3	0	100	25.3%
N4	0	50	12.7%
N5	0	45	11.4%

b) Methods Overview

For the local MCE implementation, we chose the Ideal Point Method (IPM) technique. The IPM evaluates the decision alternatives with reference to a specific goal, which in this case is the maximization of the EBI score. The final output of IPM is the ordered set of decision alternatives based on their separations from the ideal reference point.

The results of local IPM can be analyzed with the spatially-explicit approach for two different watershed delineation levels (HUC10 and HUC12) separately. The results of spatially explicit UA are then presented on a pair of maps: a mean suitability map and an uncertainty map (represented by standard deviation). These maps are further categorized into high-low suitability and uncertainty maps. Subsequently, the results of spatially-explicit SA, given by the spatially distributed values of first and total-order sensitivity indices, are mapped to depict the contribution of each criterion weight to model output variability. These maps can be

summarized into dominance maps to analyze the distribution of dominant factors at each discrete location (e.g., a polygon or a raster cell). A flowchart depicting the methodology is presented in Figure II-19.
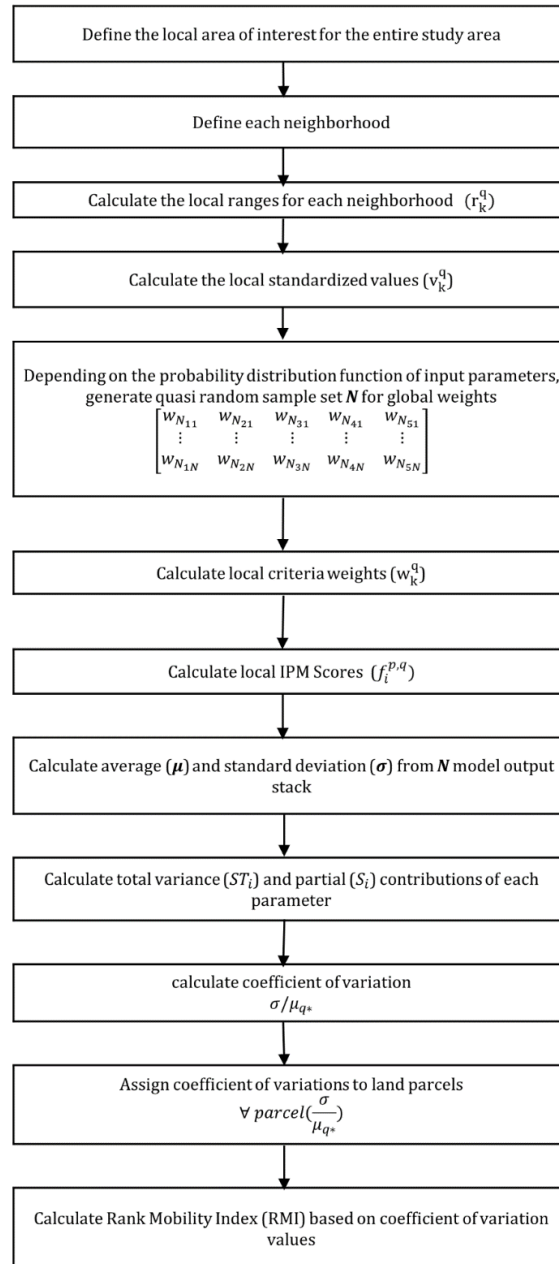
Figure II-19 . Flowchart with the methodology for Uncertainty and Sensitivity Analysis

(1)   Local Ideal Point Method

In this study, vector-based (polygon) watersheds were used as analysis units. The reason for choosing watershed as the analysis unit has been its function of natural division unit demarcating transitions in physical phenomena driving the EBI factors. Consequently, transitions in the factor values can be expected at watershed boundaries. For this study, the watershed (HUC10 - coarse) and sub-watershed (HUC12- fine) levels were used to construct Queen-type neighborhoods in the local IPM implementation of EBI model. Queen-type scheme includes the watersheds sharing either an edge or a point, thus preserving the contiguity among neighbors. With this scheme, each neighborhood has at least two members, which ensures variability in local criterion values.

Criteria values are the five input factors in EBI, which are benefit-type – meaning their values are maximized. To bring the factors to a common measurement scale they must be standardized. For the local IPM, the standardization formula for the benefit criterion (k) for the ith alternative is based on the local range (r_k^q) between the local maximum (ideal) and minimum (nadir) values in a given neighborhood (q) Eq. II-11.

$$r_k^q = \max_k^q\{a_{ik}\} - \min_k^q\{a_{ik}\}$$
Eq. II-11

Therefore, the local standardized criterion value (v_k^q) of the raw score (a_{ik}) for the kth criterion and the ith alternative becomes a relative measure related to the best expected score within a given neighborhood (q) for each areal unit (k) Eq. II-12.

$$v_k^q = \frac{a_{ik} - \min_k{}^q(a_{ik})}{r_k^q}$$
Eq. II-12

Local criteria weights are calculated based on the range sensitivity principle, including global weight (w_k) and global range (r_k) variables as follows Eq. II-13:

$$w_k^q = \frac{\dfrac{w_k r_k^q}{r_k}}{\sum_{k=1}^{n} \dfrac{w_k r_k^q}{r_k}} \quad 0 \leq w_k^q \leq 1 \text{ and } \sum_{k=1}^{n} w_k^q = 1 \qquad \textbf{Eq. II-13}$$

By including the global weight and global range variables, a local weight represents the importance of the given criterion reflecting the relationship between local (neighborhood) and global (study area) shifts in criterion values.

Following the calculation of local weights for each neighborhood, the overall scores of relative closeness($f^{p,q}$) to the ideal solution are calculated using weighted distances between the best ($s^{p,q}$) and the worst($d^{p,q}$)) scores and the best (ideal) ($v(a_{ik})^{q*}$) and worst (nadir) ($v(a_{ik})_*^q$) standardized values for the kth criterion and the ith alternative within the qth neighborhood Eq. II-14,Eq. II-15 and Eq. II-16.

$$s^{p,q} = \left\{ \sum_{k=1}^{n} \left(w_k^q \frac{(v(a_{ik})^{q*}) - v_k^q}{v(a_{ik})^{q*} - v(a_{ik})_*^q} \right)^p \right\}^{1/p} \qquad \textbf{Eq. II-14}$$

$$d^{p,q} = \left\{ \sum_{k=1}^{n} \left(w_k^q \frac{(v_k^q - v(a_{ik})_*^q)}{v(a_{ik})^{q*} - v(a_{ik})_*^q} \right)^p \right\}^{1/p} \qquad \textbf{Eq. II-15}$$

$$f_i^{p,q} = \frac{d_i^{p,q}}{s_i^{p,q} + d_i^{p,q}} \qquad \textbf{Eq. II-16}$$

(2)   Spatially Explicit Approach to Uncertainty and Sensitivity Analysis

A spatially explicit approach to U-SA (Ligmann-Zielinska and Jankowski 2014) focuses on model reliability evaluation, in which model output uncertainties and input factor sensitivities are quantified and mapped for every spatial entity within the study area. There are two essential components of the approach: UA based on Monte Carlo (MC) simulations and global SA based on variance decomposition. We describe both in the subsequent sections.

(a) MC Simulation-Based Uncertainty Analysis

MC simulation, which relies on multiple model executions, is the essential component of UA. The *simulation* term here corresponds to the computation of model output for the corresponding sample input dataset. The sample data are generated for the input factors considered to be uncertain. Since the study focus is on the uncertainty of criteria weights, the sample input dataset represents the criteria weights. Two key parameters for the MC simulation are the sampling algorithm for generating the sample dataset and the probability density distribution functions used in data sampling.

In the subject literature, different algorithms have been offered to produce sample datasets for MC simulation (Helton and Davis 2003; Helton et al. 2006; Sobol' et al. 2011; Wei et al. 2015). However, each algorithm results in the generated sample deviating from the true uniform distribution, which is recommended in the absence of specific information about probability density distribution for a given uncertain input factor. This deviation is referred to as the discrepancy measure and the simulation effectiveness increases with decreasing the discrepancy. A quasi-random sampling, as one of the low discrepancy sequences, follows a random pattern and fits a uniform distribution (Kucherenko et al. 2011). The quasi-random sampling algorithm "remembers" the distribution positions of previously sampled points, thus,

56

avoiding clusters or gaps in the sample space (Lilburne and Tarantola 2009; Gatelli et al. 2009; Saltelli et al. 2010). As a result, the sample discrepancy from the uniform distribution is low. Given these characteristics, we selected the quasi-random sampling technique (proposed by (Sobol' 2001)) for the sample generation. We used Simlab software to generate quasi-random samples for MC Simulation. (Simlab can be freely accessed from simlab.jrc.ec.europa.eu/).

The distribution ranges are generally derived from prior expert knowledge or from empirical observations. Since the sampled weight values depend on the value range intervals, the posterior information on the probability distributions should be updated with new information whenever possible and practical (Tarantola et al. 2002). Global criteria weights are typically assumed to range between 0 and 1 (Malczewski and Rinner 2015). Therefore, lower and upper limits for the sample distributions can be selected accordingly. However, these limits are not expected to be assigned for criteria weights, specifically in the EBI model. Therefore, instead of using a uniform distribution, a triangular distribution is more appropriate especially when the middle value of the range is more likely than the values near the either extremes (Morgan and Henrion 1990). Considering different score value ranges for EBI factors, the criterion weight samples were generated based on the triangular probability distributions using the parameters in Table II-2.

Following the specification of probability density functions, the generated weight sample set is fed into the MC simulation process and the model was run (k+2) *N times, where k is the number of uncertain model input factors and N is the number of sampled weight values. For each run, the model produced the set of EBI scores for each watershed in the study area.

57

Table II-2 Parameters for Triangular Probability Distribution

EBI Factors	Possible Lowest Value	Estimated Peak Value	Possible Highest Value
N1	0	0.78	1
N2	0	0.78	1
N3	0	0.78	1
N4	0	0.39	1
N5	0	0.35	1

(b) Variance-based Global Sensitivity Analysis

The variance-based SA, which represents a global approach, has been adopted for spatially explicit U-SA. Within this approach, the variance of model output is apportioned to individual input factors and their combinations. If the model representation takes the form of $Y = f(X_1, X_2, \cdots, X_k)$, where Y is a scalar value corresponding to the model output and X_i is the generic input factor weight, then the sensitivity measure can be expressed by first order sensitivity index as in Eq. II-17(Saltelli et al. 2010):

$$S_i = \frac{V_i}{V} = \frac{V[E(Y|X_i)]}{V(Y)}$$

Eq. II-17

Where Y is the model output, and $V[E(Y|X_i)]$ is the variance of the expectation of Y conditional on the weight i having a fixed value. If $[E(Y|X_i)]$ substantially varies across X_i value range, i is regarded as an important criterion weight.

S_i represents the major contribution of i to model output variance. However, it does not capture the interaction (second- and higher-order) effects between i and the other criterion weights, which is its major limitation. The latter can be addressed by the total effect sensitivity

index (ST_i) (Eq. II-18), which quantifies the fractional contribution to $V(Y)$ of a given weight including its all interactions with other weights and $V[E(Y|X_{\sim i})]$ is the total contribution to Y's conditional variance caused by all non-i weights:

$$ST_i = 1 - \frac{V[E(Y|X_{\sim i})]}{V(Y)} = S_i + S_{ij} + S_{im} + S_{ijm} + \cdots + S_{ijm\ldots z} \qquad \textbf{Eq. II-18}$$

For spatially-explicit U-SA, the sensitivity indices are calculated for each spatial unit, which in this case is a watershed. Therefore, an algorithm to calculate sensitivity indices for vector-based local MCE has been developed and run for both fine and coarse scale representations.

(3)   Scale Sensitivity and Rank Mobility Index

Coefficient of variation (c_v), which is expressed by the ratio of standard deviation to mean (σ/μ_{q*}), is a standardized measure of dispersion widely used to compare different analysis units (Saint-Geours et al. 2014) and it can be applied as the final rank of suitability scores.

The relative change in the ranks for each land parcel was expressed by the rank mobility index (RMI) defined by Eq. II-19, where R_{HUC10} represents the watershed rank for HUC10 and R_{HUC12} represents the corresponding rank for HUC12.

$$RMI = \frac{R_{HUC10} - R_{HUC12}}{R_{HUC10} + R_{HUC12}} \qquad \textbf{Eq. II-19}$$

The rank mobility index captures shifts in watershed (analysis unit) ranks and can be used to show how changing the analysis scale from finer (HUC12) to coarser (HUC10) affects

59

the rank-position of land parcels. For a parcel with no change in its rank position between HUC12 and HUC10 the RMI equals zero.

4. **The Implementation of Local IPM with Spatially Explicit Uncertainty-Sensitivity Analysis**

a) **Explanatory Example and Simulation Set-Up**

The weight sample sets were generated using triangular probability distributions for the five EBI factor weights. The suggested sample number is advised to be a much larger value than the number of variables (approximately 100 times for each) (European Commission - IPSC 2008). In total, 1408 samples were generated with the quasi-random sampling algorithm using the Sobol sequence mode (2^n) and the number of input parameters (k=5) (details for the algorithm can be found in: (Sobol' et al. 1992)).

To explain the procedure of calculating local suitability scores, let us consider the watershed #5 in the HUC12 watershed delineation. As depicted in Figure II-20, the 5th watershed has 6 neighboring watersheds, including itself (Queen Neighborhood is used). Therefore, only the criterion values for the following six watersheds: 1, 5, 6, 7, 8 and 9 are used for the local standardization and local range calculation Eq. II-11 and Eq. II-12 (Table II-3 a-f contains the step-by-step calculations). The neighborhoods similar to the one shown in Figure II-20 are formed for each watershed in the study area (31 for HUC10 and 158 for HUC12) following the edge and/or point contiguity requirements of Queen Neighborhood scheme. Continuing with the example for the 5th watershed, the global extreme values (Table II-3a) are determined based on the maximum and minimum criterion values for the study area. The local extremes do not necessarily correspond to global extremes due to the range sensitivity principle. For example, for the 4th criterion (N4 - Enduring Benefits), the global

maximum value is 8.13 whereas the local maximum in the neighborhood equals to 6.70. Therefore, for the 5th neighborhood, although the Enduring Benefits criterion value is less than the global maximum (N4 = 6.62), given that the value is closer to the local maximum (6.70 vs 6.62) than to the global maximum (8.13 vs 6.62), the local standardized value becomes 0.97, which is very close to ideal value 1.0. (Table II-3d).

Following the criteria standardization, local weights (Table II-3f) are calculated based on Eq. II-13. It should be noted that although the randomly generated global weights (w_k) (Table II-3b) were fixed for each neighborhood in the first simulation run, the local weights changed for each neighborhood due to local heterogeneity, which also defines the local extremes. Therefore, unlike the global MCE, in the local MCE approach the criteria weights and the suitability scores are affected by spatial heterogeneity within neighborhoods.

In the final step of local IPM computation, the relative closeness to the ideal solution was calculated by using the formula in Eq. II-16. Following the calculation of EBI scores, the U-SA was run for five EBI factors (k=5) and 1408 global weight samples (N=1408). The model was run 9856 times (N*(k+2)) for each of the two watershed delineation levels (HUC10 and HUC12).
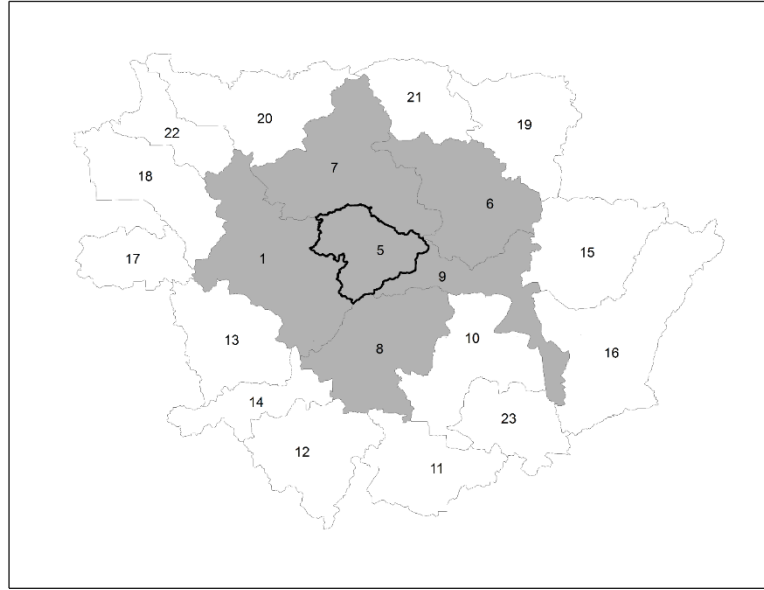
Figure II-20 Example of Queen Neighborhood for the 5th watershed

Table II-3 Calculation of local criteria values and criteria weights for the 5th neighborhood

	N1 Wildlife	N2 Water Quality	N3 Soil Erosion	N4 Enduring Benefits	N5 Air Quality
Global Max	3.76	3.58	4.30	8.13	9.04
Global Min	1.28	1.96	2.13	1.87	2.73
Global Range	2.48	1.62	2.18	6.26	6.31

(a)

Global Weights for 1st Simulation generated by quasi-random sampling and normalized to sum up 1.0)				
w_{N1}	w_{N2}	w_{N3}	w_{N4}	w_{N5}
0.2270	0.2270	0.0.2270	0.1674	0.1563

(b)

Criteria Values	N1	N2	N3	N4	N5
1	**1.76**	2.40	**3.73**	**6.70**	**5.18**
5	2.03	2.68	3.59	6.62	6.70
6	**3.11**	2.40	**3.21**	**3.61**	9.04
7	2.31	**3.40**	3.61	6.01	6.45
8	2.33	**2.18**	3.25	4.70	7.51
9	2.26	2.29	3.65	5.66	7.23

(c)

LOCAL STANDARD VALUES					
	N1	N2	N3	N4	N5
1	0.46	0.30	0.46	0.60	0.45
5	0.20	0.41	0.73	0.97	0.39
6	0.63	0.15	0.71	0.37	1.00
7	0.42	1.00	0.68	0.66	0.49
8	0.85	0.31	0	0.16	0.77
9	0.27	0.08	0.86	0.68	0.23

(d)

LOCAL RANGES					
	N1	N2	N3	N4	N5
1	1.06	1.43	1.04	3.60	5.49
5	1.35	1.22	0.52	3.10	3.86
6	1.73	1.18	0.52	3.10	3.86
7	2.48	1.43	2.17	6.26	5.11
8	0.88	0.73	1.05	2.92	3.04
9	1.18	1.40	1.19	3.01	2.34

(e)

Local WEIGHTS w_k^q (1st Simulation)					
	N1	N2	N3	N4	N5
1	0.1523	0.3159	0.1707	0.1472	0.2139
5	0.2358	0.3254	0.1030	0.1535	0.1823
6	0.2359	0.2462	0.2380	0.1842	0.0958
7	0.2407	0.2127	0.2399	0.1725	0.1342
8	0.1818	0.2298	0.2477	0.1711	0.1696
9	0.1907	0.3472	0.2207	0.1389	0.1026

(f)

b) Spatially Explicit Uncertainty-Sensitivity Analysis

For each watershed delineation scheme, the 9856 model outputs (Map Blocks in Figure II-17) were collapsed into the mean suitability and standard deviation maps. The resulting statistics are given in the scalar form in Table II-4. The scalar mean reported in Table II-4 is the mean of all watershed means for the given delineation (HUC12 or HUC10). Similarly, the scalar standard deviation is the mean of standard deviations for all watersheds.

Table II-4 Summary simulation results for mean suitability and uncertainty maps.

Neighborhood Scheme	Sample Size	Model Run	Mean Final Score (μ)	Standard Deviation (σ)
HUC 10/ 31 areal units	1408	9856	0.404	0.013
HUC 12/ 158 areal units	1408	9856	0.379	0.021

The CRP assigns a threshold value as a cut-off parameter for each bidding term. In this study, the choice of threshold values was based on the mean final score (μ) and standard deviation (σ) given in Table II-4. Hence, any location in the study area with the mean suitability and standard deviation values exceeding the mean final score and standard deviation reported in Table II-4, was interpreted as highly suitable but uncertain.

In the conventional approach, suitability scores exceeding the mean would indicate robust areas for land conservation. Hence, the application of local MCE without the UA would stop here and recommend high suitability areas for CRP selection. However, using mean suitability map without standard deviation map may conceal the areas of high suitability and high uncertainty. This means that the selection, which is based solely on suitability scores without considering an uncertainty measure, will inevitably result in picking suitable areas associated with high uncertainty. Yet, U-SA inform the decision-making process by providing

confidence levels on the suitability results (Figure II-21). The analysis results presented in the following section focus on the suitable areas with high uncertainty. Focusing on the so-called high-high areas (high suitability and high uncertainty) is predicated on the premise that those areas comprise the next best candidates for inclusion in the CRP program following the obvious winners – the high suitability and low uncertainty areas.
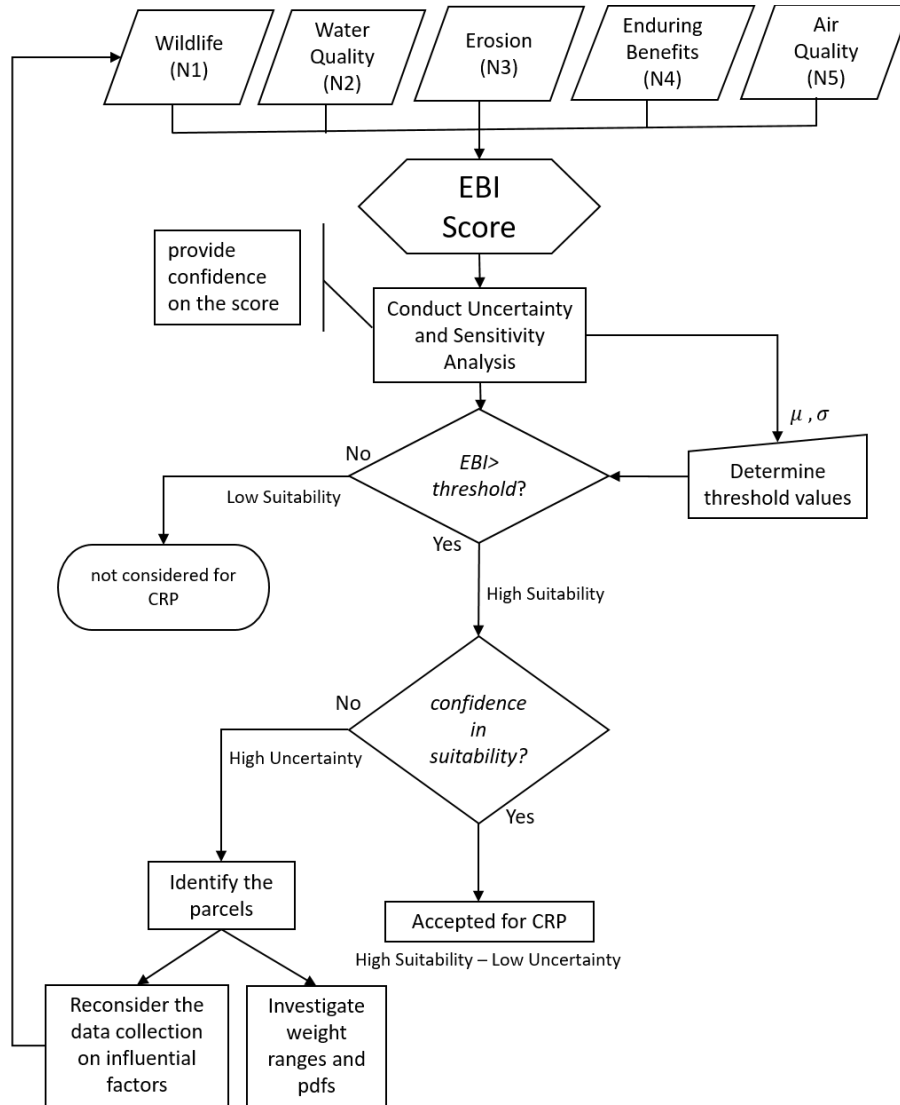
Figure II-21 Flowchart for land conservation decision making informed by Uncertainty and Sensitivity Analysis

5. **Results and Discussions**

In this section, the results of EBI model UA at two model scales; HUC10 and HUC12 are presented. This is followed by the global SA of factor weights using the variance decomposition and the calculation of spatially distributed first-order and total interaction sensitivity indices. Next, the sensitivity of model output to changes in analysis unit scale with Rank Mobility Index is analyzed. The section is closed by interpreting the results of weight SA in concert with scale SA.

a) **Mean Suitability and Uncertainty of EBI Candidate Areas**

Based on the outcomes of mean suitability and uncertainty maps, watershed delineations can be further categorized as (1) high suitability-high uncertainty, (2) high suitability-low uncertainty, (3) low suitability-low uncertainty, and (4) low suitability-high uncertainty. The watersheds falling into the category 1 were high confidence priority regions. The categories 3 (high uncertainty) and 4 (low suitability) were not considered in the analysis that followed. The focus was on candidate watersheds (category 2) that potentially might broaden the pool of obvious choices.

For the HUC10 watersheds, 11.48% of the study area (4 out of 31 watersheds) had mean suitability values higher than the corresponding threshold $(\mu \geq 0.404)$ and was accompanied by the uncertainty higher than the threshold $(\sigma \geq 0.013)$ which falls into high mean suitability and high uncertainty category represented as candidate areas (Figure II-22a – category High-High). For the HUC12 watersheds $(\mu \geq 0.379\ and\ \sigma \geq 0.021)$, the respective high-suitability-high-uncertainty area increased to 18.09% (32 out of 158 watersheds) (Figure II-22b-category High-High).
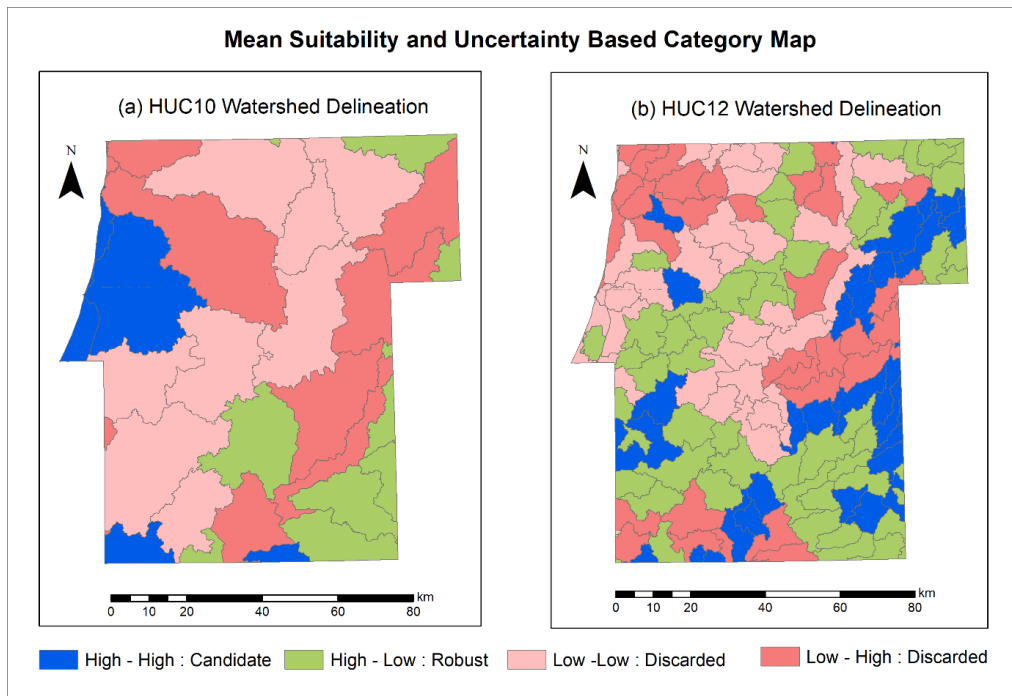
Figure II-22 Spatial distribution of land suitability and its uncertainty based on the cross tabulation of high-low values: (a) for HUC10 watershed delineation, (b) for HUC12 watershed delineation

These results are important in terms of identifying the areas suitable for CRP and assessing their uncertainty due to factor weights. However, to better understand the influence of factor weights on the uncertainty of EBI suitability scores, the sensitivity indices of weights can be mapped and their distribution examined.

b) Sensitivity Analysis of Factor Weights

The first-order and total-order sensitivity indices were computed using the Eq. II-17 and Eq. II-18 and the data from MapBlocks (Figure II-17). The indices account for the variability of EBI scores (model output) and apportion it to each factor weight. For the ease of visual interpretation, five first-order sensitivity index maps were combined into two dominance maps – one for each watershed delineation scheme (Figure II-23).

66

The dominance maps (Figure II-23a-b) were compiled by assigning to each analysis unit (HUC10 or HUC12 watershed, respectively) the attribute code representing a factor with the highest first-order sensitivity index value (i.e., the dominating factor in terms of weight sensitivity). The maps reveal factor weights contributing the most to the uncertainty of model (EBI) output. For the HUC10 watershed delineation scale (Figure II-23a), the EBI scores are sensitive to the (N3) factor weight (erosion) for the majority of the study area. For the HUC12 watersheds, (N5) air quality is the major dominant factor weight except for the north-western region where almost every factor shows dominance in terms of first order sensitivity index value.

First Order Sensitivity Index Dominance Maps

(a) HUC10 Watershed Delineation

(b) HUC12 Watershed Delineation

N1 - Wildlife   N2 - Water Quality   N3 - Erosion   N4 - Enduring Benefits   N5 - Air Quality
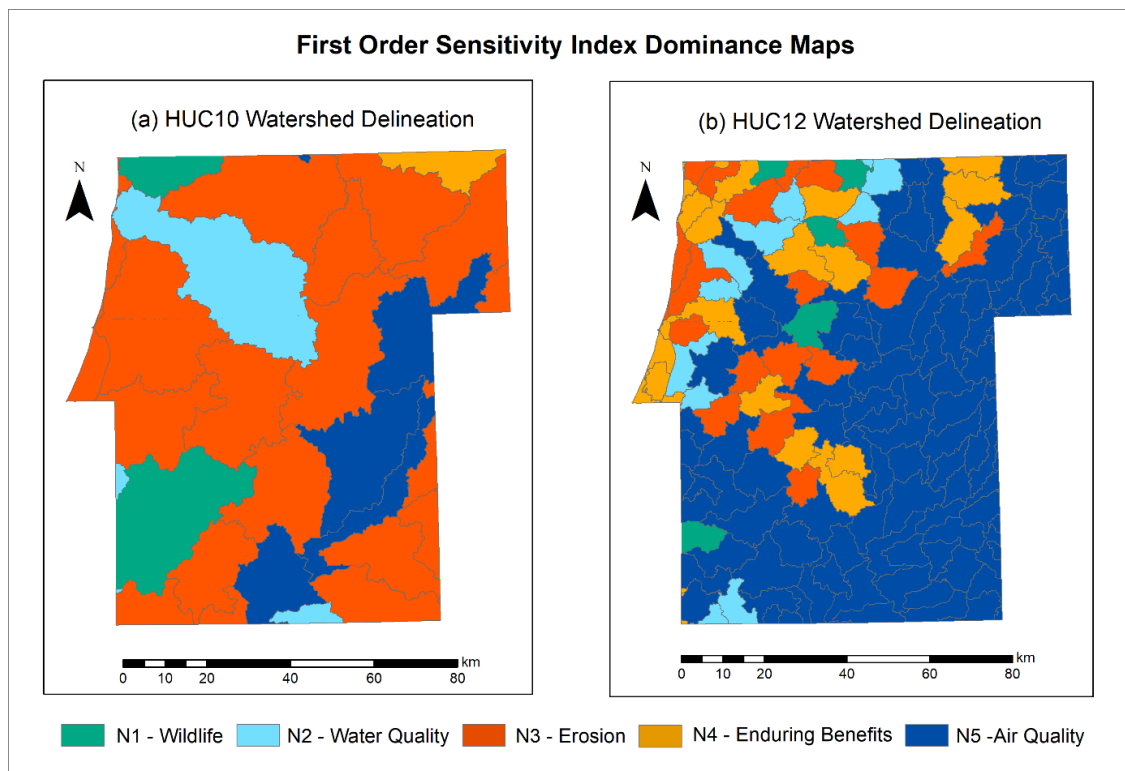
Figure II-23 First-order sensitivity index dominance maps for HUC10 and HUC12 watershed delineations

Similar dominance maps were also compiled for the total-order sensitivity indices (Figure II-24a-b). Where the first order sensitivity indices only measure the individual effect

of each factor, the total order effects capture interactions between factors. This is especially important in modeling systems where individual input factors can have complex interactions. Such interactions, called higher order effects, can be revealed through the interpretation of total order index maps. Visualizing and comparing the total-order dominance maps (Figure II-24), one can observe the same dominant influence of air quality weight throughout the study area. However, for HUC10, the dominance of (N3) erosion has been replaced by (N5) air quality for some of the watersheds. Similarly, the dominance effect of air quality is expressed in HUC12 in interaction maps. Despite the fact that the individual contribution of air quality weight is less insignificant (Figure II-23) especially in north-western region, its influence becomes dominant when interacting with other factor weights.
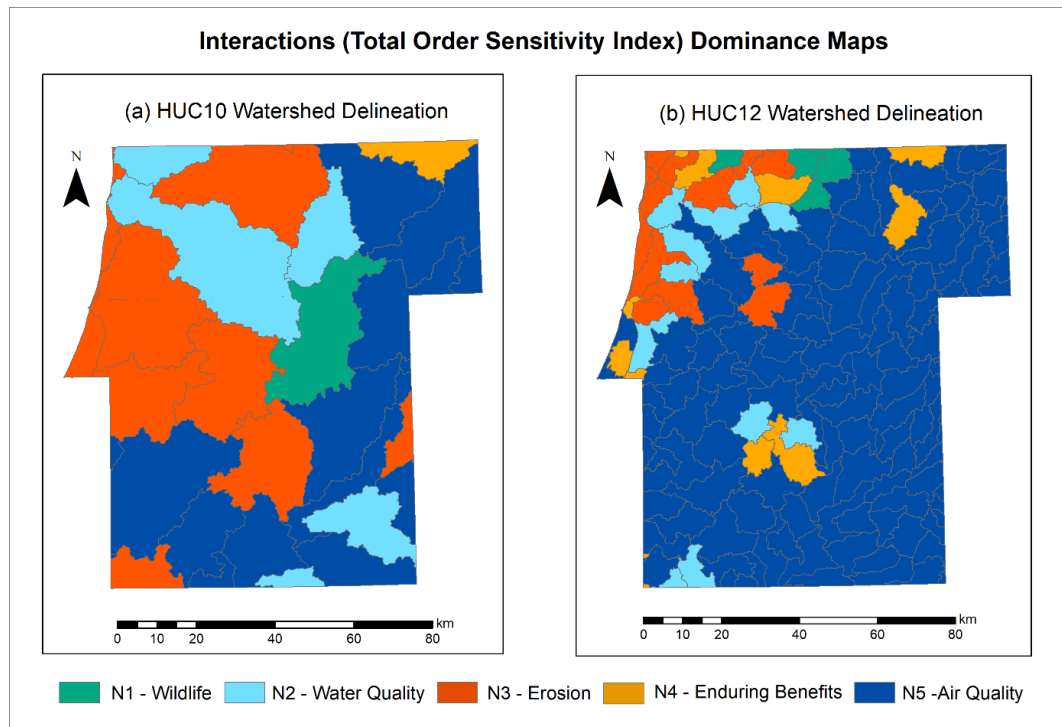
Figure II-24 Interactions (Total-order Sensitivity Index) dominance maps for HUC10 and HUC12 watershed delineations

c) Scale Sensitivity

To compare high-suitability-high-uncertainty areas identified at two different scales of analysis (Figure II-22), the results of U-SA were represented at the parcel level by running spatial query and assigning mean suitability and standard deviation values to each parcel (the CRP decision unit, Figure II-25). Each parcel was assigned a coefficient of variation value (the level of uncertainty relative to suitability) for the spatially intersecting watershed by using an iteration script. The coefficient of variation was calculated twice; ones for HUC10 and next for HUC12. Then, the land parcels were rank-ordered in the descending order, based on the corresponding coefficient of variation values, yielding two rankings: one for HUC10 and another for HUC12. Out of 19,988 parcels in the study area, there were no parcels with the zero RMI value. However, there were 139 parcels (0.67%) showing only minimal rank shifts, for which the RMI values ranged between -0.007 and 0.007. Hence, the EBI scores for this small set of parcels can be deemed as insensitive to changes in the analysis scale.

The increasing absolute values for RMI imply the increasing divergence between the ranks of a parcel computed at two different analysis scales. A negative RMI ($R_{HUC10}<R_{HUC12}$) implies that a parcel with a higher position in the ranking (rank 1 is the highest-ranking position) at the HUC10 (coarser) scale drops to a lower ranking position at the HUC12 (finer) scale. Conversely, a positive RMI indicates that a parcel's rank declines when moving from the finer to the coarser scale of analysis. For example, a parcel with the coefficient of variation 0.02 (HUC10) and 0.03 (HUC12), and the corresponding ranks of 1120 (HUC10) and 2340 (HUC12), yields the RMI value of -0.3526 ($R_{HUC10}<R_{HUC12}$) indicating an upward rank shift associated with changing the scale from finer to coarser. In general, the higher the absolute

69

value of RMI, the higher the shift (and sensitivity) of parcel rank to change in the scale (size) of analysis unit.

Figure II-25 and Figure II-26 show the RMI values mapped at the parcel level for the high-high category, computed at two different scales of analysis (Figure II-22a-b). For the HUC10 watershed delineation, 79.9% of parcels in that category (1678 out of 2099 high-high parcels) have negative RMI values representing a downward shift in ranks in response to change in the analysis scale from coarser (HUC10) to finer (HUC12). (Figure II-25). The remaining 20.1% of parcels (symbolized in orange and red in Figure II-25) have positive RMI values representing an upward shift in ranks in response to scale change from HUC10 to HUC12. This means that all of the land parcels in the high-high category are sensitive to scale change, but for over 79% their ranks tend to increase with the change from finer to coarser scale. For the HUC12 watershed delineation scheme (Figure II-26), the percentage of parcels with negative RMI values decreases to 14.9 % (536 out of 3608 parcels). This means that for almost 15% of land parcels in the high-high category, their ranks tend to drop with the change from coarser (HUC10) to finer (HUC12) scale.

Although these results suggest that the choice of scale (resolution) for analysis unit plays a role in EBI ranking, they should be interpreted in concert with factor weight sensitivities.

Rank Mobility Index Map for HUC 10 Delineation Scheme
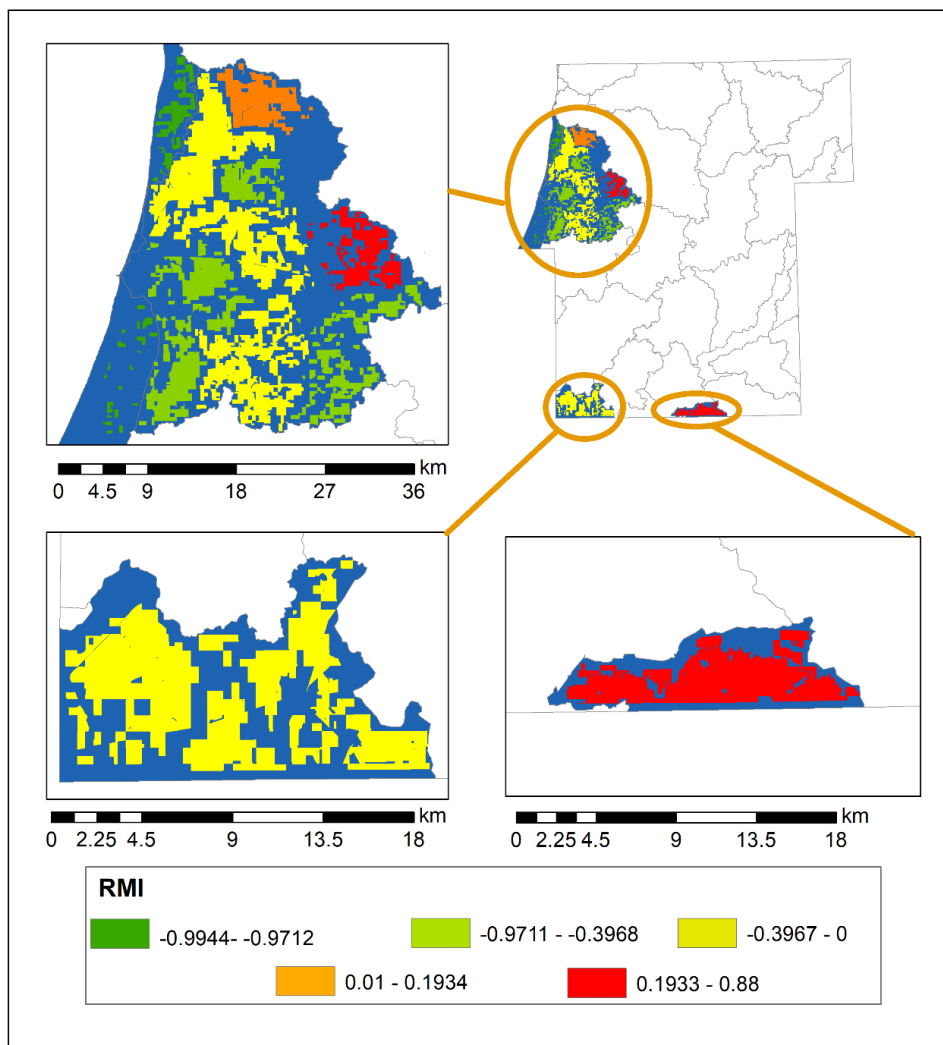
Figure II-25 Rank mobility index maps for land parcels located in high mean suitability and high uncertainty watersheds (in blue) for HUC10 delineation scheme

Rank Mobility Index Map for HUC 12 Delineation Scheme

RMI

| ██ -0.5048 - -0.2430 | ██ -0.2429 - -0.1522 | ██ -0.1521 - -0.3835 | ██ -0.3834 - -0.6258 | ██ 0.6257 - 0.9043 |
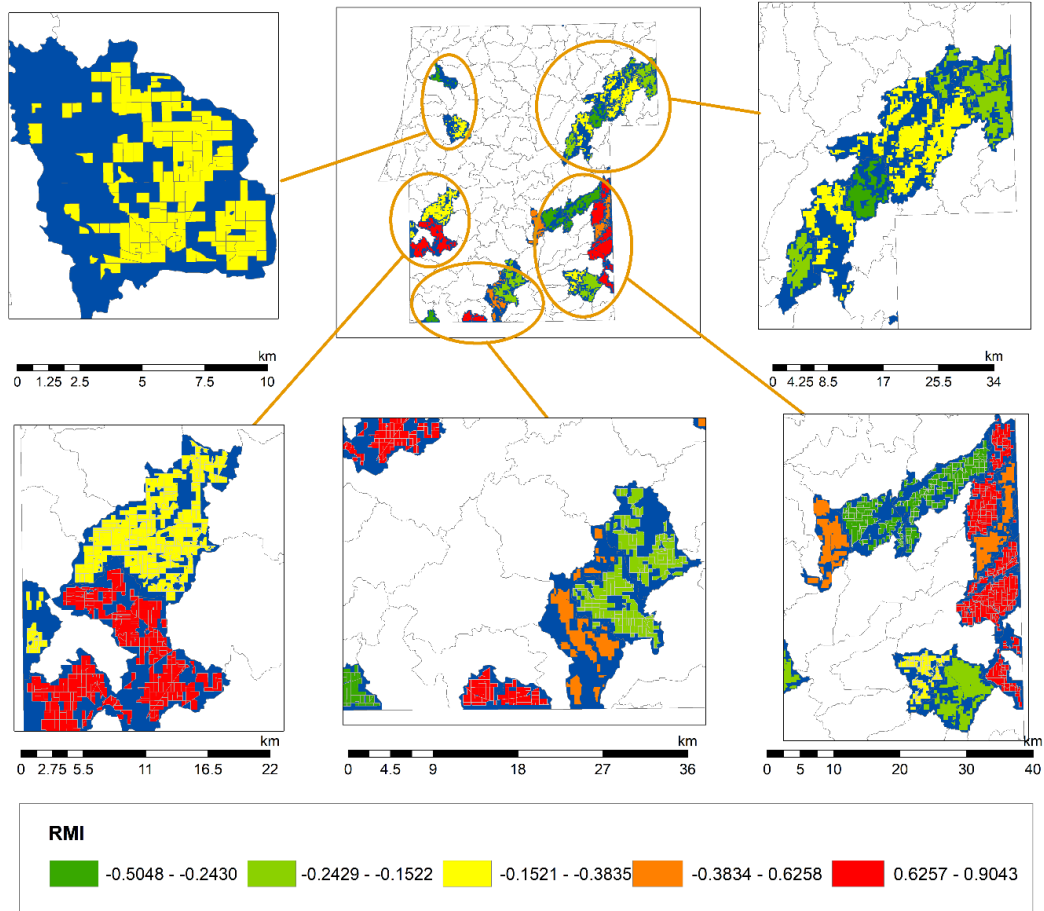
Figure II-26 Rank mobility index maps for land parcels located in high mean suitability and high uncertainty watersheds (in blue) for HUC12 delineation scheme

d) Integrating the Sensitivity Analysis Results

To integrate the scale and factor weight SA results, parcels located in the candidate (high-high) areas common to both scales of analysis were selected. Figure II-27 shows the parcels located in candidate areas (HUC12 sub-watersheds), which are common to both HUC12 and HUC10 delineations. This can be also visually confirmed by comparing with the candidate areas (represented in blue) in Figure II-22a and Figure II-22b. The parcels in Figure II-27 fall into two categories; parcels with positive RMI values denoting an upward shift in

72

ranks in response to change in the analysis scale from HUC10 to HUC12, and parcels with negative RMI values representing a downward shift in ranks in response to change from HUC10 to HUC12.

Candidate Areas with the Associated Uncertainty and RMI
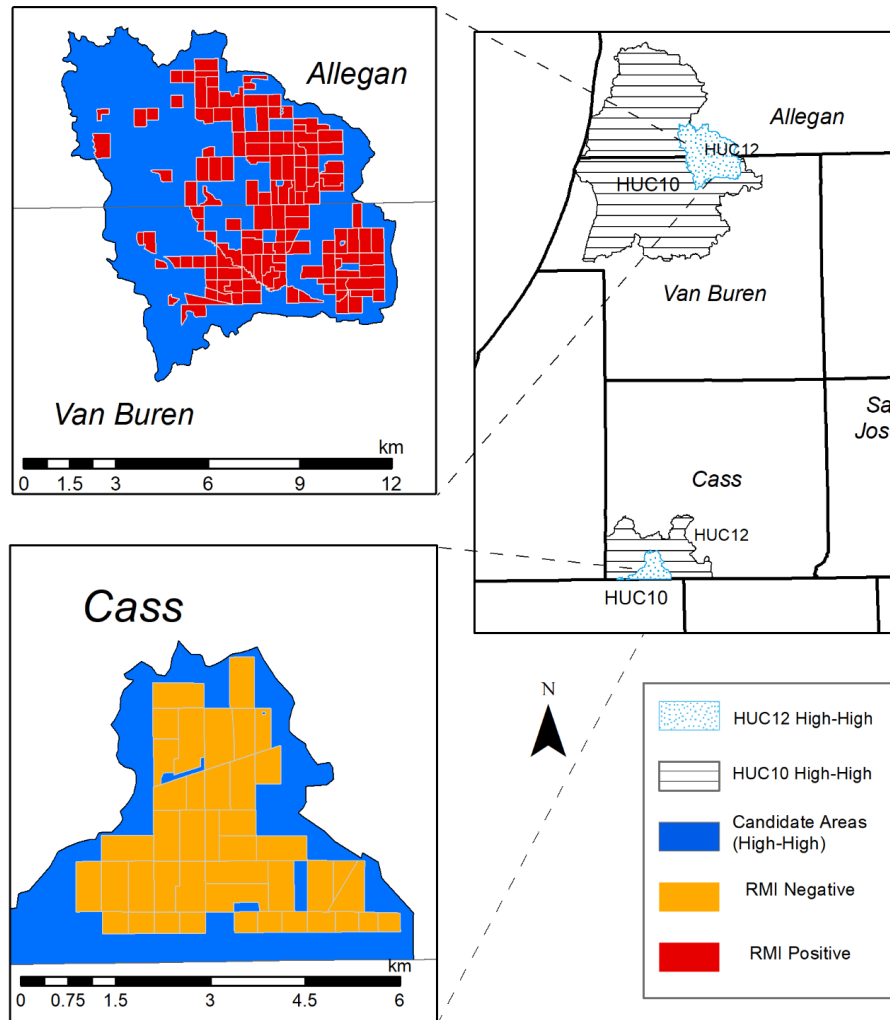
Figure II-27 Candidate areas with the associated rank mobility index category. The three map insects show the areas common to HUC12 and HUC10

In total, there are 171 parcels located in the candidate areas common to both delineations, out of which 42 parcels have negative RMI values ($R_{HUC12} > R_{HUC10}$) indicating

that their position in the rank order will drop when the scale of analysis changes from coarser (HUC10) to finer (HUC12). For the remaining 129 parcels with positive RMI values ($R_{HUC10}>R_{HUC12}$) their rank will increase in response to the same change of scale from HUC10 to HUC12. This finding indicates that the ranks of all 171 parcels are sensitive to scale change. However, the parcels with positive RMI values located in the north-western part of the study area overlapping Allegan and Van Burren Counties will stand a better chance of getting selected for CRP (their ranks will be higher since RMI is positive) if the analysis is carried out at the finer scale (HUC12). Conversely, a smaller group of parcels (42) with negative RMI values will do better in terms of ranking and the subsequent selection for CRP if the analysis is carried out at a coarser scale (HUC10 delineation).

To put this finding in the context of factor weight sensitivities, the parcels in the candidate areas (Figure II-27) were overlaid with the dominant first order and total effect sensitivity indices (Figure II-28).

The sensitivity dominance map including the high-high areas common to both scales is shown in Figure II-28. The bivariate map design is based on the crosstabulation of two scales (HUC12 and HUC10) and the dominant factors (N2, N3 and N5) common to the first and total order indices.

Out of five possible factor weights affecting the parcel ranks three were found influential for the candidate areas: water quality (N2) and erosion (N3) in Cass County and erosion (N3) and air quality (N5) in Allegan and Van Buren Counties. (Figure II-28)

74
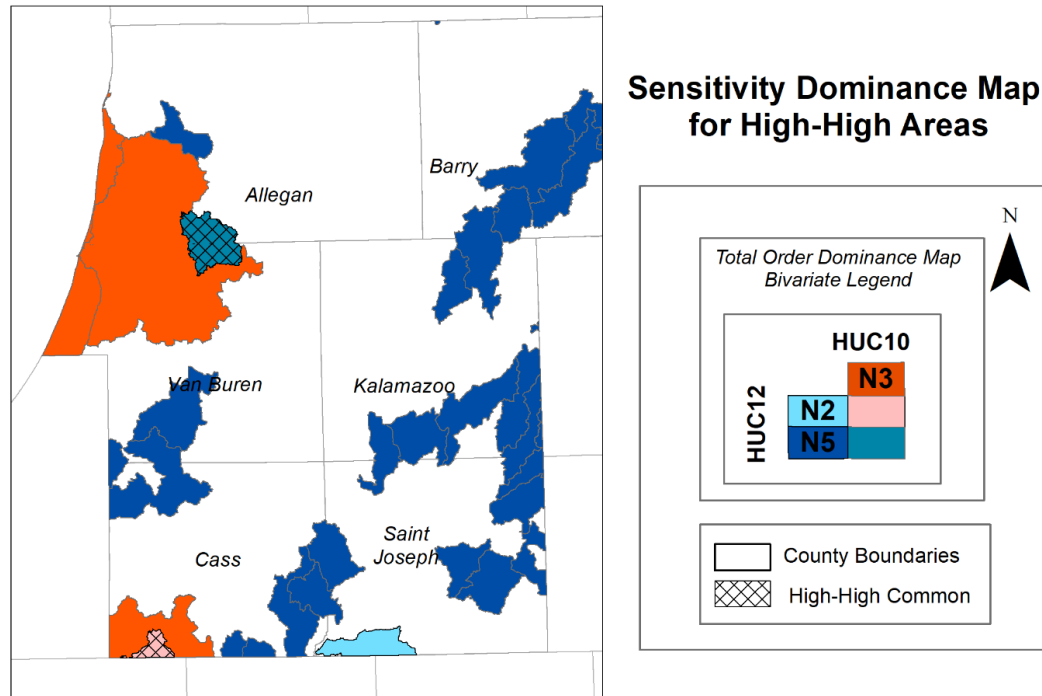
Figure II-28 Sensitivity Dominance Map for high-high areas common to both scales

Given the results in Figure II-27 and Figure II-28, one can interpret the joint influence of scale and factor weights on the parcel ranks. The ranks of the parcels located in the candidate areas, common to both scales of analysis, are sensitive to scale change. The scale sensitivity is confounded though, by the factor weight sensitivity, which exhibits a simpler spatial pattern for the first order effects than for the total order effects. Specifically, for the north-western candidate area overlapping Allegan and Van Buren Counties attention should be paid to the weights for erosion (N3) and air quality (N5). These two factor weights may affect the upward shift in parcels ranks due to the change from finer (HUC12) to coarser scale (HUC10). Further on, for the south-western candidate area (Cass County) the weights for water quality (N2), erosion (N3), may affect the upward shift in parcels ranks due to the scale change from HUC12 to HUC10.

6. **Conclusion**

SA is a common analytic method utilized in a variety of disciplines that rely on modeling including the physical sciences, environmental modeling, and operations research. In spatial multi-criteria evaluation, SA has largely been applied in a perfunctory manner, and frequently confused with UA. In this paper, an approach featuring spatially-explicit UA integrated with SA was used to analyze the influence of input factor weights on the model output in the form of rank-ordered list of decision alternatives (agricultural land parcels). In addition to factor weights, the sensitivity of parcel rank order to changes in the scale of analysis unit was analyzed with rank mobility index (RMI).

The results of UA included the robust set of parcels for CRP selection. Those were the parcels characterized by above-the-mean EBI scores (high suitability) and below-the-threshold uncertainty of rank change. Next, the candidate parcels characterized by high suitability and high uncertainty, were analyzed by focusing on two potential sources of uncertainty: factor weights and scale of analysis unit. Following the SA of factors weights and the SA of scale, the results were collated by focusing on the candidate areas common to both scales of analysis. All of the parcels located in the candidate areas showed some sensitivity to scale change with the majority (over 75%) increasing their rank positions in response to change from HUC12 to HUC10. The upward shift in parcel ranks caused by the change from finer to coarser scale was likely amplified by the sensitivity of model output to three factor weights: water quality (N2), erosion (N3), and air quality (N5). However, the spatial manifestations of combined scale and factor weight influences on the model output were uneven. In Cass County, the calculation of EBI scores at a lower scale of analysis (HUC10) will contribute to rank increase for the candidate parcels (Figure II-27). Moreover, the parcel ranking will be influenced by water

quality and erosion weights (Figure II-28). In the area overlapping Allegan and Van Buren counties, the ranks of candidate parcels will increase when EBI scores are calculated at a larger scale of analysis (HUC12), and the parcel ranking will be influenced by erosion and air quality weights (Figure II-27 and Figure II-28).

A question can be asked: what is the practical value of extensive U-SA, presented in this paper, to the decision maker who needs to decide on the selection of parcels for CRP? Clearly, if the CRP budget in any given year suffices only to accept the robust parcels (high suitability/low uncertainty) the presented analysis aids in identifying such parcels, and their number can be increased or decreased by lowering (relaxing) or raising (tightening) thresholds corresponding to high suitability and low uncertainty. If, however, the available budget allows expanding beyond the robust parcels by including high suitability/high uncertainty parcels (the so-called candidate parcels), the presented approach offers additional insights into the drivers of model output uncertainty, which in turn can be used by the decision maker to select from the high-high parcels based on their rank sensitivities.

From the methodological standpoint, the integrated and spatially-explicit approach to U-SA in land allocation problems can guide modelling effort by focusing data collection on influential model input factors. In particular, investigating weight value ranges and their probability density functions in weighted index models such as EBI may result in smaller variability (uncertainty) of model output. Therefore, the integrated uncertainty and sensitivity approach benefits from considering various probability distribution functions and selecting the ones that fit the best the uncertain model parameters.

Reporting on model output uncertainty and understanding its drivers is simply a good modeling practice. Therefore, improving the visualization of uncertainty and sensitivity

quantification is expected to make an improvement in the explanatory power of land use modeling. Future research efforts should focus on developing further integrated methods of analyzing model output sensitivity to multiple sources of uncertainty, beyond scale and factor weight, and to offer effective means of their visualization.

III.   Spatio-Temporal Uncertainty and Sensitivity Analysis for Land-Use Forecasting Model

This chapter presents a computationally efficient meta-modeling approach to spatially explicit uncertainty and sensitivity analysis in a cellular automata (CA) urban growth and land-use simulation model. The uncertainty and sensitivity of the model parameters are approximated using a meta-modeling method called polynomial chaos expansion (PCE). The parameter uncertainty and sensitivity measures obtained with PCE are compared with traditional Monte Carlo simulation results. The meta-modeling approach was found to reduce the number of model simulations necessary to arrive at stable sensitivity estimates. The quality of the results is comparable to the full-order modeling approach, which is computationally costly. The study shows that the meta-modeling approach can significantly reduce the computational effort of carrying out spatially explicit uncertainty and sensitivity analysis in the application of spatio-temporal models.

A.   Introduction

Increasing urban population directly affects the pressure on the available urban and sub-urban land with negative impacts on biodiversity in favor of urbanization. To represent these land-use dynamics, a cell-based spatial diffusion approach called cellular automata (CA) has been frequently used for urban growth and land use change (UG-LUC) modeling (de Almeida et al. 2003; Torrens and Nara 2007; Clarke 2008; Moreno et al. 2008; van Vliet et al. 2016). CA-based models mostly involve many input factors including variables and structural elements (e.g. transition rules). Any confidence in the results depends highly on these input factors. It is therefore expected that some of the initial conditions may be the

drivers of model uncertainty (Kocabas and Dragićević 2006; Li et al. 2014a; Dahal and Chow 2015). In the same context, it is critical to evaluate the influence of input factors on model's output so as to provide decision makers with confidence in their actionable information. To this end, uncertainty and sensitivity analysis offer a way forward.

Uncertainty analysis (UA) quantifies the model output variability and sensitivity analysis (SA) investigates how this uncertainty is apportioned among the model input factors (Saltelli et al. 2000; Crosetto and Tarantola 2001). In particular, an uncertainty and sensitivity analysis (U-SA) approach that is both independent from model structure and capable of handling interaction effects is important for complex, non-linear models. (Halls 2002; Chen et al. 2010; Roura-Pascual et al. 2010; Moreau et al. 2013a; Xu and Zhang 2013; Saint-Geours et al. 2014). Moreover, for spatio-temporal models, where the simulation results are spatially distributed, it is additionally important to identify not only the source(s) of uncertainty but also its location(s) at a specific time (Herman et al. 2013; Abily et al. 2016). The resulting uncertainty maps can assist in locating uncertainty hot spots, and the sensitivity maps help further in identifying the spatial pattern of influential input factors behind the high uncertainty areas (Ligmann-Zielinska 2013; Şalap-Ayça and Jankowski 2016). However, the traditional Monte Carlo-based methods for U-SA require a large number of model evaluations, which make these approaches intractable for computationally expansive models (Saltelli et al. 2010).

One approach to overcoming the computational bottleneck is high-performance computing in the form of distributed and/or parallel computing (Tang and Jia 2014; Hu et al. 2015). Tang and Jia (2014) and Erlacher et al. (2017) accelerated U-SA with graphics processing units (GPU) and Ligmann-Zielinska and Jankowski (2014) used a supercomputer

to overcome intractable models. Yet another approach without the need of access to supercomputers or computationally powerful hardware is the use of surrogate or meta-models (Saltelli et al. 2000). The meta-model, which is fitted to the model by a set of experiments or model runs, replicates the behavior of the original model in the domain of its influential input parameters (Oakley and Hagan 2000; Marrel et al. 2011).

Although it is common to calibrate and validate CA models for achieving a desirable land use pattern accuracy, only limited attention has been paid to spatially-explicit U-SA. In this study, it is aimed to contribute to the body of knowledge on spatio-temporal U-SA by using a meta-modeling technique called Polynomial Chaos Expansion (PCE), which can reduce the computational effort of performing a U-SA. This approach was implemented on a CA-based model, called SLEUTH (Clarke et al. 1997), which has been widely used for simulating UG-LUC. The results of PCE to the full order Monte Carlo (MC) approach was also compared to show how close the PCE reproduces uncertainty measures with fewer model computations than MC. For the implementation, first model output uncertainty on UA maps was analyzed to observe where and when the range of variations is most influential. The uncertainty analysis was followed up by studying sensitivity maps to identify the most influential inputs.

In the remainder of the chapter, the background information on UG-LUC forecasting is provided, including SLEUTH modeling, and on the spatially-explicit approach to integrated U-SA. In section three we explain the basis of the PCE method. Then, it is showed, in section four, how PCE can be applied in concert with U-SA to reveal the influence of the spatio-temporal variations of input parameters on the model output.

B.   *Background*

This section provides a brief introduction to CA as a simulation method for UG-LUC

modeling, followed by an introduction to U-SA and meta-modeling.

1. **Cellular Automata based Urban Growth and Land-Use Forecasting**

Cellular automata (CA), pioneered by Ulam and Von Neumann (Ulam 1952; von Neumann

1966), is based on the generated dynamic behaviors under defined rules and constraints for

certain configurations (neighborhoods) (Holland 1999). Due to the similarity between

cellular automata and field representations (i.e. a grid), especially for spatial systems based

on grid representations, the applications of CA proliferated in the understanding of complex

geographical systems (pioneering examples include: Tobler 1979; Couclelis 1985; White and

Engelen 1993; White and Engelen 1994).

Within a set of regular cells, the cellular automaton, *A*, is defined by the set of states,

S, that change in discrete time steps based on transition rules, *T*, within a specified

neighborhood, *N*. Therefore, the basic formulation of a cellular automaton can be written as:

$$A \sim (S, T, N)$$

For urban growth, the cell's state is guided by transition rules, which reflect the

complexity of the environment. These rules act as a link between the spatial patterns and the

underlying spatial process. The transition rules are applied within the cell's neighborhood in

temporal increments. The rules are not necessarily applied uniformly to all cells since the

evolution does not encapsulate each land form (i.e. water bodies in UG-LUC modeling).

However, the rules capture the intrinsic variability of the model's nature. As a result, CA

model design is highly sensitive to the transition rules (White and Engelen 1993; Torrens and O'Sullivan 2000; Ménard and Marceau 2005; Kocabas and Dragićević 2006; Samat 2006; Yeh and Li 2006; Pan et al. 2010; Pontius and Neeti 2010).

2. **SLEUTH for Urban Growth and Land-Use Change Modeling**

SLEUTH is a widely used CA based UG-LUC model, which is available along with a data repository for various cities on the United States Geologic Survey (USGS) affiliated, National Center for Geographic Information and Analysis (NCGIA) Project Gigalopolis website (NCGIA). Comprehensive reviews on its usage and application areas can be found in the literature (Clarke et al. 2007; Clarke 2008; Chaudhuri and Clarke 2013).

SLEUTH is the acronym for slope, land use, exclusion, urban extent over time, transportation, and hill-shaded backdrop layers. The model is initialized with these 6 input layers and a scenario file containing all the necessary parameters for simulation (i.e. UG forecast parameters and time steps for forecast) (Figure III-1). The model is run for each year of the simulation time frame [$t_1...t_T$] and the output is the urban growth/land use for each year.

SLEUTH simulates UG by using four transition (growth) rules, which include spontaneous growth $F_S(\delta, \gamma)$, new spreading center $F_{NS}(\beta, \gamma)$, edge growth $F_E(\chi, \gamma)$ and road influenced growth $F_R(\beta, \rho, \delta, \gamma)$ where, δ symbolizes a value for diffusion, β breed, χ spread, γ slope resistance, and ρ road gravity coefficients given as UG forecast parameters (Candau et al. 2000). Urban growth transition rules are bounded by suitability defined by the exclusion layer and the slope gradient. The exclusion areas (such as water bodies, preserved areas, or parks) or slopes greater than a critical level (often 21%) are considered as less likely to be urbanized. The resulting urban growth, achieved with four different transition rules,

serves as the basis for calculating the growth rate expressed by the ratio of the number of growth pixels to the total urban pixel population in SLEUTH (Clarke et al. 1997).
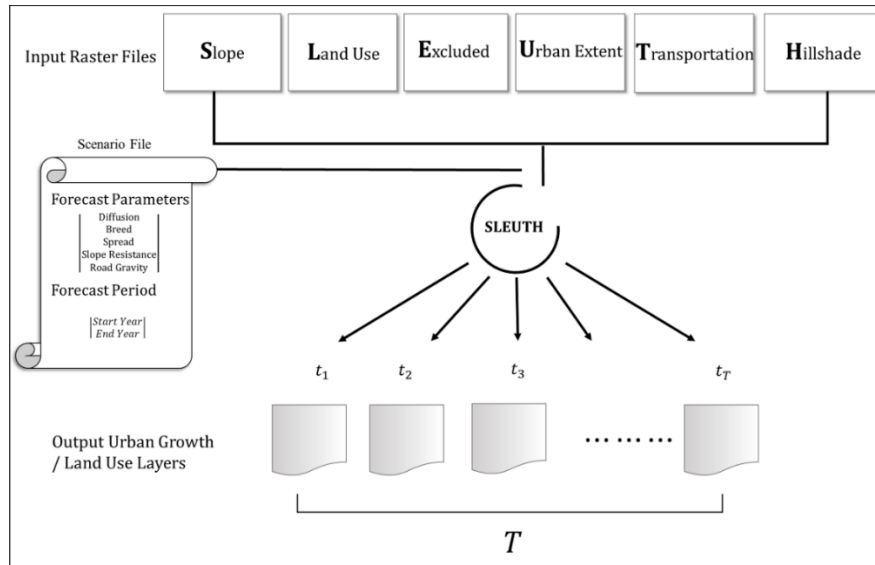
Figure III-1 SLEUTH Workflow

3. Uncertainty and Global Sensitivity Analysis for Complex System Models

In spatial models, UA is usually referred to as error propagation, and SA is considered as the analysis which aims to understand the behavior of the error/uncertainty and its reflection on the predictions made by the models (Heuvelink 1989; Heuvelink and Burrough 1993; Heuvelink 1998; Heuvelink and Burrough 2002).

For CA based UG-LUC models, early examples of SA focused on cell by cell inspection (White et al. 1997), finding an optimum neighboring size and type (Ménard and Marceau 2005; Kocabas and Dragićević 2006), investigating the variations in the output by applying different cell sizes and cellular configurations (Chen and Mynett 2003; Samat 2006; Pan et al. 2010) or comparing different scenario maps for land use change and validating

results with historical data (Pontius and Neeti 2010) . However, relatively little attention has been paid to the transition rules.

SLEUTH, like any other CA model, is subject to various uncertainties associated with the transition rules. The model employs a calibration process to define the best fit range for each forecast parameter used in the transition rules, however, the parameter values highly depend on the data and the user's expertise. The reliability of SLEUTH simulations depends on the forecast parameters, the model's sensitivity to these parameters and their interactions. A simple one-at-a-time (OAT) approach or (mono-looping) approach to quantifying the influence of different forecast parameter values on simulation results fails to catch the higher order effects resulting from parameter interactions nor does it reveal their partial contribution to the overall variance of the model results. In light of the above mentioned studies, U-SA is essential to increase the credibility of the UG-LUC models, as well as to test the model robustness in producing realistic outputs for future implementations (Jantz et al. 2003; Jantz and Goetz 2005; Kim 2013). Additionally, a spatially-explicit approach is also crucial for spatial models that do not entirely depend on scalar inputs but that are also affected by spatial relationships (Herman et al. 2013; Abily et al. 2016),

Variance, which is a central measure in error propagation and SA, allows partitioning the effects of uncertainty in the input factors on model output (Kyriakidis and Goodchild 2006). There is a range of different theoretical and methodological approaches to variance-based SA in the literature. Generally, SA is discussed under two categories: local and global (Saltelli et al. 2000; Helton and Davis 2002). In a local approach, one investigates the input variations by estimating partial derivatives of model input factors as varying one and keeping others constant (OAT approach) (Crosetto and Tarantola 2001). OAT is computationally

efficient and it does not need a large number of model executions. However, since it only investigates individual variations, it is mostly applied when no higher order interactions are expected (Crosetto et al. 2000; Gómez-Delgado and Tarantola 2006; Lilburne and Tarantola 2009).

Interactions among model inputs and non-linear output responses can be addressed by global SA (GSA) techniques where the sensitivity of the model input factors is not only determined individually (first order effects), but also as overall interactions (total order effects). Specifically, in variance-based GSA, the model factors influence on model output variability is represented by first-order (S) and total order (S_T) sensitivity indices. The first-order index (S) , sometimes referred to as the main effect sensitivity, estimates directly the selected single variable's portion of the overall variance (Sobol' 2001). The total order index (S_T) measures the total contribution of pairs of factors, i.e., first and higher order interactions of the selected single variable (Saltelli et al. 2010; Saint-Geours et al. 2014). Since CA models are characterized by interactions among input factors and non-linear output responses, the variance-based GSA is potentially an attractive SA method for different types of spatio-temporal models, including for the CA based SLEUTH, where higher order interactions result from the transition rules.

4. **Variance-Based Global Sensitivity Analysis and Polynomial Chaos Expansion**

GSA variance-decomposition based methods (e.g. *Fourier Amplitude Sensitivity Test* (FAST) (Cukier et al. 1973), *Extended FAST* (E-FAST) (Saltelli et al. 1999c), *Sobol Decomposition* (Sobol' 1993)) use MC simulation (Metropolis and Ulam 1949) as a sampling method during uncertainty propagation to draw multiple random samples from a given input distribution. A model is then run for each random sample set to obtain simulated outputs. The

computational cost of input sample generation (required to run MC) is insignificant in

comparison to the cost of model simulations (required to quantify the output uncertainty),

especially for complex models with large input datasets (Crosetto et al. 2000). Consequently,

the high number of simulations results in an expensive uncertainty evaluation and SA

becomes impractical (Helton 1993; Heuvelink 2003).

As a practical solution to this problem, meta-models can evaluate a model's response by

using a mathematical model approximation. SA based on meta-modeling starts with the

selection of the ranges and distribution for each input factor and continues with the

development of the experimental design to define the combinations of factor values, on

which the model evaluation will be based. Therefore, although the sequence of steps seems to

be exactly the same as in the comprehensive SA, the experimental design that uses the

selection of design points (points representing parameter values in sampling space) makes the

meta-model approach distinct (Saltelli et al. 2000). The approximation is based on these

design points and their selection is determined according to the presence of higher-order

effects, the number of variables under consideration, and the computational effort required to

evaluate the model. Different types of experimental designs are available such as multiple

linear, nonlinear regression (e.g. Ratto & Pagano 2012), neural networks (e.g.Villa-Vialaneix

et al. 2012), cubic splines (Rutherford et al. 2015), Gaussian processes (e.g. Marrel et al.

2011), and orthogonal polynomials (e.g. Sudret 2008).

One of the most frequently used meta-modeling techniques, Polynomial Chaos

Expansion (PCE), originally proposed by Norbert Wiener in 1938, propagates uncertainty

(which the 'chaos' term refers to) by expanding a complex function into orthogonal

polynomials that could be solved for relatively more easily than the original function (Wiener

1938). These polynomials are selected from a family of polynomials which are orthogonal with respect to the probability distribution of the corresponding input parameter (Burnaev et al. 2017). For example, Legendre polynomials, which are defined over the range [-1, 1], are orthogonal to a uniform distribution. Therefore, if PCE is applied for an input parameter set that has a uniform distribution, Legendre polynomials are used for expansion. PCE is preferable compared to other meta-modeling methods due to its applicability for dynamic stochastic systems, where there is an unavoidable uncertainty term in the system parameters. Theoretical studies with different polynomial functions and the applicability of various probability density functions are discussed by Xiu and Karniadakis (2002), Sudret (2008), and Crestaux et al., (2009).

Since PCE reduces the computational expense of uncertainty propagation, it has been widely applied in complex environmental problems including water quality modeling (Moreau et al. 2013a), large scale socio-hydrologic modeling coupled with Agent-Based Models (Hu et al. 2015), groundwater hydrogeological modeling (Deman et al. 2016) and in other dynamic modeling examples such as crop modeling (Lamboni et al. 2009) and seawater intrusion (Rajabi et al. 2015). Moreover, an extensive review of basic principles and applications of PCE in computational fluid dynamics was conducted by Najm (2009). PCE has also been used in the geostatistical literature under the term bivariate isofactorial models in the context of disjunctive kriging (Wackernagel 2003). The objective in those applications was to decompose a bivariate distribution into a series of orthogonal polynomials, therefore, finding isofactorial representations which help later to determine recurrence relations between factors (Armstrong and Matheron 1986; Chiles and Delfiner 1999).

There are only a few studies that have employed PCE in spatio-temporal modeling. In one study, PCE was applied for a CA-based lava flow forecasting model to evaluate the model's input parameters (Bilotta et al. 2012). They improved the use of the forecasting model by assessing the impact of measurement errors on the results of simulation and subsequently identified the model's critical parameters. In another study, a PCE-based SA was combined with high-performance computational techniques for a spatially explicit, large-scale socio-hydrological model developed by Hu et al. (2015). The combination of the PCE with high-performance computing made possible the analysis of the effect of spatio-temporal variations of the input parameters on the output of a model even with big multi-dimensional data (Hu et al. 2015). Their result of PCE based variance decomposition helped to identify the influential parameters, quantify their interactions, and prioritize the factors.

C.   *The Polynomial Chaos Expansion Method*

PCE starts with the selection of input parameters where the largest uncertainty is expected, or to which the model is suspected to be most sensitive. The number of selected input parameters is represented by *M*, which determines the dimension of the random variable matrix **X**. The random variables are independently defined based on a probability distribution (e.g. uniform, normal, log-normal, etc.) and the model output Y is defined as $Y = f(X)$. This expansion can be represented by a series of independent random variables and orthogonal polynomials (Wiener 1938):

$$Y = f(\boldsymbol{X}) \approx f_{PC}(\boldsymbol{X}) = \sum_{j=0}^{P-1} \beta_j \psi_j(\boldsymbol{X}) \qquad \textbf{Eq. III-1}$$

where ψ_j denotes the type of the *j*-th (out of *P-1*) orthogonal polynomials, β_j denotes the unknown response coefficient, and *P* is the number of unknown response coefficients (*β)* to be estimated. The variable set *β* is also referred to as the design points and these coefficients are used during the post-processing stage when calculating the results for SA. A **β** matrix is calculated as in Eq. III-2:

$$\left| \begin{matrix} \beta_0 \\ \vdots \\ \beta_P \end{matrix} \right|_{(P,(mxn))} = \left| \left(|A^T|_{(P,N)} |A|_{(N,P)} \right)^{-1} \right|_{(P,P)} * |A^T|_{(P,N)} * |Y|_{(N,(mxn)} \qquad \textbf{Eq. III-2}$$

where (*m*x*n*) is the model output size (*m* = number of columns and *n*= number of rows) for a single run, **A** is the experimental matrix and **Y** is the output matrix coming from *N* model simulations (i.e. the number of runs necessary to solve *β* coefficients). PCE is applied in this work at the local spatial level, which means calculation is done for each pixel independently in matrix **Y**. Following Eq. III-2, SA results depend on the specific model output type, and presumably, they can be different for different model output constituents. Likewise, the order of importance of input factors could vary for different output constituents.

The value selected for *N* (number of model runs) should at least be equal to $k *$ *P where* $k \in [2,3]$ (the selection of *k* is explained in detail in Sudret 2008) where $P =$ $\binom{M+p}{p} = \frac{(M+p)!}{p!M!}$ which means that the number of unknown coefficients to be solved

depends on the number of input variables under interest (M) and the experimental degree of the polynomial (p).

Therefore, to build the meta-model which approximates the full approach and to calculate the estimated mean and variance for U-SA, there are five key steps:

(1) Determining the input parameters and the probability distribution functions for the selected parameters (which also defines the orthogonal polynomials)

(2) Selecting an experimental design degree, p, and calculating the number of unknown response coefficients, P

(3) Forming the experimental matrix, **A** and calculating the unknown response coefficients, **β**

(4) Computing mean and total variance for UA

(5) Computing Sobol indices

1. **Orthogonal Polynomials**

The type of orthogonal polynomials, ψ_j, is derived from the orthogonal bases of input factor probability density functions (PDFs). This affords the reduced dimensionality by taking advantage of the resemblance of weight functions (i.e. inner product vector) to the PDF of certain random distributions (Xiu and Karniadakis 2002). Therefore, depending on the PDF of input parameters, a corresponding orthogonal polynomial scheme is selected for PCE. The most frequently used orthogonal polynomials are Legendre for the uniform and Hermite for the Gaussian (normal) distribution, and these polynomial functions for a 5th degree model are given in Table III-1 (Xiu et al. 2002; Sudret 2014).

Table III-1 Orthogonal Polynomials for Selected Probability Distribution Types
(Sudret 2014)

Distribution Type	Orthogonal Polynomials	First five polynomials
Uniform	Legendre $P_k(x)$	$P_0(x) = 1$ $P_1(x) = x$ $P_2(x) = \dfrac{1}{2}(3x^2 - 1)$ $P_3(x) = \dfrac{1}{2}(5x^3 - 3x)$ $P_4(x) = \dfrac{1}{8}(35x^4 - 30x^2 + 3)$ $P_5(x) = \dfrac{1}{8}(63x^5 - 70x^3 + 15x)$
Gaussian (Normal)	Hermite $H_k(x)$	$H_0(x) = 1$ $H_1(x) = x$ $H_2(x) = x^2 - 1$ $H_3(x) = x^3 - 3x$ $H_4(x) = x^4 - 6x^2 + 3$ $H_5(x) = x^5 - 10x^3 + 15x$

2. **Experimental Design Degree and Expansion Terms**

For a full analytical solution, experimental design degree equals model degree. The difference between full order solution, where P is calculated as $M=p$, and any p value where $p<M$, gives the overall computational gain. Sudret (2008) suggested a two-step strategy starting with a low order expansion degree for factor prioritization, then continuing with a higher order design degree to compute the main sensitivity indices. The relative error between the full analytical solution and its approximation can be obtained by experimenting with different p values (several functional model comparisons are presented in Sudret (2008)). However, increasing p values does not necessarily guarantee that the distribution is well approximated (O'Hagan 2011). Therefore, the PCE approximation results were checked with MC simulation for estimated mean and standard deviation surfaces.

3. **Experimental Matrix and Computation of the Response Coefficients**

After selecting p and calculating N, a random sample set of $\boldsymbol{\xi} = \{\xi_1, \dots, \xi_n\}$ from the

corresponding distribution function of each input parameter $\boldsymbol{X} = \{\xi^{(1)}, \dots, \xi^{(N)}\}$ is generated,

and the model is evaluated for each sample to produce the output $\boldsymbol{Y} = \{Y(\xi^{(1)}), \dots, Y(\xi^{(N)})\}$.

Then, for each pixel, the experimental matrix $\boldsymbol{A}_{ij}$ can be computed using the previously

defined orthogonal polynomials (Table III-1) as follows:

$$\boldsymbol{A}_{ij} = \psi_j(x_n) \quad n = 1, \dots, M, \qquad i = 0, \dots, P-1 \; and \; j = 1, \dots, N$$

$$\boldsymbol{A}_{ij} = \begin{vmatrix} \psi_0(x_1, x_2, x_3, x_4, x_5)^1 & \dots & \psi_{P-1}(x_1 x_2, x_3, x_4, x_5)^1 \\ \vdots & \ddots & \vdots \\ \psi_0(x_1, x_2, x_3, x_4, x_5)^N & \dots & \psi_{P-1}(x_1, x_2, x_3, x_4, x_5)^N \end{vmatrix} \; \text{for M=5}$$

Finally, after calculating $\boldsymbol{A}_{ij}$ and gathering simulation results as $\boldsymbol{Y}$, response coefficients can

be estimated from Eq. III-2. From the first response coefficient, β_0, the estimated mean, $\mu =$

$E\left[\sum_{j=0}^{P-1} f_i \psi_j(\boldsymbol{X})\right]$, can be obtained at almost no additional cost, since $\mu = \beta_0$.

4. **Computation of Sobol Sensitivity Indices for Variance Decomposition**

Sobol's variance-based decomposition (usually referred to as Sobol decomposition)

decomposes the output variance into fractions so that the contribution of each input can be

traced with the first order and total effects (Saltelli et al. 2010). Sensitivity indices derived

from PCE are also referred to as PCE-based Sobol indices (SU) (Sudret 2008). First order SU

and total order SU^T PCE-based Sobol indices can be computed using Eq. III-3 and Eq. III-4.

The first order index represents the main influence of the ith term on the total variance for all

the input parameters from $(i_1, \cdots, i_s)$ set and the SU^T is the influence from higher order

interactions among all the parameters from the integer sequence of $\mathcal{I}_{(j_1,\cdots,j_t)} =$

$\{(i_1,\cdots,i_s),(j_1,\cdots,j_t) \subset (i_1,\cdots,i_s)\}$ (for more details see Sudret, 2008):

$$SU_{i_1,\cdots,i_s} = \sum_{\alpha \in \psi_{i_1,\cdots,i_s}} f_\alpha^2 E[\psi_\alpha^2] \Big/ D_{PC} \qquad \text{Eq. III-3}$$

$$SU_{j_1,\cdots,j_t}^T = \sum_{(i_1,\cdots,i_s)\in\mathcal{I}_{j_1,\cdots j_t}} SU_{i_1,\cdots,i_s} \qquad \text{Eq. III-4}$$

where D_{PC} corresponds to the total variance determined with PCE and can be computed from

Eq. III-5:

$$D_{PC} = Var\left[\sum_{j=0}^{P-1} f_i\psi_j(\boldsymbol{X})\right] = \sum_{j=1}^{P-1} f_i^2 E\left[\psi_j^2(\boldsymbol{X})\right] \qquad \text{Eq. III-5}$$

D. *Application of PCE-based GSA in a Probabilistic CA based UG-LUC Model*

1. SLEUTH Set-up

Santa Barbara, California was selected for the case study due to: (1) availability of data, and

(2) the authors' familiarity with the study site. SLEUTH produces distributed (spatially-

explicit) output for each time step selected in the forecast scenario. UG in SLEUTH takes

place in a three-step cycle: setting up the growth coefficients, applying the growth rules, and

finally evaluating the growth rate. The general function governing SLEUTH simulations can

be written as:

$$y(t) = f(x, \varepsilon, t)$$

where x represents the vector of input variables (input layers), ε is the vector of behavior control parameters (forecast parameters) and t is the time step (each year in time span T). The input vector (x) is composed of an array of size (486x2074) for the Santa Barbara area and kept constant for every simulation. ε is replaced by the **X** quasi random-sample matrix. The forecast period, T, is set from 1999 to 2016 (18 years).

2. **The Uncertainty-Sensitivity Analysis**

Quasi-random sequences produce random numbers but the selected numbers "know" the positions of previously sampled numbers and therefore, they do not form clusters or gaps in the sample space. Since there is no a priori information about the distribution of these parameters, each is assumed to be uniformly distributed. The lower and upper bounds for each parameter are used as ranges for the uniform distribution for quasi-random sample generation. The quasi-random sample matrix is generated based on the ranges in Table III-2. The uniform distribution is also used when selecting the polynomial basis for PCE, which corresponds to Legendre orthogonal polynomials. The samples generated with the quasi-random sampling scheme are normalized to a [-1, 1] uniform distribution interval.

Table III-2 Selected Input Parameters for SA

	Diffusion	Breed	Spread	Slope	Road
Calibrated/Optimum	40	41	100	1	23
Lower Bound	36	36.9	90	0.9	20.7
Upper Bound	44	45.1	110	1.1	25.3

The model is run for *N* times for *(mxn)* pixels and produce the urban growth land use extent for each year of the simulation time frame [t_1...t_T] as output. The model outputs are collected to analyze urban growth and change by comparing the intermediate simulation results. Since the interest is how the forecasted urban growth changes at each time step, the

volume of data required to estimate the Sobol sensitivity indices at each particular pixel at each time step is *T x N*. The variance decomposition is expected to show the influence of forecast parameters on the urban land use output.

3. **Calculation of PCE-based Sobol Sensitivity Indices**

Since there are five forecast parameters (diffusion, breed, spread, slope and road gravity), the degree of the model becomes *M=5*, and if the experimental design degree is selected as *p=3* and take *k=2*, the number of model simulations necessary to solve the unknown coefficients becomes $= k * P = 2 * \frac{(5+3)!}{3!5!} = 112$ yielding the Y output matrix of (112*(486(rows)*2074(columns))) size. Therefore, for PCE based U-SA, 112 runs are enough to calculate the sensitivity indices for the time period (which yields 18*112=2016 model outputs). For a full-order approach, where *p=5*, *N* will be $= k * P = 2 * \frac{(5+5)!}{5!5!} = 504,$ which requires 78% more computations for each pixel. Another comparison can be made for the Monte Carlo based variance-decomposition described by Saltelli et. al. (2010), where the number of simulations required to compute the Sobol indices equals *(k+2) *N* where *k* is the number of uncertain model factors, and *N* is the number of factor samples. *N* is recommended to be large enough (>= 1000) to give reliable estimates for the sensitivity indices. However, large values for *N* are computationally expensive and require more processing memory and time. Even for the number of samples *N*=112 used in PCE-based approximation, at least $N = (5 + 2) * 112 = 784$ simulation samples would be required to perform the full variance-based decomposition described by Saltelli et al. (2010).

Although 112 simulations were found to be enough to conduct PCE-based U-SA, SLEUTH was run 1000 times to have enough runs to compare the PCE approximation with

the sample-based MC simulation for the mean and total variance. After solving the polynomials and calculating coefficients for the five input parameters, the PCE-based Sobol decomposition resulted in the calculation of first, second, third, fourth and fifth order indices, which were summed to yield the total Sobol indices.

E.   *Results and Discussion*

1. **Uncertainty Analysis**

For PCE, 112*18 simulation outputs were used to compute statistical moments of estimated mean, total variance, first order and total order indices. Figure III-2 depicts an example of these outputs for 2016 just showing the urban land use class extent. Starting with the initial land-use layer, the urban extent was calculated from the cumulative result of equally probable growth cycles completed in SLEUTH.
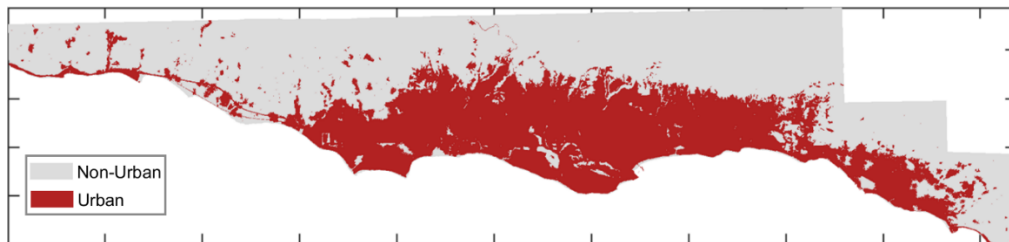
Figure III-2 Forecast Urban Extent for 2016

For the mean value comparison, the first (1999), middle (2008) and the last simulation year (2016) were selected to show the PCE-based estimated mean compared with the mean resulting from 1000 MC model simulations. Figure III-3Figure III-5 show that the estimated mean surfaces, calculated from only 112 model simulations, is a very close approximation to the mean of the 1000 simulations. As can be seen in the difference maps in Figure III-3(bottom) to Figure III-5 (bottom), the maximum value of the difference between

97

the two approaches is 0.4, which is only observable for less than 10% of the urban pixels. Still, the accuracy of the estimated mean can be enhanced by experimenting with different p values for PCE approximation. Increasing p values will require a higher number of model simulations, which results in longer computational time. There is a trade-off between the computational time required to execute 1000 simulations and the desired accuracy of PCE-based approximation of mean and standard deviation, which can be assessed.
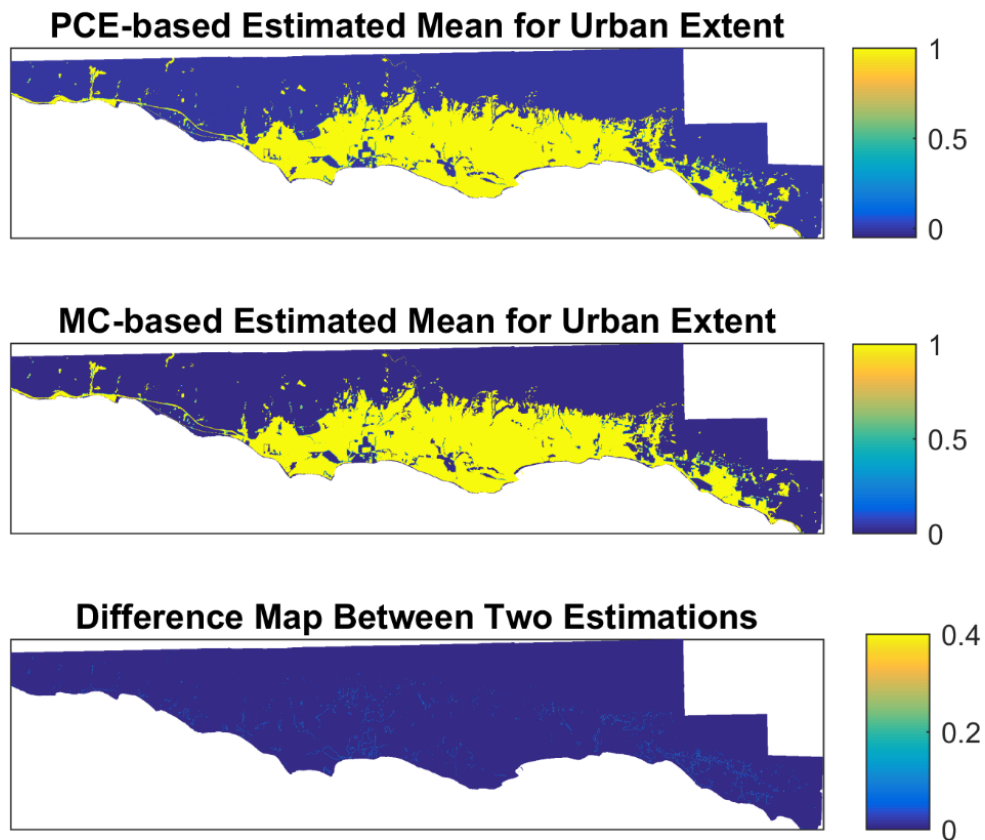
Figure III-3 The estimated means for the probability of a cell to change into urban land use for the year 1999: PCE-based Estimated Mean (top), MC-based Estimated Mean (middle), difference between the PCE-based Estimated and MC-based Estimated Mean Surfaces (bottom)
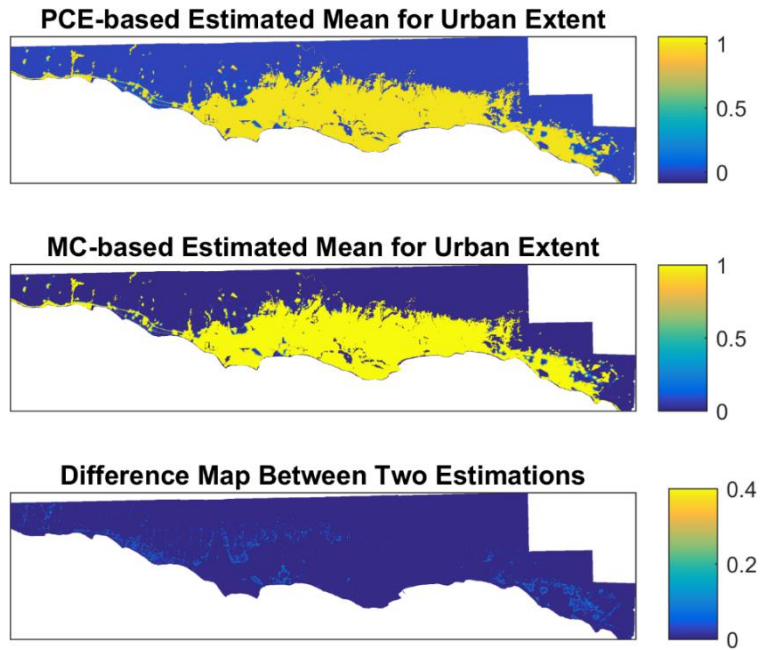
Figure III-4 The estimated means for the probability of a cell to change into urban land use for the year 2008: PCE-based Estimated Mean (top), MC-based Estimated Mean (middle), difference between the PCE-based Estimated and MC-based Estimated Mean Surfaces (bottom)
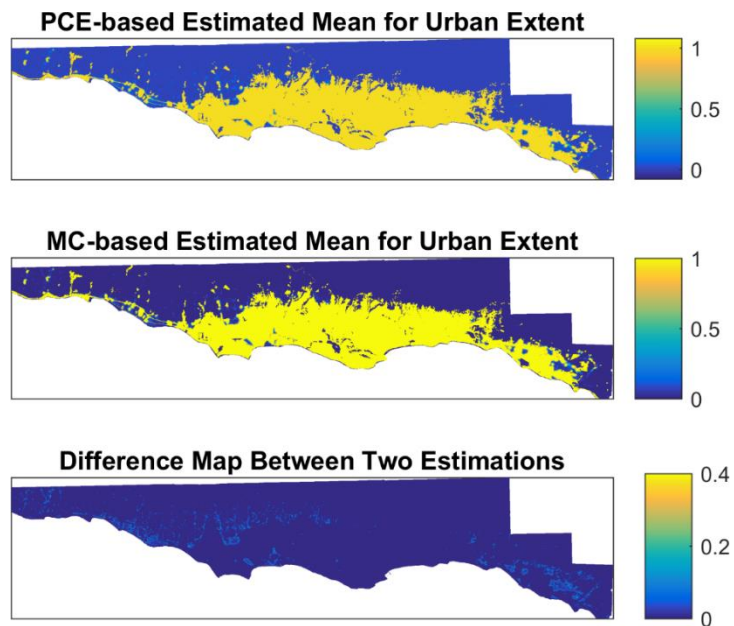
Figure III-5 The estimated means for the probability of a cell to change into urban land use for the year 2016: PCE-based Estimated Mean (top), MC-based Estimated Mean (middle), difference between the PCE-based Estimated and MC-based Estimated Mean Surfaces (bottom)

The comparison can be extended by plotting the model's forecast accuracy over the simulation time interval. For this comparison, the difference between the mean computed with 1000 Monte Carlo samples and the mean obtained with 112 PCE samples was calculated and plotted against the simulation time interval (Figure III-6). The graph shows that the difference between the means is converging throughout the forecast period and ranges from 0 to 0.2. To better understand this difference, one can examine the distribution of pixels comprising the study area. The number of pixels with the observed difference greater than 0.12 is less than 1000 and for the overall urban area, this difference of 1.3% can be considered negligibly small.

Another interesting observation can be drawn from the decreasing pattern of differences. Neither the parameters nor the procedure to calculate the PCE or MC measures differ as the simulation progresses. As expected, the differences occur in places where SLEUTH forecasts a high probability of a cell changing its state to urban. As discussed in the methodology section, PCE estimation is based on the produced output to approximate the model. Therefore, the differences between MC and PCE estimates not only depend on the characteristics of the methods but also on the model output as well.
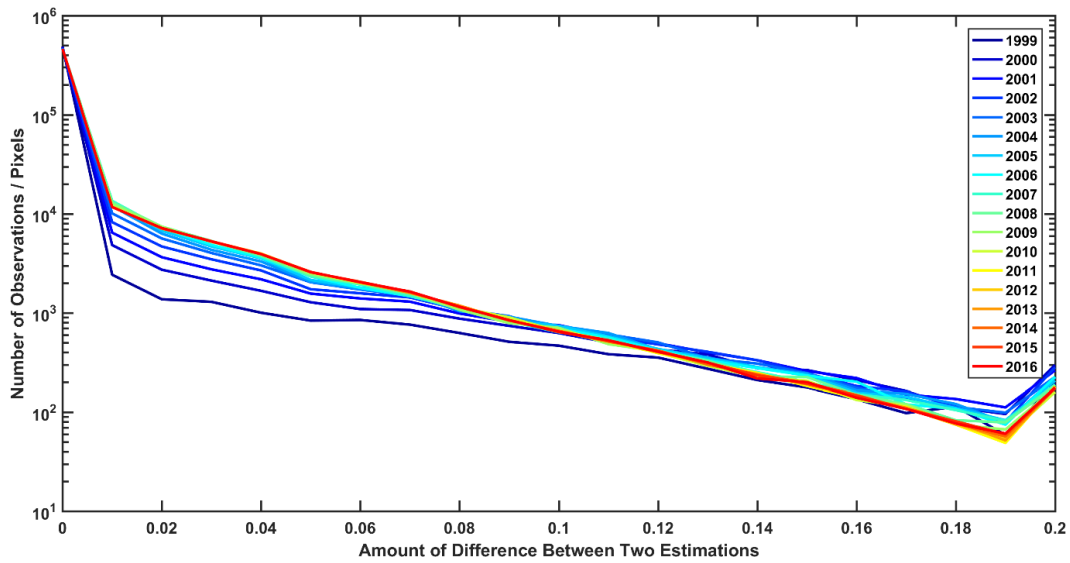
Figure III-6 The comparison of difference between PCE-based estimated mean and MC-based mean

The estimated mean maps are helpful to locate the regions where urban growth is expected to occur. They summarize the forecasting results of all simulations based on the calculated mean for each pixel. Similar to the mean maps, the simulation years 1999, 2008 and 2016 were selected to depict the uncertainty (represented by standard deviation from the mean) resulting from transition parameters (Figure III-7-Figure III-9). The uncertainty maps, showing a similar pattern, can be further investigated in concert with the mean maps.
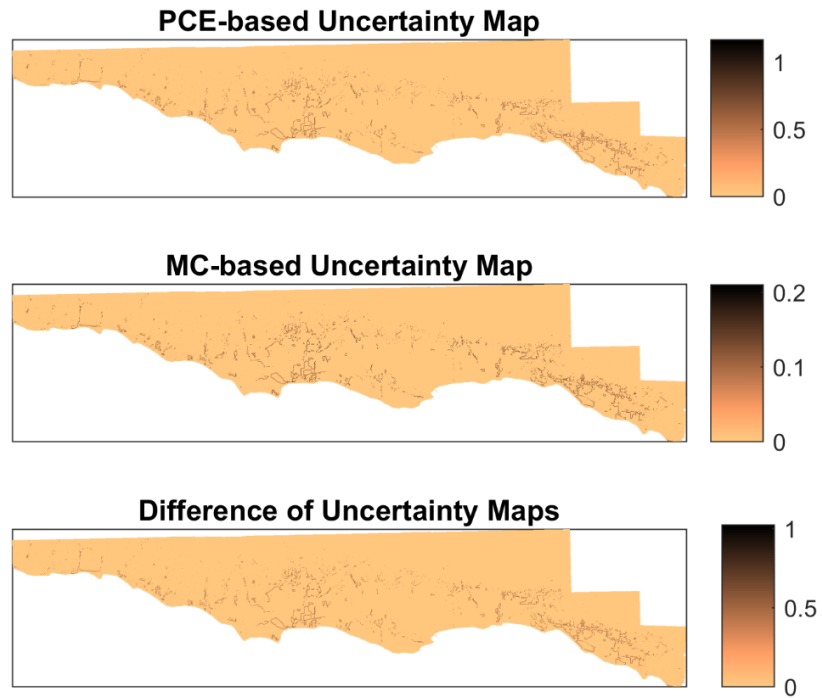
Figure III-7 The standard deviations of the forecasted urban land use change for the year 1999: PCE-based Uncertainty (top), MC-based Uncertainty (middle), difference between the PCE-based and MC-based Uncertainty Surfaces (bottom)
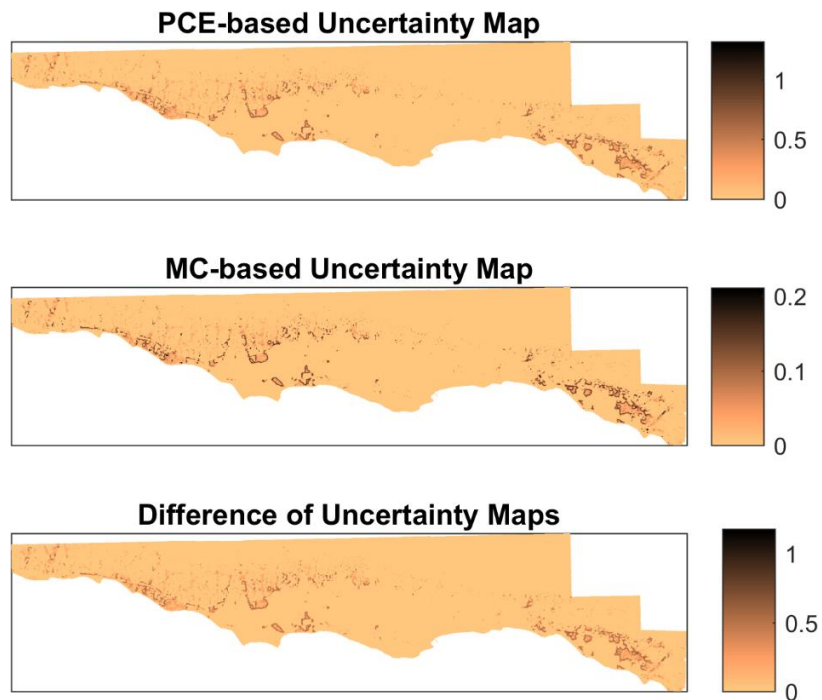
Figure III-8 The standard deviations of the forecasted urban land use change for the year 2008: PCE-based Uncertainty (top), MC-based Uncertainty (middle), difference between the PCE-based and MC-based Uncertainty Surfaces (bottom)
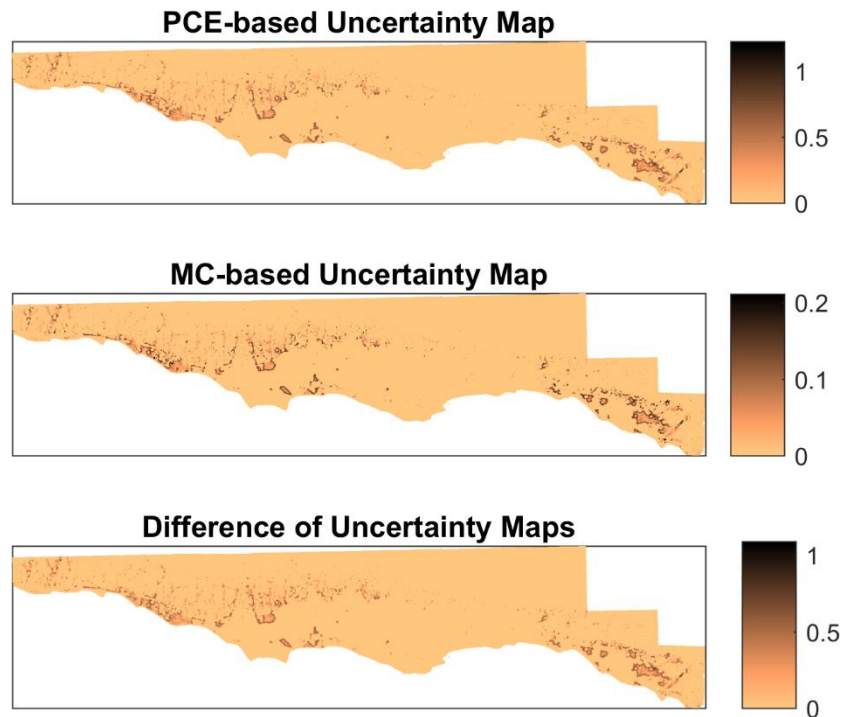
Figure III-9 The standard deviations of the forecasted urban land use for the year 2016: PCE-based Uncertainty (top), MC-based Uncertainty (middle), difference between the PCE-based and MC-based Uncertainty Surfaces (bottom)

In order to categorize the study area based on high/low probability of change to urban land use and high/low uncertainty (standard deviation) of the change, a categorical map can be compiled to show four distinct categories: (1) high probability of changing into the urban class with high uncertainty (HH), (2) high probability of changing into the urban class with low uncertainty (HL), (3) low probability of changing into the urban class with high uncertainty (LH), and (4) low probability of changing into the urban class with low uncertainty (LL) (Ligmann-Zielinska and Jankowski 2014). The thresholds for high/low probability and high/low uncertainty can be selected by examining the logarithmically-scaled histograms of mean probability for land use change (Figure III-10) and standard deviation (Figure III-11) for years 1999, 2008, and 2016. A threshold value of 0.5 was selected for the mean probability (Figure III-10), and the value of 0.5 was selected for the standard deviation

(Figure III-11). The selection is based on the distributions of mean urban land use change probability and standard deviation of the mean urban land use change probability; however, the ultimate selection of thresholds is an arbitrary choice (reflecting the mean value of the frequency distribution) made by the analyst.
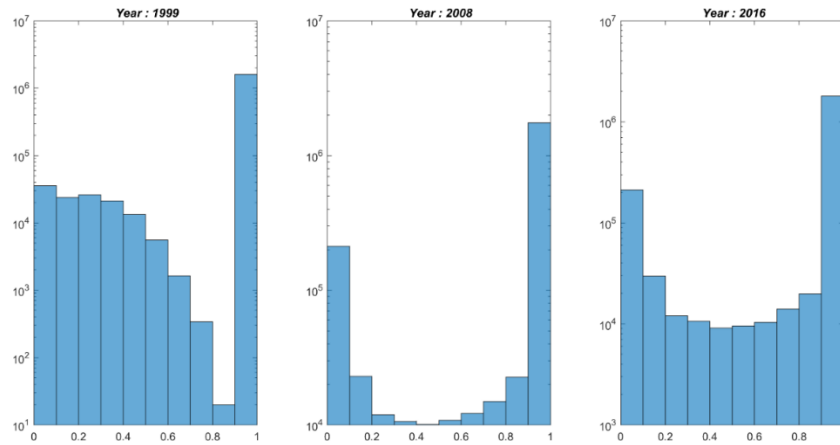
Figure III-10 Mean land use change probabilities for years 1999, 2008 and 2016
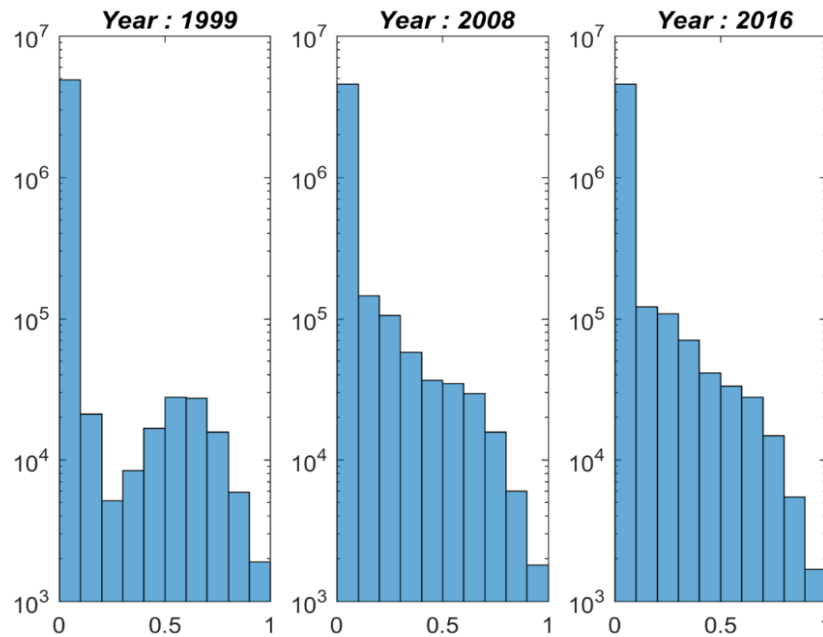
Figure III-11 Standard deviation of mean land use change probability for years 1999, 2008 and 2016

The regions (pixels) falling into the 2nd category (HL) are considered as reliable predictions (low uncertainty) of urban land use change. The regions falling into the 3rd and 4th categories can be discarded due to low confidence in the result (LH) and low probability of land use change (LL). For SA, the analysis continues by investigating the regions in the 1st category (HH) to establish how the relatively high uncertainty in these regions is apportioned to the transition parameters.

After applying the threshold values, categorical maps were produced for three selected simulation years (Figure III-12). The clusters of the high probability of land use change accompanied by high uncertainty are depicted in red and these zones are particularly important when evaluating the results of SA due to the first and total order interactions of transition parameters. An area in the lower-right of the map (Figure III-12) where the HH category seems clustered, was selected for further investigation with SA.
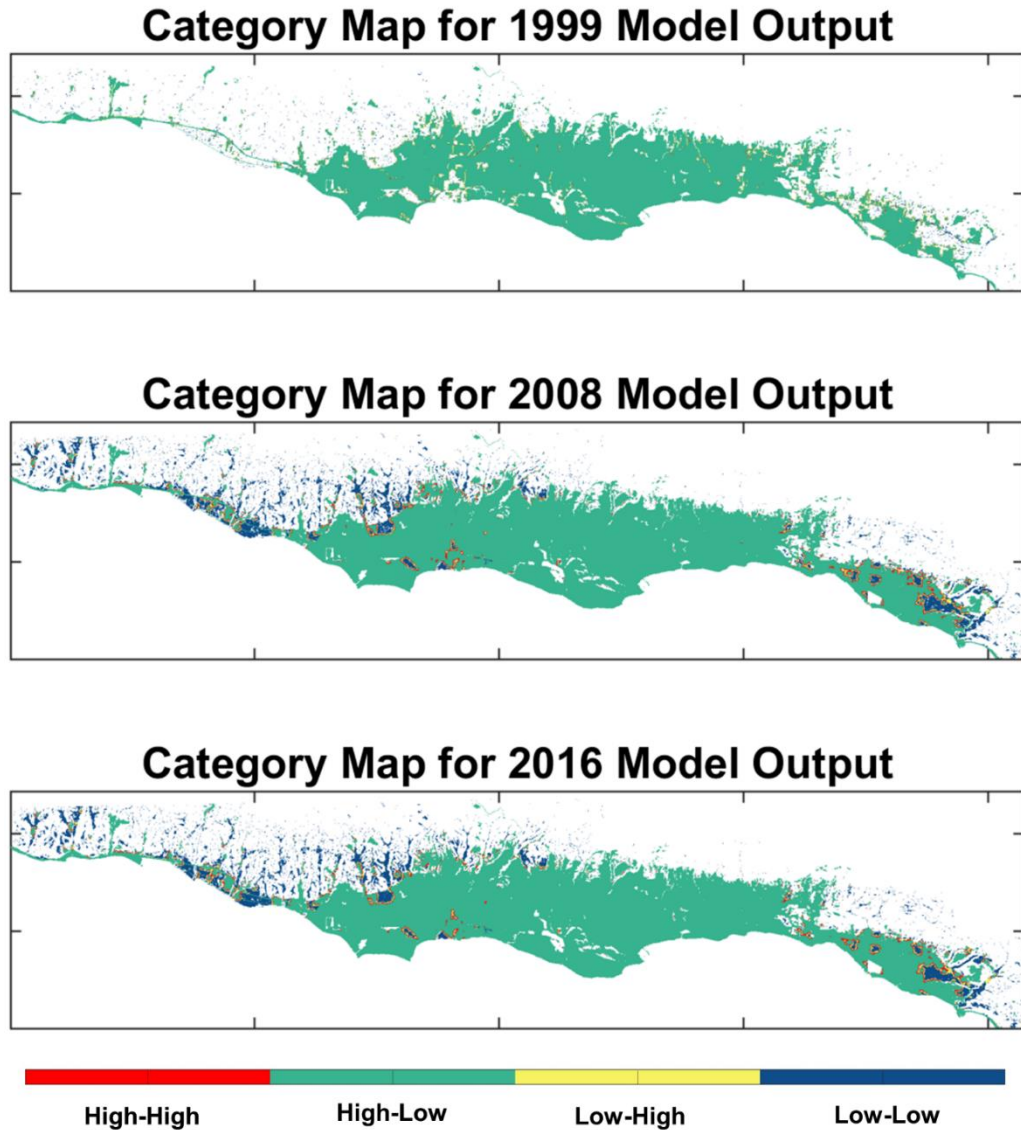
Figure III-12 Categorical maps based on the probability of land use change (High/Low) with the associated uncertainty (High/Low) for years 1999, 2008, and 2016

2. **Sensitivity Analysis**

Sobol first and total order sensitivity indices were computed for the five forecast parameters for each simulation year resulting in 90 maps (5 parameters * 18 years) per each sensitivity index. To reduce the cognitive load of visualizing 90 maps, each sensitivity index is represented by its mean value with the confidence intervals and plotted for the simulation

period for each analyzed parameter (Figure III-13). After having compared these indices,

one can return the produced spatial sensitivity maps for each year for each parameter to see

spatial patterns of sensitivities. For different forecast years, the effect of each input parameter

on the model's output varies. The effect of breed, slope and road parameters is relatively

small (the model is insensitive to these parameters when taken singly or in isolation from one

another) during the simulation time interval. This cannot be said about diffusion and spread

parameters, which show much larger and oscillating influence on the model's output.

Moreover, one can observe that during the forecast period, most of the parameters show a

steady dispersion after 2010. For the simulation period before 2010, diffusion and spread

show a decreasing pattern, whereas breed, slope and road show an increasing pattern.
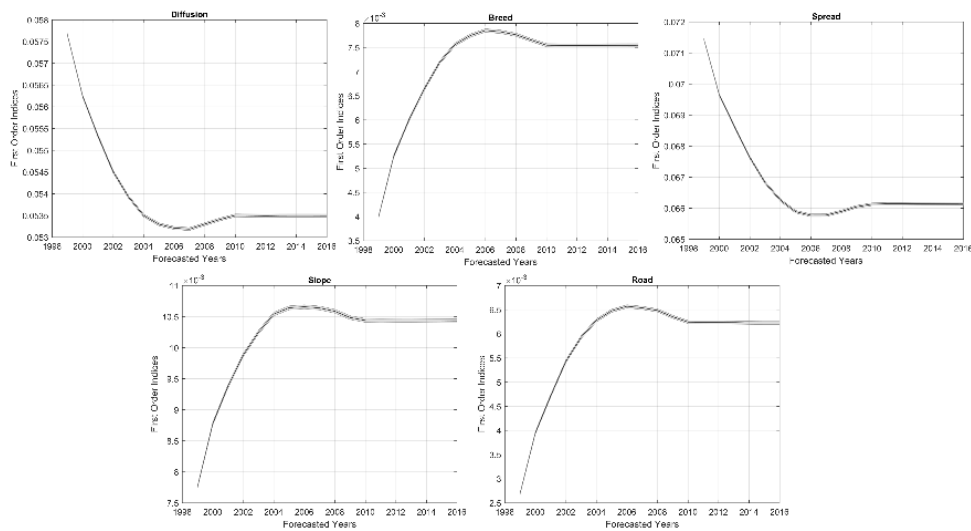
Figure III-13 PCE-based Sobol First Order Indices for years 1999 to 2016

To visualize the interaction among forecast parameters and interaction dynamics,

higher order interactions, calculated as the difference between total order indices and first

order indices, were plotted (Figure III-14). The relatively high values represent high

interactions among the parameters. For the interval 1999 – 2010, the higher order interactions

follow an increasing trend for diffusion, slope and road parameters and a decreasing trend for

the breed and spread parameters. After 2010, there is no change in the level of interactions among the parameters. These graphs show that the sensitivity of slope and road parameters increases as the simulations progress for both SA measures. However, for diffusion, breed and spread, the sensitivity dynamics change between no interaction and interaction measures.
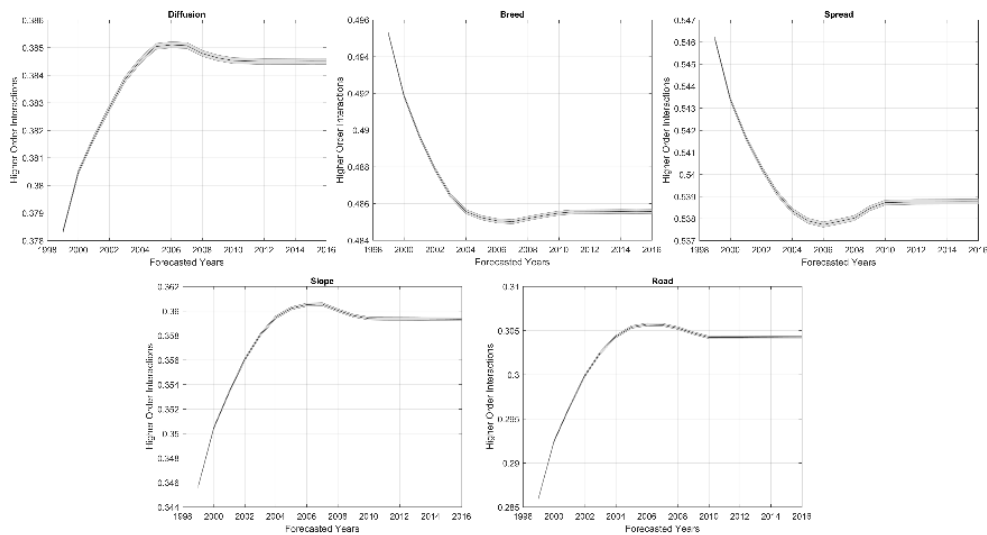
Figure III-14 PCE-based Sobol Higher Order Indices (ST-S) for years 1999 to 2016

In order to understand the spatial pattern of parameter sensitivity, it is the sensitivity maps for a region located in the lower-left of the study area were also examined, where the model prediction has high uncertainty. The reason of this selection is the HH category pixel cluster for this region. The dominant sensitivity indices for years 2005, 2007, and 2010 where the forecast parameters change behavior were mapped (Figure III-15) (Ligmann-Zielinska and Jankowski 2014). Out of five parameters, spread has the major influence on the output variability when the first order indices are considered. For higher order indices, diffusion dominates the other parameters in influencing output variability. Spread is a parameter driving edge growth and diffusion is effective during spontaneous growth and road influenced growth. One possible explanation for the dominance of spread and diffusion is a

cyclical pattern of urbanization driven by edge and road influenced growth. The road

parameter, associated with road influenced growth, is the second single (no interaction) most

influential model parameter after spread (see the First Order Dominance Maps in Figure

III-15).
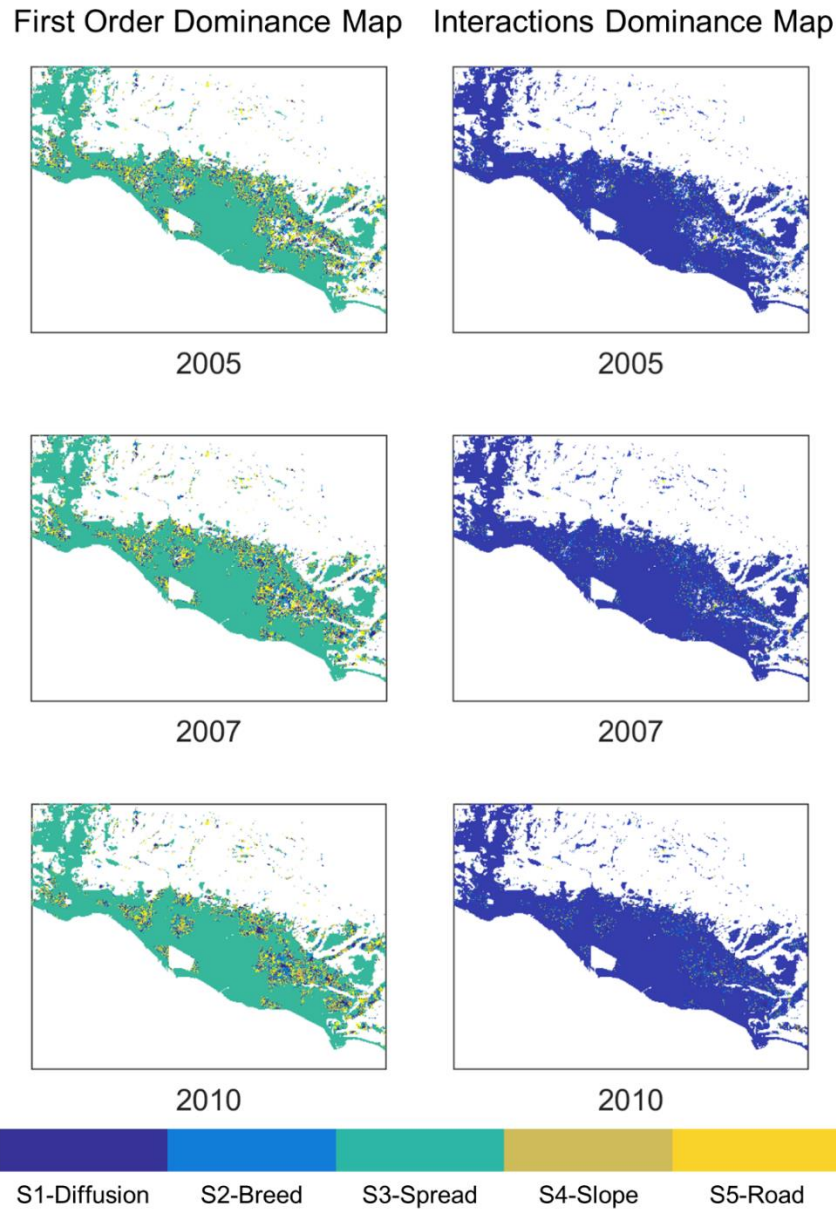
Figure III-15 First Order and Higher Order Dominance Maps for 2005, 2007 and 2010

Following the examination of the sensitivity maps, the contributions of the model parameters to the model output variance can be considered during model calibration, especially considering small perturbations in the value range of input parameters resulting in different levels of model output variance. For the HH zones (high probability of land use change and high uncertainty – Figure III-12), to increase the confidence in the model output, attention must be paid to the diffusion and spread forecast parameters since they have shown the most variability within the simulation time interval.

F.   *Limitations and Future Work*

As discussed in the methodology section, PCE is a model approximation based on design points. Compared with an analytical solution, which includes every high order interaction, PCE approximation only takes into account the subset of interactions defined by the design points. Therefore, the decimal accuracy of the indices may be lower than that for the full order based variance decomposition. However, given the results of tests for various models (Sudret 2008), PCE can be a good guide to prioritize input factors with smaller computational cost compared to full order variance decomposition. For a higher level of accuracy, the experimental design can be reset with higher p values, resulting in higher order polynomials in the expansion.

In addition to sensitivity index accuracy, another limitation of the work presented is the visualization of U-SA outputs for spatio-temporal models. Future research efforts should focus on effective means of visualizing parameter sensitivity both in space and time including the capability of examining spatial patterns for any time period. Additional topics for future research include:

- Further parallelization of the integrated U-SA approach to reduce computation cost for larger datasets.

- Applying the PCE-based Sobol decomposition to a different type of CA neighborhood (Von Neumann) to investigate whether there is a neighborhood effect on the model forecasts.

- Changing the experimental design size (N) and polynomial degree (p) to test the effect of different N and p values on the accuracy of the SA results.

- Comparing the output sensitivity indices of PCE-based Sobol decomposition with Quasi-Monte Carlo based Sobol decomposition to examine the convergence of analysis results obtained with these two model variance decomposition methods.

- Examining in detail the regions with the most and least sensitivity and uncertainty, to test for and explain spatial autocorrelation in the modeling results.

G. Conclusions

SA, especially in its global approach, has received much attention in the research community over the past decade. However, the main challenge lies in the implementation stage due to the increasing amount of data and model complexity. These issues also highlight the problem of computational cost, which is especially high for spatially explicit, integrated U-SA for dynamic models. The proposed meta-modeling approach based on PCE-enabled model variance decomposition is an attractive alternative to conducting U-SA for nonlinear, non-monotonic, and high order spatio-temporal models. The PCE implementation presented in the paper is also valuable in terms of its applicability to any spatio-temporal model due to its model-independent workflow. For high dimensional models with potentially interacting

input parameters that can influence the overall model variability, in particular, PCE can be applied as an initial screening approach to find the most influential variables. This enables further experiments with a smaller subset of model parameters.

IV.   Assessing the Effectiveness of Visualization Techniques for Spatial Sensitivity Analysis

Visualization of sensitivity analysis output in spatially explicit models can potentially enhance the interpretation of uncertainty in model inputs. Yet, it is not obvious which visualization techniques are effective in the context of spatial and spatio-temporal models as the difficulty of selecting an appropriate visualization increases with model complexity and the number of input-output linkages.

This study examines the effectiveness of adjacent and coincident maps depicting the results of global sensitivity analysis applied to a widely used spatio-temporal model of urban growth called SLEUTH. The efficacy of both types of maps is tested for expert and novice end-users with a web-based survey to understand which of the maps is more effective in supporting the comprehension of global sensitivity analysis results. Additionally, the survey results are analysed to determine which map type (adjacent versus coincident) is more effective in gaining user's confidence to discern influential model inputs form non-influential ones, and correctly interpret sensitive locations in a model's study area.

A.   *Introduction*

Many process representations in land-use models are subject to uncertainty, which imposes a limit on the confidence in model output. As a solution to this problem, land-use models' reliability can be assessed by quantifying and representing model output uncertainty followed by a sensitivity analysis (SA). As the end product, reporting the model output uncertainty and its drivers is simply a good modeling practice.

113

As a result of an integrated approach to uncertainty quantification with global sensitivity analysis (GSA), where not only main effects but also interactions between parameters are analysed, several sensitivity maps are produced to depict the contributions of individual model input factors to model output uncertainty and contributions due to their interactions. Precisely, the number of output maps equals twice the number of input parameters under investigation—the sum of individual variances and the variances due to the interactions among the factors (Ligmann-Zielinska and Jankowski 2014; Şalap-Ayça et al. 2018). The choice of appropriate technique(s) for visualizing input parameter sensitivity becomes more challenging with increasing model complexity caused, for example, by the number of model variables, by the degree of interactions or by adding a time dimension to spatial representation.

Although the literature on sensitivity visualization is scarce, the usability of different visualization techniques for depicting uncertainty has been investigated by some scholars (Slocum et al. 2003; MacEachren et al. 2005; Brodlie et al. 2012; Potter et al. 2012; Kinkeldey et al. 2015). Resolving the issue of whether to depict uncertainty in one integrated display or separately (coincident/adjacent) is one of the main questions in investigating techniques applicable to uncertainty visualization. In this research, the question of whether to use integrated or separate displays is extended to model output sensitivity due to uncertain model input parameters.

The separate displays, also called visually separable methods (MacEachren 1992; MacEachren et al. 1998; Viard et al. 2011), is the traditional way of visualizing model output maps, in which individual maps are arranged one next to each other. This approach has been successfully used in several dynamic model applications, including Potter et al (2009) and

Shu et al (2016), to enable interactive explorations for spatiotemporal data analysis. In this representation, no information loss occurs since the output maps are displayed as is (i.e., without aggregation). It is also possible to compare every output map with one another for any given pixel/polygon within the entire study area. However, when the number of parameter increases, the effectiveness of comparison between several juxtaposed maps can be compromised.

In addition to the selection of visualization technique, the issue of the dimensionality of model output plays an important role especially in models with multi-dimensional outputs. For example, for zero or one-dimensional output data, a standard approach such as boxplots, error bars, or glyphs (Brodlie et al. 2012) could be sufficient for depicting only uncertainty whereas for 2-D data a three-dimensional space can be used to represent different levels of uncertainty. However, with more than two dimensions (e.g. attribute + location + time), the visualization of uncertainty becomes more complex. Therefore, most of the visualization techniques attempt to reduce the dimensionality of output by way of producing composite displays. Morgan and Henrion (1990) suggested that each dimension of variation could be aggregated over geographic regions and weighted to obtain an aggregate value effect as a composite representation (Morgan and Henrion 1990).

For a composite representation, which is also referred to as the visually integral method, dominance maps can be used where the maximum value of a sensitivity index at each map location (e.g. a raster cell) is used to represent multiple index values (Ligmann-Zielinska and Jankowski 2014). In other words, based on this approach, the maximum value will be selected as the dominant value and the sensitivity index maps will be aggregated into one single representation. Dominance maps offer data summary that may be helpful for

certain tasks such as getting a general idea about the co-location of sensitive areas and model input parameters or finding places/location clusters that are significantly different from others (Andrienko and Andrienko 2001b). However, as stated by Ligmann-Zielinska and Jankowski (2014), this method is inadequate when the differences between sensitivity index values are small (i.e. approaching zero), obviating the need for more sophisticated visualization techniques.

In the research reported herein, the dominance map concept has been improved upon by adding a parallel coordinates plot (Andrienko and Andrienko 2001a). Parallel coordinates plots make it easier to differentiate the ranking between parameters, thus improving the dominance map. However, for large areas involving high numbers of pixels, the parallel coordinates plot becomes crowded and hard to read. In order to provide the analyst with references in such situations, also the mean value plot line was included in order to show the trend of plot lines representing sensitivity indices for individual pixels. This visualization technique was tested in this research by selecting adjacent representation as the control approach, which is the most popular mapping of SA.

For the temporal dimension, following the aggregating approach, stream graphs were used for spatiotemporal sensitivity visualization. Stream (stacked) graphs display the changes in data over time where the size of the stream shape is proportional to the value in that category (Byron and Wattenberg 2008). The data represented by a stream graph has reference axes, and the graph creates noticeable aspect ratios that can have a significant effect on readability at different levels of detail (Bertin 1983; Cleveland 1993). The most varying parameter is placed on the edges and least varying parameter towards the center. Therefore, the closer a parameter is to the center, the less variability can be observed in the model output.

116

By comparing the adjacent and coincident displays, it is aimed to assess the effectiveness of different visualization techniques in depicting spatial SA results. Both techniques were tested with expert and novice users in order to understand (1) the effectiveness of different visual representations for input factor sensitivity in a land-use model, and (2) the relationship between level of expertise and the choice of preferred visualization technique.

For models where input parameters have higher order interactions, the benefits of GSA over the one-at-a-time approach has been discussed thoroughly in the SA literature. Therefore, for the final research question (3), the extent to which the interaction maps inform the interpretation of land-use model SA results was tested.

Testing the effectiveness of uncertainty and sensitivity visualization is expected to make an improvement in the explanatory power of land-use modeling. As pointedly stated by Richard Hamming, a Turing Award recipient, "*The purpose of computing is insight, not numbers.*" Therefore, in the spirit of improving the communication of numbers, the proposed visualization techniques are expected to contribute to the model-based decision support tools.

In the remainder of the chapter, background information was provided on GSA for urban growth forecasting and visualization techniques for uncertainty and SA. In section three, the web-based questionnaire design was explained including questions and maps used in the questionnaire. Then , in section four, the results from the web survey and discuss findings were presented in section five. The paper concludes with final remarks and recommendations for future work.

B.   *Background*

1.   Global Sensitivity Analysis for Urban Growth Modeling

Simulation models are arguably difficult to validate due to the impossibility of forecasting the future without uncertainty. Van Vliet et al.,(2016) state that validation of a land-change model simply focuses on the performance of the model rather than its underlying forecasting capability. In this sense, SA for a land-use change model is a useful method to access a model's reliability by identifying input factors that contribute to the model's output uncertainty.

Land use change modelling is always shaped by the definition of candidate variables, processes and system boundaries (van Vliet et al. 2016). Cellular automata (CA) models are not an exception to this assertion. Therefore, the input parameters in the CA model that affect the output will most definitely determine the output of the model. In this sense, how sensitive the model is to these parameters is important for determining output confidence. Moreover, in complex systems, where individual model parts can have complex interdependencies, the effects of interactions among the components on the variability of model output have to be studied (Ligmann-Zielinska and Sun 2010; Moreau et al. 2013b; Li et al. 2014b).

Gaining popularity among the methods of SA applied to complex models, GSA addresses both interactions among model inputs and non-linear output response such that the sensitivity of model input factors is not only determined individually (main effects), but also as a result of their interactions (Crosetto et al. 2000; Saltelli et al. 2008; Marrel et al. 2011). Specifically, the model's factor influence on model output variability is represented by first-order (S_i) and total-order (S_T) sensitivity indices.

118

The main effect sensitivity maps, consisting of first-order indices, show the selected single variable's portion of the overall variance. These maps are helpful to visualize the parameter's effect on the model output. They depict how much (magnitude) and where in the study area (location) a small variation in a single input parameter will affect the model output; the greater the value at the given map location, the greater the sensitivity of the model to that parameter.

The interaction maps, consisting of total-order sensitivity indices, show the total contribution of pairs of parameters expressed by a total sensitivity index S_T. For example, the sensitivity index S_{T_1} represents the total contribution of the 1st parameter to the model variance resulting from the parameter's interactions with other model parameters. A low S_1 and high S_{T_1} means that the contribution of the 1st parameter to the overall variability of model output is more due to this parameter interactions with other parameters than to this parameter treated singly.

For this research, the SLEUTH Land Use Change Model (LUC) has been selected as an example of a widely used CA-based land use change simulation model (Clarke et al. 1997). SLEUTH simulates urban growth by using four transition rules, which include spontaneous growth $F_S(\delta, \gamma)$, new spreading center $F_{NS}(\beta, \gamma)$, edge growth $F_E(\chi, \gamma)$ and road influenced growth $F_R(\beta, \rho, \delta, \gamma)$ where, δ symbolizes diffusion, γ slope, β breed, χ spread, and ρ road gravity coefficients given as forecast parameters (Candau et al. 2000). The reliability of SLEUTH simulations depends on these forecast parameters, the model's sensitivity to these input parameters and their interactions. Accounting for higher order effects is especially crucial for spatial-temporal models that do not entirely depend on scalar inputs but are also affected by spatial relationships. Therefore, a robust sensitivity analysis

119

approach accounting for both individual model parameters and their interaction effects is necessary to assess the confidence of model simulation results.

C. *Visualizing Results of Spatially Explicit Global Sensitivity Analysis*

The curse of uncertainty extends to the visualization stage of modeling, as "representing the uncertainty in our representations is an uncertain endeavour" (MacEachren 1992, p.17). The choice of appropriate technique(s) for visualizing model output uncertainty becomes more difficult with increasing model complexity caused, for example, by the number of model variables, or by adding time to spatial representation.

Multivariate data representation is a challenging task which occurs when the attribute space has higher dimension than Cartesian space (e.g. urban growth, land use change, fluid dynamics, climate change, etc.). One solution is to compress/combine the multivariate information in a static(non-spatial) point source representation by using bar chart, pie chart, glyphs, star plots (Spense 2014). A second option is to reduce dimensionality by using scatterplots which can be further extended to scatterplot matrices (Cleveland 1993); parallel coordinates plots where the multiple variables are displayed on parallel axes (Inselberg 1985); or principal component analysis (PCA) where the data is projected to the axes of largest variance (Jolliffe 2002). However, each technique suffers from limitations in usability affected by the number of variables or visual clutter.

Although uncertainty visualization has gained some attention, not much has been done to systematically evaluate the effectiveness of various uncertainty visualization techniques in terms of enhancing the cognition of uncertainty and SA results. The effectiveness of communicating model output uncertainty to decision makers or even

analysts has paramount importance especially for spatial decision-making problems where model results sometimes fail to disclose full information by falsely conveying a sense of certainty and reliability. One can assess the effectiveness of communicating uncertainty, for example, by designing a questionnaire measuring the comprehension of data and information depicted on visuals in a group of randomly or non-randomly selected model users or their proxies (Slocum et al. 2003; Çöltekin et al. 2009). Aerts and his co-authors (2003) used a web-survey of 66 participants to assess the effectiveness of two visualization techniques (static comparison and toggling) for spatial decision-making purposes. The Chi-square test was used to analyse the survey results and compare the two visualization techniques. The results showed some degree of difference in the preferences of novice versus expert users. The static comparison was preferred over toggling by both expert and novice users. The results were also similar to those obtained by Leitner and Buttenfield's (1997; 2000) who found out that representing uncertainty as color lightness, saturation and texture (integrated with certainty information) was more clear to end-users when compared with a complex graphical representation (Leitner and Buttenfield 1997, 2000; Aerts et al. 2003). Sanyal at el., (2009) evaluated four different visualization techniques for one-dimensional and two-dimensional outputs with 36 participants. For analysis, they computed full factorial ANOVA from survey results to assess the effectiveness for different techniques. According to their findings, error bars had the poorest results among the four techniques. They also concluded that the comprehension of uncertainty in 1D model output data (i.e. scalar output) was higher than in 2D counterparts (Sanyal et al. 2009). Bisantz and his co-authors (2011) tested the effect of numeric annotation accompanying information on the probability of category's membership , which is defined by the degree to which the icons were crisp representations

of the category, or were blurred and combined representations, by comparing it with graphical representation (Bisantz et al. 2011). Their experimental design included twelve randomly assigned participants and they analysed the survey results by using a normalized score and chi-square statistic. Their results indicated better outcomes when the participants toggled between numerical and graphical representations than when using only one or the other.

D.   *Web-based Survey Design*

For the SLEUTH modeling, San Diego County - SILVIS data set compiled by Syphard and her co-authors, was used in this study (Syphard et al. 2011). The effectiveness of SA visualizations for UGM was tested in the study, with a meta-modeling framework developed by Salap-Ayca et al (2018). For 5 input forecast parameters (diffusion, breed, spread, slope and road), a set of 252 quasi-random numbers were generated based on a triangular distribution. Then, by using these samples as the input parameter, SLEUTH model simulated the yearly urban growth from 2001 to 2050 yielding 252 x 50 output forecast maps for the fifty-year period. An example output probability map of urban development for San Diego for 2050 has been given in the survey introduction (Figure IV-1). These maps were utilized in the survey.

Figure IV-1 Probability Map of Urban Development for San Diego for year 2050 – Colors indicate the probability of a cell to become urbanized

The survey was published through San Diego State University (SDSU), Department of Geography web host which was active from 25th of April to 12th of June 2018. Participants were recruited by distributing the questionnaire in selected upper division Geography courses. Additionally, students and faculty members via email listservs were contacted. Each participant who accepted the consent form was directed to the first section of the survey, which had an imaginary-case story composed of a brief explanation of the urban growth modeling, the meaning of sensitivity maps, and solicited participant's responses based on the model output maps (Figure IV-2). The participants were also reminded that full confidence in responses was neither a requirement nor an expectation in their answers. In the second section, participants were directed to questions related to the randomly assigned visualization technique. Ethical clearance for the survey was obtained from SDSU Institutional Review Board for Human Subject Research.

123

Visualizing Urban Growth Future Forecast

Imagine you are a city planner for San Diego County and you have been asked to forecast a geographical boundary of the city by 2050. To make your forecast you are using an urban growth model (UGM), which has been used by over 90 cities. However, you have a meticulous boss who wants detailed information about the city's geographical extent forecast. In particular, your boss is interested in the reliability of the forecast and the uncertainty of predicted future urban expansion.

In order to provide your boss with information about the uncertainty of future growth, you have decided to use sensitivity maps compiled by your office colleague. Sensitivity maps can tell you how the model output changes when the model input parameters are changed. The change in the model output can be interpreted as the forecast uncertainty. This means that if the model is more sensitive to an input parameter, any small change in that parameter can alter the model results.

Below you see the example of UGM result map for 2050 (Figure 1). This map shows the probability of a cell to become urbanized in the future (i.e. the pixels in red have 100 to 90% probability to become urbanized in 2050). In order to analyze the sensitivity of input parameters, the model was run for 252 times with randomly generated input parameters to calculate the variation in the outputs. The maps in the next section (Section 2) have been compiled based on these output maps for the selected region inside the black rectangle.

Please select the best possible choice in the upcoming questions. In answering your questions, full confidence is neither a requirement nor expected.

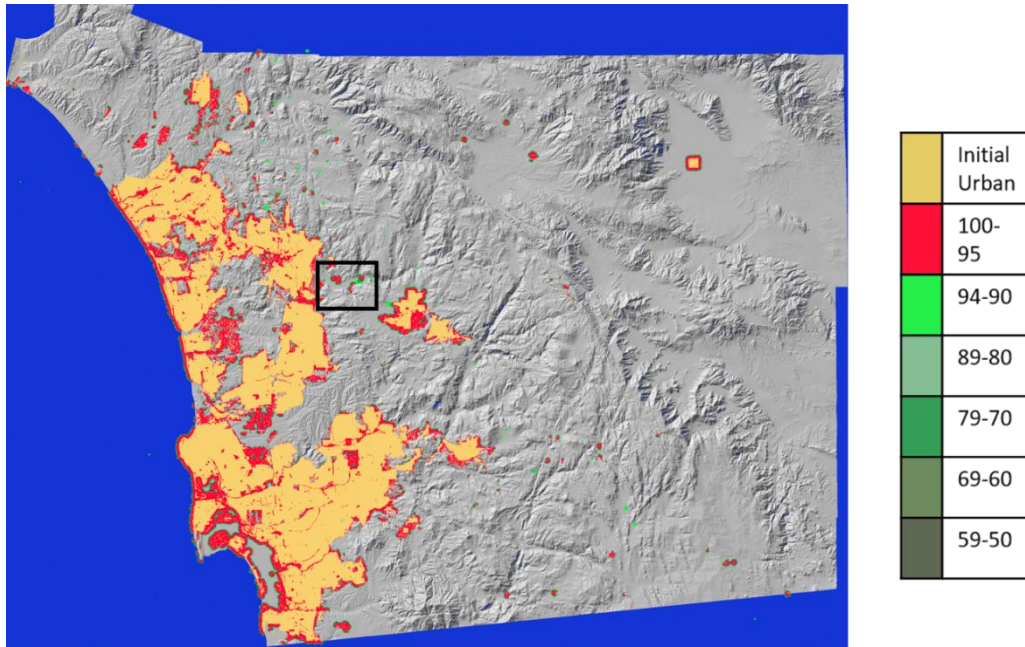|	Initial Urban
(red)	100-95
(green)	94-90
	89-80
	79-70
	69-60
	59-50

Figure 1. Probability Map of Urban Development for San Diego for 2050
*colors indicate the probability of a cell to become urbanized

NEXT   Page 1 of 3

Figure IV-2 Survey Introduction Screen

E.   *Survey Overview*

1.   Participants

65 volunteer participants responded to the survey including undergraduate and graduate

students from Geography departments at SDSU and University of California, Santa Barbara, University of Southern California Engineering graduate students, and participants reached through listservs who were coming from a variety of expert groups including urban planning, map visualization, GIS, environmental management, data analysis and engineering.

After collecting the survey responses, participants were grouped according to the visualization technique (adjacent - control group, and coincident - test group). Assignment of participants to groups was randomly made based on the 50% chance random number generation giving each participant the known probability of selection. Each response was also later grouped based on responder's professional background classifying those with background in urban planning, GIS, and map visualization as experts, and those with background in engineering and others as non-experts.

2. Survey Instrument

All participants were given a set of 12 questions including 10 map-related questions and 2 demographic questions. The first 5 questions in each group were related to spatial sensitivity analysis visualization; only the sensitivity maps resulting from 2050 urban growth forecast output were used in those questions. The fifty-year period sensitivity analysis results were summarized for Question 6 to depict temporal change. Questions 7 to 10 solicited participant's general opinion on the given visualization technique and sensitivity visualization in general. Questions 11 and 12 were about the education level and professional speciality area. Table IV-1 summarizes the questions, variables investigated, and provides the short version of question wordings.

Table IV-1 Survey Measures

Question ID	Variable Name	Question Wording
Q1	DecisionQuality	The most influential parameter selection
Q2	Confidence_1	Confidence in S_3 (the dominating factor of the main effect comparison)
Q3	Confidence_2	Confidence in S_1 (the second highest of the main effect comparison with the highest interaction effect)
Q4	InteractionMaps	Usage of interaction maps
Q5	Importance	Importance of interaction maps
Q6	Confidence_3	Confidence on spatio-temporal main effect
Q7	Confidence_4	Confidence on visualization technique
Q8	Ease	Ease to comprehend
Q9	InfoAcq_1	Complexity of usage
Q10	InfoAcq_2	Helpfulness of the SA visualization

For the main effect sensitivity maps, which show the contribution of single variables to output variability, the five input parameters under investigation are referred to as S_1, S_2, S_3, S_4 and S_5. The higher order indices, which account for the interaction effects and their contribution to output variability are referred to as $S_{T_1}, S_{T_2}, S_{T_3}, S_{T_4}$ and S_{T_5} and depicted on the corresponding maps.

F.   Adjacent Maps with Static Graphs

For the adjacent representation, the main effect sensitivity maps (Figure IV-3) were produced with MATLAB's plotting function to depict the result of 2050 forecast for each model parameter. The maps show sensitivity analysis results for a selected sub-region (the black rectangle area in Figure IV-1) in San Diego County. The background color (gray) indicates

no data values and the color bar shows the range of change the sensitivity values for each parameter. The color selection was intentionally made to increase the contrast to help visualize changes in small pixel clusters. Figure IV-3 and Figure IV-4 are used for questions Q1 to Q5 in adjacent representation group.

When only the main effect sensitivity maps are examined, the ranking of parameters with respect to their contribution to model output variability yields $S_3 > S_1 > S_2$ with two additional parameters regarded as equally important ($S_4 = S_5$) and contributing relatively little to the output variability. Figure IV-4 shows the result of interaction maps for 2050 forecast for each forecast parameter, representing the total contribution of the pairs of parameters expressed by the total sensitivity index S_T. The ranking of parameters with respect to their output variability contribution yields $S_{T_1} > S_{T_5} > S_{T_3} > S_{T_2} > S_{T_4}$. Therefore, when considering the overall variance of a single parameter, S_1 should be interpreted as the most influential parameter for the selected study area.

To represent the model variability change in time, all sensitivity maps for the forecast period (2001-2050) were summarized in a single measure, which is the mean sensitivity index value per simulation year, and the results were plotted on a static X-Y graph. In Figure IV-5, each plot represents one parameter's course of change of sensitivity index value over the simulation time. S_1, S_2, S_4 and S_5 show a relatively similar increase of the influence, whereas the influence of S_3 shows a reverse trend, which means less variability in the model output. Figure IV-5 is used for questions Q6 in adjacent representation group.

127

MAIN EFFECT SENSITIVITY MAPS
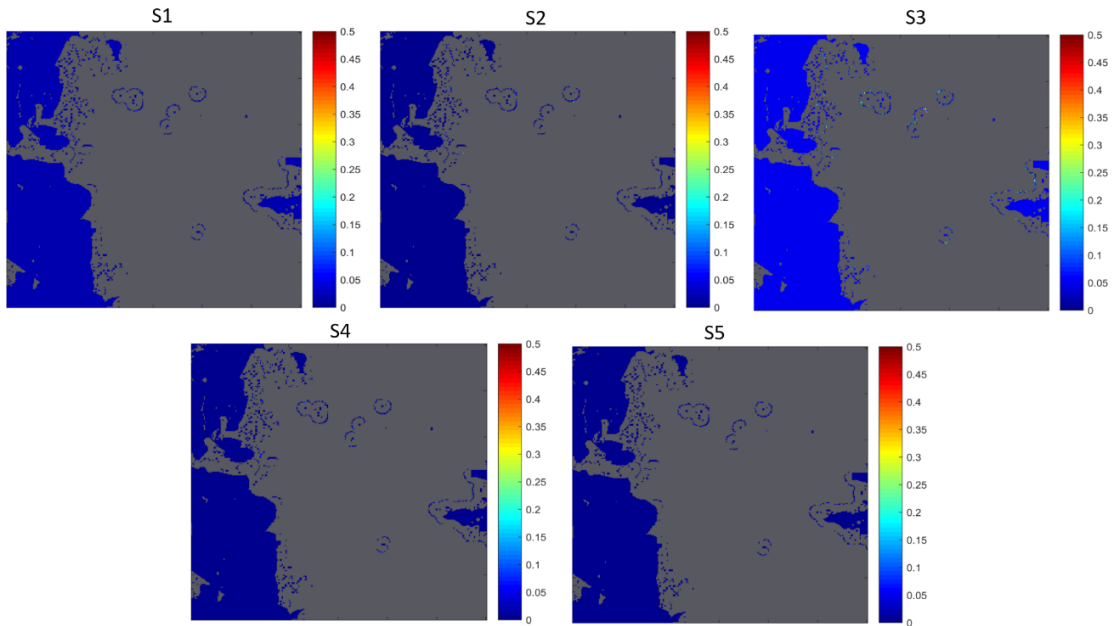
Figure IV-3 Main Effect Maps for Adjacent Representation - the background color (grey) indicates no data values and the color bar shows the range of change in sensitivity values

INTERACTION MAPS
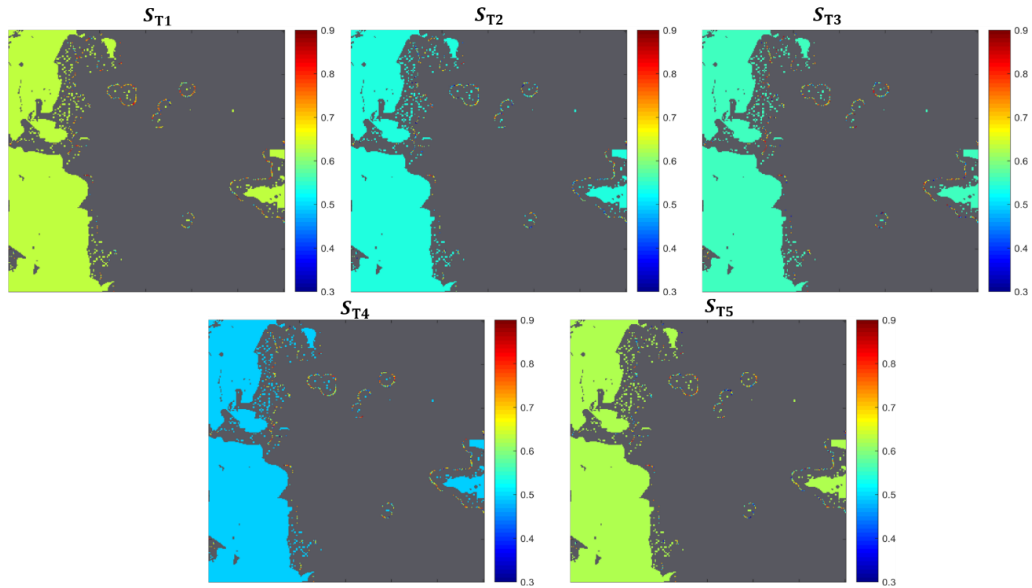
Figure IV-4 Interaction Maps for Adjacent Representation- the background color (grey) indicates no data values and the color bar shows the range of change in sensitivity values
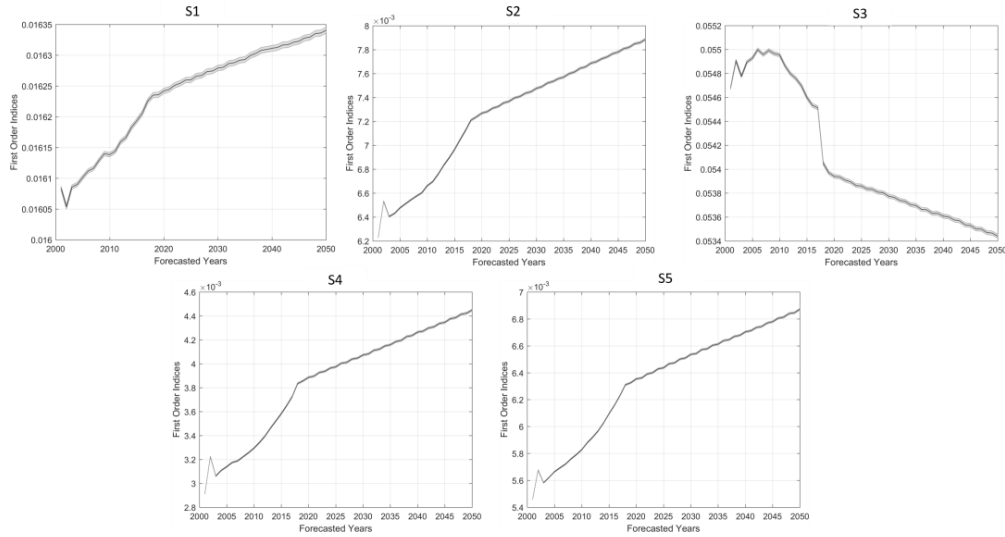
Figure IV-5 Static Graphs for Adjacent Representation

G. *Dominant Map with Stream Graphs*

For the coincident representation of simulation results, the main effect dominance sensitivity maps were arranged to emphasize at each pixel the dominating factor among all five model factors (Figure IV-6). Figure IV-6 is used for questions Q1 to Q5 in coincident representation group. The parallel coordinate graphs, produced with MATLAB's parallel coordinates plot function, show how the sensitivity index values change for each pixel location. The blue lines represent the change in sensitivity values for each pixel and the red line represents the mean of the sensitivity values for each parameter. Although by looking at the main effect dominance map, it is not possible to derive the rank order of model parameters, the parallel coordinates graph shows the general trend in the ranks. The interpretation of the lower part in Figure IV-6, depicting the interaction dominance map, is the same as for the main effect dominance map. The only difference is that it refers to the higher order interaction between parameters.
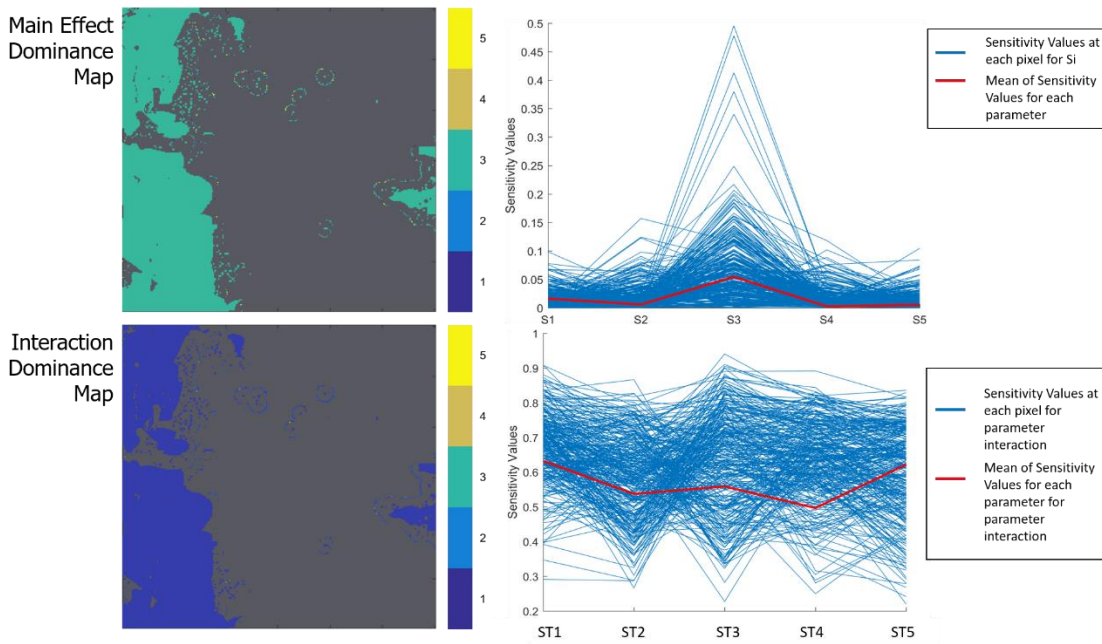
Figure IV-6 Dominant Maps for Coincident Representation

Figure IV-7 is used for question Q6 in coincident representation group. For temporal variability in coincident representation, a stream graph, produced in R with *ggplot2* and *ggTimeSeries* libraries, was used to depict parameter's sensitivity index change over time (Figure IV-7). In order to introduce this visualization technique, a brief explanation about stream graphs was given to the survey participants. The participants were informed that the most varying parameter was placed on the graph's edges and the thickness of the stream corresponded to parameter's value. The increase in the fluctuations of parameter's values is represented by peaks and jagged boundary lines whereas the smooth edges are symptomatic of steady parameter values. Although the axes of the stream graph do not represent the exact measured values, they are used as a reference and the relative rank of the parameters can be established over the simulation time period. Table IV-2 shows the range rank and value rank

of the five parameters. Range rank is used for the placement of the parameter in the graph and it is based on the difference between maximum observed and minimum observed variance. For example, S_3 has 1st rank (highest range among the five) and S_2 has the 2nd rank when the range of variance values are compared, therefore, these two values are placed on the edges of the graph. Value rank is used for a guidance to interpret the thickness in the graph. S_3 has the highest variance value and S_4 has the minimum variance value, therefore, S_3 is the thickest whereas S_4 is the thinnest represented parameter on Figure IV-7 Stream Graph for Temporal Change in Sensitivity ValuesFigure IV-7.

Table IV-2 Stream Graph Orders and Thickness for Parameters

Range Rank (Placement on the Stream)	Value Rank (Thickness in the Stream)
S_3	S_3
S_2	S_1
S_4	S_2
S_5	S_5
S_1	S_4

Stream graphs display the changes in data over time where the size of the stream shape is proportional to the value in that category. The data represented on a stream graph is not exact and axes are used as a reference.
The most varying parameter is placed on the edges, and least varying parameter towards the center. Therefore the closer a parameter is to the center for the time period, the less variability can be observed on the model output.
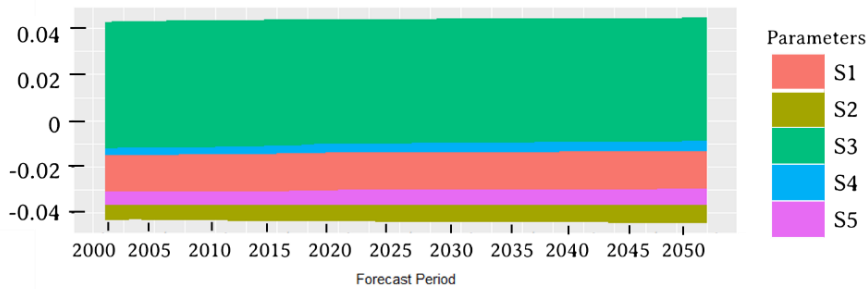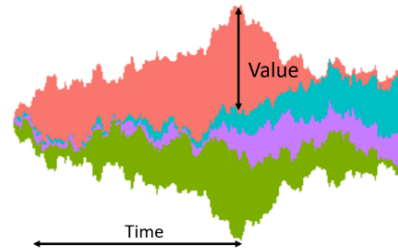
Figure IV-7 Stream Graph for Temporal Change in Sensitivity Values

H.   Results

There was a total of 65 completed survey forms, of which 32 pertained to adjacent and 33 to coincident visualizations. Depending on the answers to two categorical question about educational level (Q11) and professional expertise (Q12), participants were divided into novice and expert categories. The participants who had at least an undergraduate college degree and background in one or a combination of the following disciplines: urban planning, or map visualization, decision support, GIS, environmental management/environmental sciences or statistics/data analytics were considered as experts. Participants with only engineering background or lacking a college degree were designated as novices (Table IV-3). Overall, 48% of participants were classified as expert and 52% as novice users.

The majority of participants had a positive attitude toward sensitivity visualization (Q10, Table IV-1). The results showed that 56% of the participants thought that sensitivity visualization was helpful in interpreting the urban growth model output (Figure IV-8). The

132

differences in responses to Q10, between adjacent and coincident representations (chi square=5.419; p=0.067; Cramer's V=0.289), and expert versus novice respondents (chi square=0.682; p=0.711; Cramer's V=0.102), were statistically non-significant and the association was weak indicating that the positive attitude toward SA was no greater than expected due to chance. For Q10 , the lack of opinion ("not sure" response) was also included in the response choices in order to help respondents who might not wish to appear uninformed or did not have an opinion on the subject (Krosnick and Presser 2010). Among the respondents who did not have a positive attitude toward SA visualization, for both levels of expertise, the selection between a disagreement ("no") and uncertain answer ("not sure") had an almost equal percentage distribution.

Table IV-3 Frequency Table of Categorized Groups (Expertise and Visualization Technique) (N=65)

	Adjacent		Coincident	
	Absolute Number	Percentage	Absolute Number	Percentage
Expert	13	20%	18	28%
Novice	19	29%	15	23%
TOTAL	32		33	
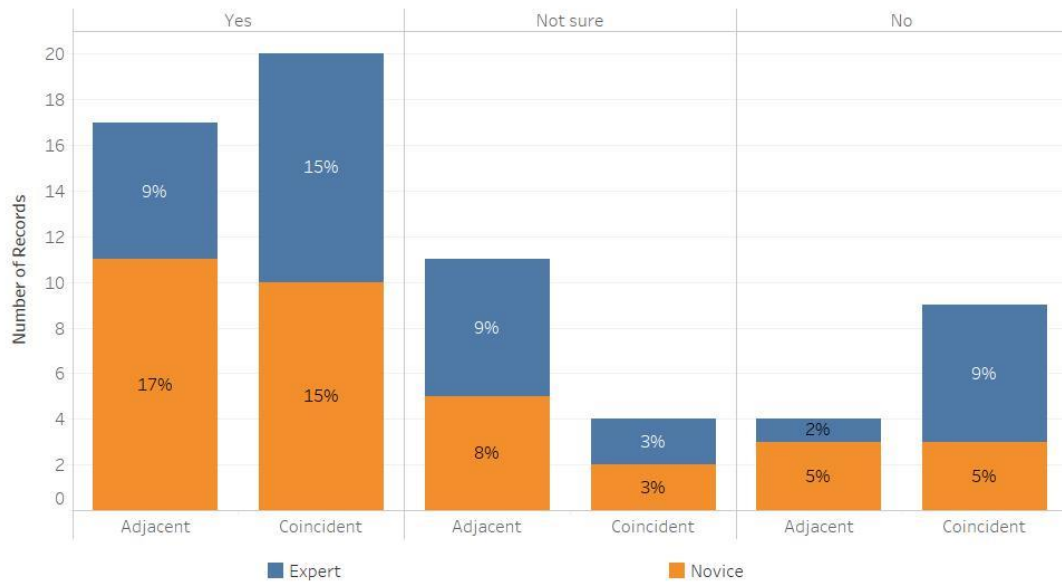
Figure IV-8 Frequencies of the Item: "Sensitivity visualization (Figures 3, 4 and 5 for adjacent and Figures 6 and 7 for coincident) helps in interpreting the urban growth model output" (Q10)

The responses for all of the questions were tested with Shapiro-Wilk Test for normality (Table IV-4) and the distribution of responses significantly deviated from a normal distribution. Given that, skewness and kurtosis of responses for each question also indicated a non-normal distribution, and the dependent variable was not normally distributed, a non-parametric test was selected for the analyses. The Mann-Whitney U Test was used to determine the significance of (1) the dependence of level of expertise (expert versus novice users – independent variables) and (2) the efficacy of both types of visualization (adjacent versus coincident -independent variables) on confidence in SA maps (dependent variables).

Table IV-4 Shapiro-Wilk Statistic for Testing Normality

Group		Shapiro-Wilk				Shapiro-Wilk		
		Statistic	df	Sig.		Statistic	df	Sig.
Q1	Adjacent	0.803	33	0.000	Novice	0.727	31	0.000
	Coincident	0.809	32	0.000	Expert	0.846	34	0.000
Q2	Adjacent	0.911	33	0.011	Novice	0.894	31	0.005

134

	Coincident	0.911	32	0.012	Expert	0.913	34	0.010
Q3	Adjacent	0.852	33	0.000	Novice	0.879	31	0.002
	Coincident	0.906	32	0.009	Expert	0.888	34	0.002
Q4	Adjacent	0.596	33	0.000	Novice	0.619	31	0.000
	Coincident	0.540	32	0.000	Expert	0.498	34	0.000
Q5	Adjacent	0.842	33	0.000	Novice	0.839	31	0.000
	Coincident	0.873	32	0.001	Expert	0.869	34	0.001
Q6	Adjacent	0.900	33	0.005	Novice	0.901	31	0.008
	Coincident	0.886	32	0.003	Expert	0.886	34	0.002
Q7	Adjacent	0.803	33	0.000	Novice	0.790	31	0.000
	Coincident	0.770	32	0.000	Expert	0.799	34	0.000
Q8	Adjacent	0.907	33	0.008	Novice	0.893	31	0.005
	Coincident	0.901	32	0.007	Expert	0.912	34	0.010
Q9	Adjacent	0.902	33	0.006	Novice	0.906	31	0.010
	Coincident	0.904	32	0.008	Expert	0.919	34	0.015
Q10	Adjacent	0.671	33	0.000	Novice	0.745	31	0.000
	Coincident	0.745	32	0.000	Expert	0.686	34	0.000

The relationship between two groups (expert versus novice and adjacent versus coincident) was addressed by using ordinal regression. Additionally, to understand the usage and benefit of GSA, the results of Q1 and Q4 were analysed to determine which representation was more effective in correctly interpreting the sensitivity maps with confidence.

1. Importance of Expertise Level in SA Result Interpretations

The frequency of response categories based on novice versus expert is illustrated in Figure IV-9. These divergence bars represent the level of agreements ranging from disagreement ("Not at all") to complete agreement ("Completely"). Bars starting to the right of center zero-line mark (0%) represent questions that received more positive than negative responses. For example, the most positive response (66%) was received from novice users to Q5. In general, the novice users had more confidence on their answers than the expert users. However, this

difference was statistically not significant when tested with Mann-Whitney U-test (Table IV-5).

Table IV-5 Expert versus novice users: U-statistic, Chi-Square and P values for responses to confidence questions

QuestionID	Significance (U Statistic)	Chi Square	Z	Asymptotic Significance (2-tailed)
Q2	478.5	0.435	-0.66	0.510
Q3	495	0.190	-0.436	0.663
Q5	505	0.088	-0.297	0.766
Q6	476.5	0.462	-0.679	0.497
Q8	461	0.805	-0.897	0.370
Q9	495	0.180	-0.425	0.671
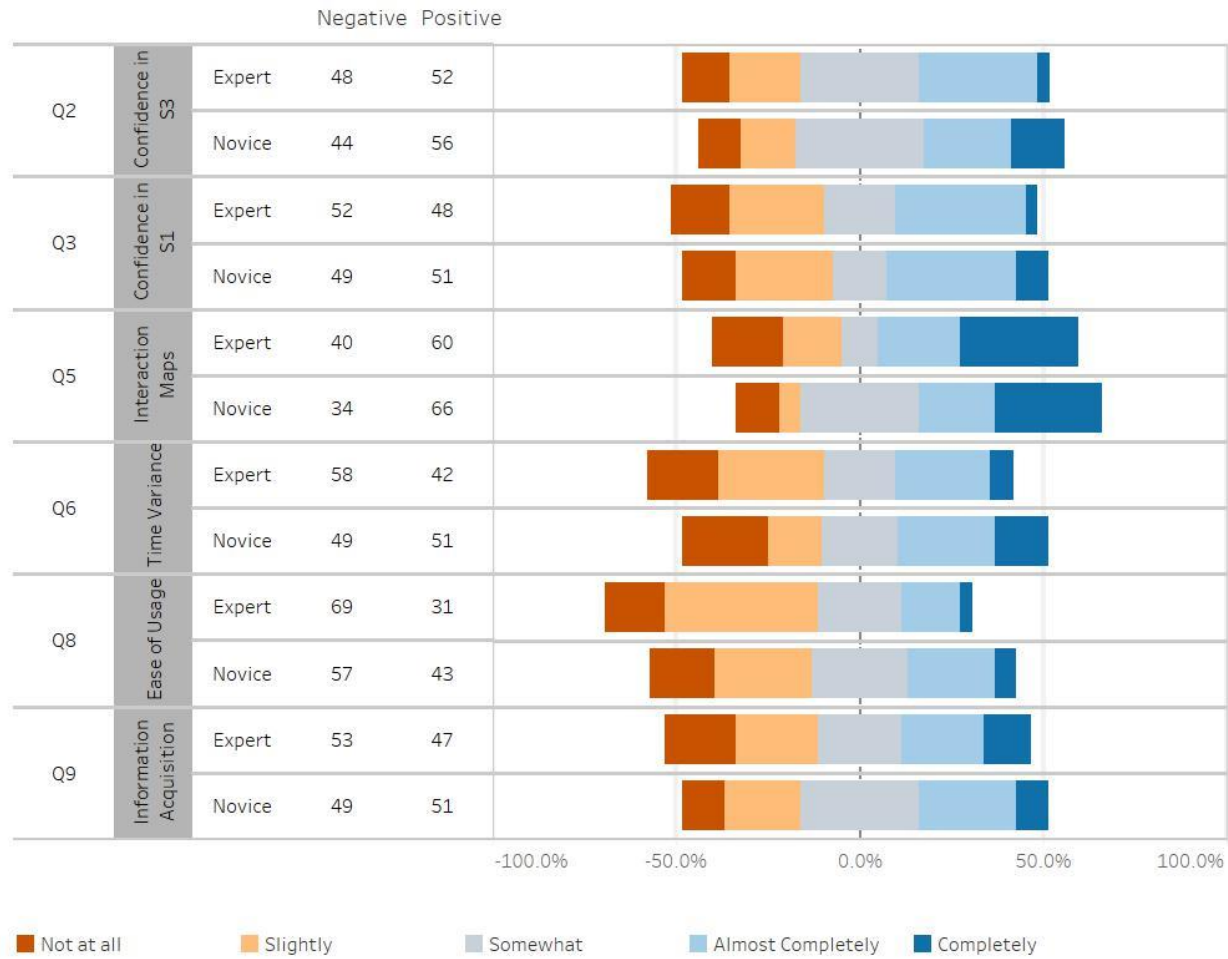
Figure IV-9 Confidence Level Frequencies for Level of Agreement Questions (Expert versus Novice)

137

2. Comparison of Effectiveness of Visualization Techniques

Q7 measures the participants preference for a visualization technique. Almost a quarter of participants assigned the coincident representation (11% of experts and 11% of novices) were uncertain of their preferences for this visualization technique, whereas a similar percentage of participants (9% experts and 14% novices) expressed their preferences for the adjacent visualization (Figure IV-10). However, the difference in preferences for these two visual representations of SA results was not statistically significant (chi square= 4.877; p=0.087; Cramer's V=0.274).
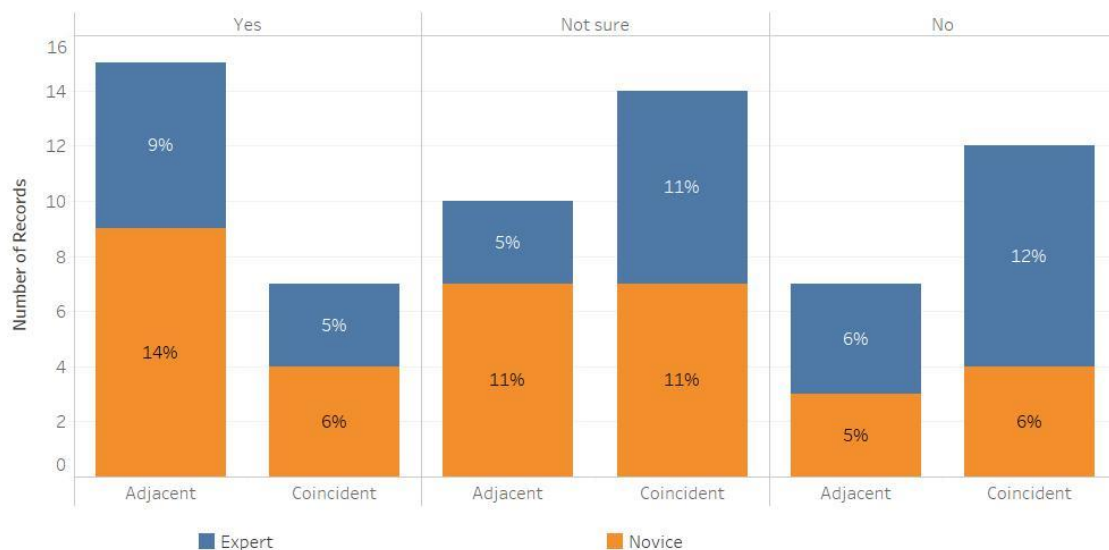
Figure IV-10 Frequencies of response categories to the question: "If you had to explain sensitivity in this urban growth model to other people, would you prefer to use this type of visualization?" (Q7)

A similar frequency distribution of responses based on the dichotomy between adjacent versus coincident representations is illustrated in

Figure IV-11. In responses to Q2, Q3, Q8, and Q9, the participants showed more
confidence in the coincident representation. For Q5 and Q6, the participants had more
confidence in the adjacent representation. The greatest difference in preferences for
adjacent versus coincident representations was in Q9 that asked whether the sensitivity
visualization made the interpretation of model output too difficult and complex to use. The
coincident representation was deemed by 62% of participants as complex and difficult to
use in interpreting the results of SA versus 36% of participants indicating the complexity of
adjacent representation. This difference was statistically significant (p = 0.009, Table IV-6).

**Table IV-6 Adjacent versus coincident representation: U-Statistics, Chi-Square
and P values for responses to confidence questions**

	Mean Rank		Significance (U Statistic)	Chi Square	Z	Asymptotic Significance (2-tailed)
	Adjacent	Coincident				
Q2	31.23	34.71	471.5	0.589	-0.768	0.443
Q3	30.06	35.85	434	1.637	-1/279	0.201
Q5	33.25	32.76	520	0.012	-0.108	0.914
Q6	36.22	29.88	425	1.916	-1.384	0.166
Q8	32.95	33.05	526.5	0	-0.020	0.984
Q9	26.92	38.89	333.5	6.862	-2.62	0.009
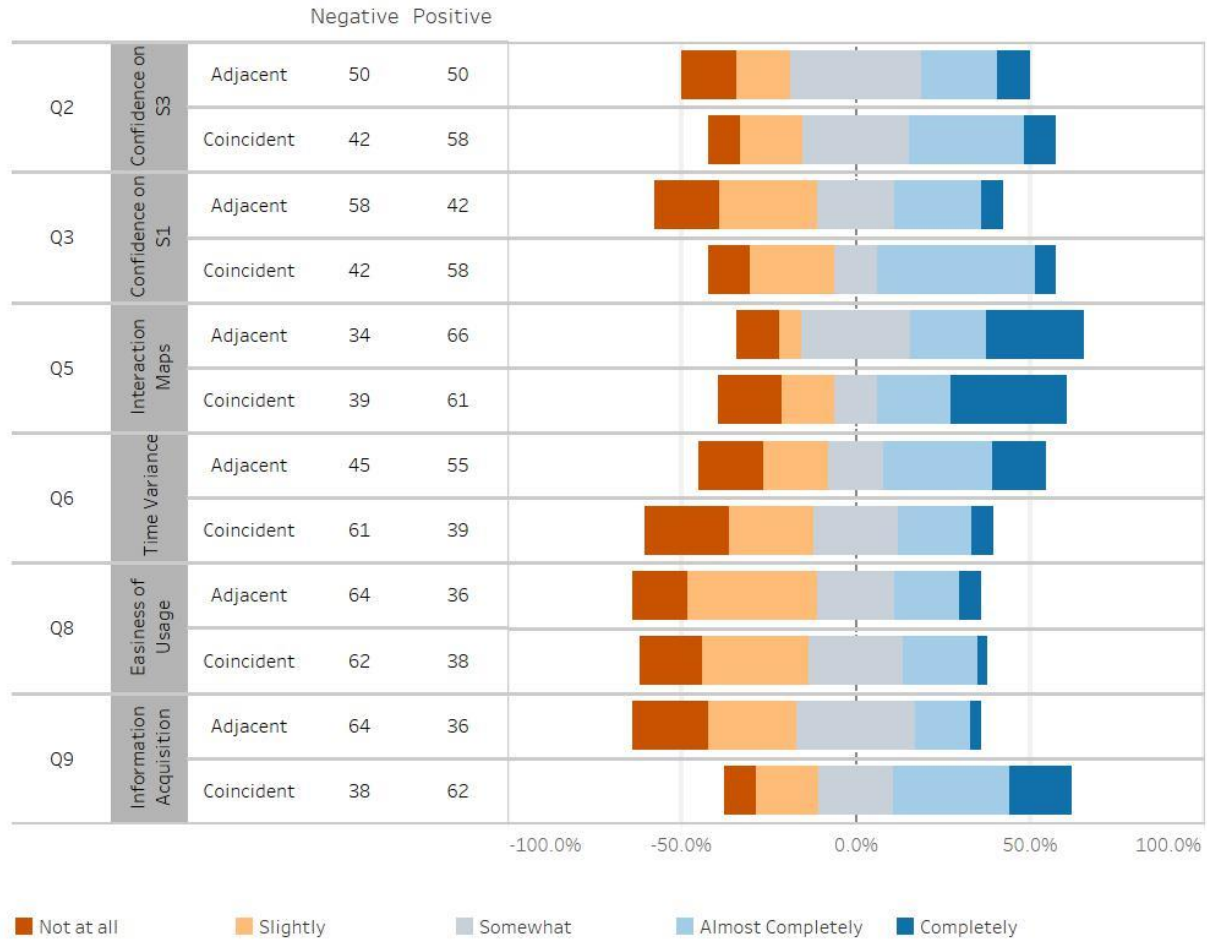
Figure IV-11 Confidence Level Frequencies for Level of Agreement Questions (Adjacent versus Coincident)

3. The Relation Between Two Categorical Variables: Expert versus Novice and Adjacent versus Coincident Representations

In order to examine the form of the relationship between the dependent (confidence in SA map interpretation) and independent (visualization technique and expertise level) variables, an ordinal regression was applied. The resulting statistics are given in Table IV-7 and the significant values are indicated in bold. The base category is represented by adjacent*novice interaction.

Odds ratio column gives the odds of an outcome increase or decrease when the explanatory variables change. For example, for Q9, shifting from adjacent to coincident representation with an increase in expertise level, a 0.42 decrease is expected in the ordered log odds of being in a higher level of confidence.

Model fitting is an estimate to determine whether the regression model improves our ability to predict the confidence in SA interpretation. This is done by comparing the base model against the final model with all explanatory variables. Thus, one can observe whether the final model has significantly improved the data fit. In this study, for all confidence level measures except for the information acquisition (Q9), the final model did not significantly improve over the baseline model (Model Fit values in Table IV-7). However, the goodness of fit was significant indicating that the data and the model predictions were similar, which is a mark of a good model. R^2, given by Nagelkerke statistic, is the coefficient of determination, and larger values indicate more variation in the confidence levels. For example, for Q2, 1.9% of the variance of the confidence level is due to model interaction (Table IV-7).

For the last statistics in Table IV-7, test of parallel lines, the significance values greater than 0.05 mean that there is no difference in location parameters (interaction between two independent variables given in exploratory variable column in Table IV-7 groups) across the response categories.

4.   Interpretation of Interaction Maps

Q1 was analysed using a simple percentage of correct versus incorrect answers. With 65 participants, almost 37% answered the question correctly by selecting S_1 as the most influential model parameter and considering both main and interaction effects (Figure IV-12), which shows that those participants were able to interpret both maps. However, the ability to interpret maps differed by visual representation (44% of correct answers for adjacent versus 30% correct answers for coincident representations), which means that the visualization assignment introduced some difference in terms of map-reading skills. Moreover, there was also some difference in correct answers among the different levels of expertise (25% correct answer from experts versus 12% correct answers from novice).

Figure IV-12 Frequencies of responses to the question: "Which parameter is more influential than the others?" (Q1)

Table IV-7 Ordinal Regression Statistics for Two Independent Variable Interactions

	Variable Name	Exploratory Variable	Estimate	Significance	Odds Ratio	Model Fit	Nagelkerke R^2	GOF	Test of Parallel Lines
Q2	Confidence_1	*Coincident*Expert*	0.44	0.941	1.55	0.751	0.019	**0.788**	**0.711**
		Coincident*Novice	0.361	0.562	1.43				
		Adjacent*Expert	-0.383	0.553	0.68				
Q3	Confidence_2	*Coincident*Expert*	0.338	0.569	1.40	0.557	0.033	**0.564**	**0.441**
		Coincident*Novice	0.649	0.303	1.91				
		Adjacent*Expert	-0.259	0.688	0.77				
Q5	Importance	*Coincident*Expert*	-0.149	0.799	0.86	0.991	0.002	**0.253**	**0.248**
		Coincident*Novice	-0.76	0.901	0.47				
		Adjacent*Expert	-0.186	0.771	0.83				
Q6	Confidence_3	*Coincident*Expert*	-0.775	0.191	0.46	0.348	0.052	**0.268**	**0.159**
		Coincident*Novice	-1.077	0.086	0.34				
		Adjacent*Expert	-0.698	0.279	0.50				
Q8	Easiness	*Coincident*Expert*	-0.347	0.557	0.71	0.683	0.024	**0.633**	**0.501**
		Coincident*Novice	-0.284	0.657	0.75				
		Adjacent*Expert	-0.789	0.227	0.45				
Q9	InfoAcq_1	*Coincident*Expert*	0.857	0.150	2.36	**0.028**	0.136	**0.833**	**0.665**
		Coincident*Novice	1.729	**0.008**	5.64				
		Adjacent*Expert	0.146	0.821	1.16				

Q4 asked about the usage of interaction maps during the interpretation of sensitivity index measures. Figure IV-13 and Figure **IV-14** show the drill-downs by visualization category and expertise level. In Figure IV-13 and Figure **IV-14**, row values 1 ("no") and 3 ("yes") represents the given answers to Q4 and column values corresponds to sensitivity index values for each parameter as 1 (S_1),. 2 (S_2), 3 (S_3), 4 (S_4), and 5 (S_5). For example, in Figure IV-13 the first column and the second row of the figure; the orange color bubble (38%) means that 38% of the participants of adjacent group (32 people), selected 1st parameter, S_1, and used interaction maps.

58% of the experts stated they used the interaction maps, whereas this ratio was 77% for the novice users. Among the 44.6% participants who selected S_3 as the most influential parameter, 41.3 % (12 out of 29) stated that they did not use the interaction maps. This is an expected outcome since S_3 is the obvious choice when only the main effect sensitivity maps are considered. Similarly, out of 70.7% of the participants who used interaction maps, 41.3% (19 out of 46) selected S_1 as the most influential parameter, which means they not only used the interaction maps, but also successfully interpreted the map content.
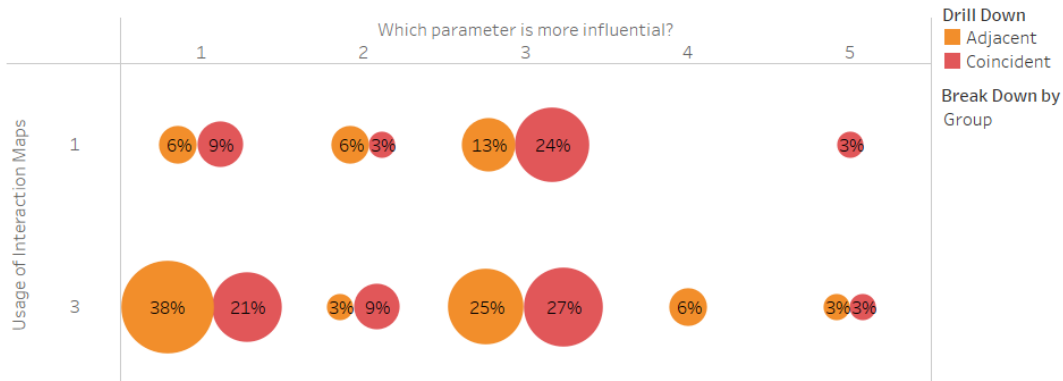
Figure IV-13 Frequencies of responses to the question: "Which parameter is more influential than the others? (Q1) versus Usage of Interaction Maps (Q4) – Break Down by Visualization Technique

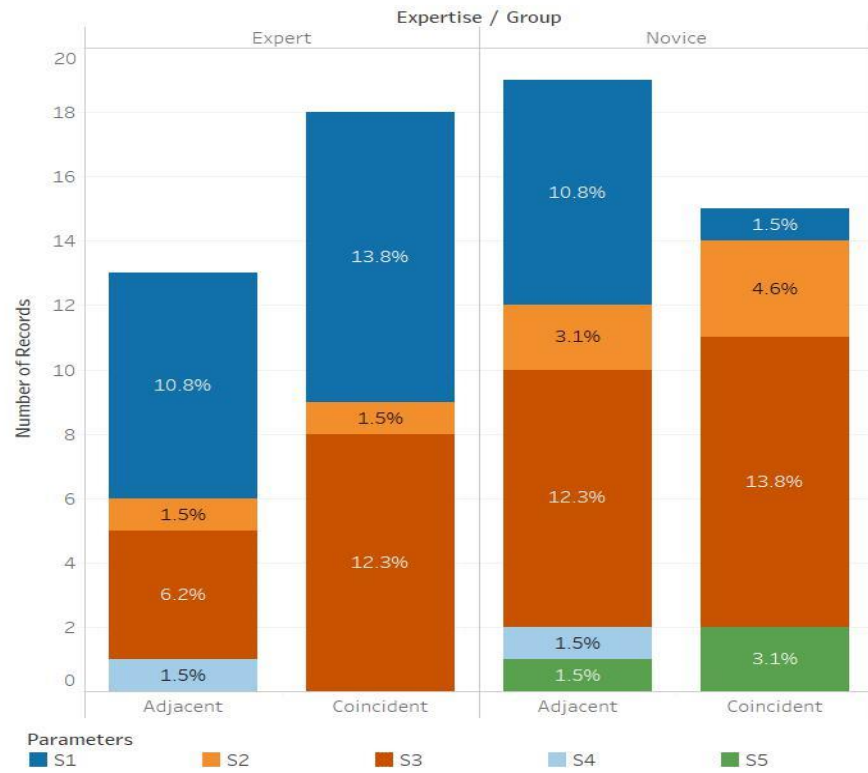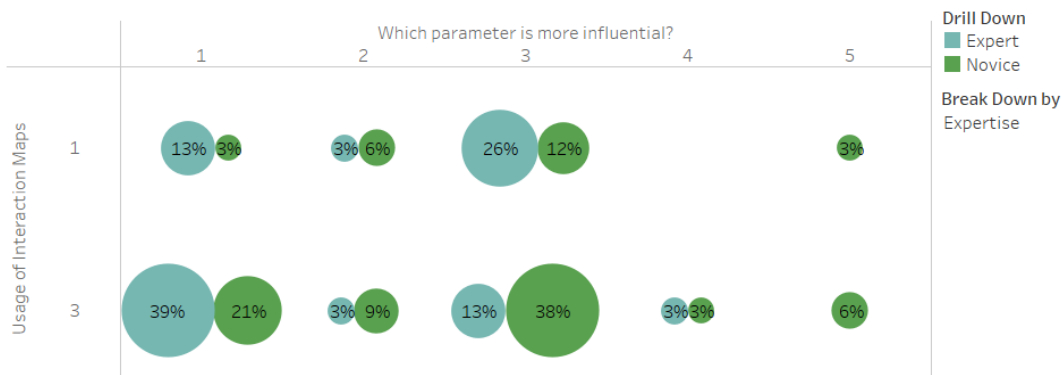**Figure IV-14 Frequencies of responses to the question: "Which parameter is more influential than the others? (Q1) versus Usage of Interaction Maps (Q4) – Break Down by Expertise Level**

I.   *Discussion*

The aim of this study was to assess the effectiveness of different visualization techniques in depicting spatial uncertainty and sensitivity analysis results with the expectation that the participants assigned the composite representation would exhibit more confidence in the analysis results. Overall confidence level frequencies for the level of agreement questions for each group (expert/novice) and for each representation (adjacent/coincident) are illustrated for visual comparison in Figure IV-15. However, for only one of the questions (Q9), a

statistically significant association between visualization technique and agreement on the question was observed.

For the first research question, it was hypothesized that the participants assigned a composite (coincident) representation would exhibit higher confidence in the map interpretation of SA results than the participants assigned a single (adjacent) representation. Based on the survey results, this hypothesis must be rejected. The effectiveness of the selected two visual representations of input factor sensitivity in the land-use model does not significantly differ between composite and adjacent representations. For Q9, which has a negative meaning, the negative answers mean a positive attitude. For example, almost half of the expert users (47.5%) don't agree on the complexity of coincident method (Figure IV-15). This could be interpreted that coincident maps are too complex for novice users despite the intent to synthesize multiple maps into one map.

The different perception between novice and expert users can be explained by visualization concepts introduced by DiBiase (DiBiase 1990) and expanded as cartography cubes by MacEachren and Taylor (MacEachren and Taylor 1994) and MacEachren and Kraak (MacEachren and Kraak 1997, 2001). The commonality in these studies is that they all interpret the importance of visualization as a communication tool to reach the audience and as a support to analysis for private visual thinking (MacEachren and Kraak 2001). For example, when we move from exploratory maps (which are mostly used by scientist and expert) to communication maps (mostly used by stakeholders, students or citizens), the success of communication of visuals mostly depends on the cartographic language used. For this study, although the interaction level was kept at a minimum to embrace larger audience, the relationship with the data might be reconsidered in order to reach the public. It can also

147

be deduced from the survey results that fitting of single visualization tool may not always be possible for all levels of expertise.

In reference to the "*uncertain endeavour*" (MacEachren 1992, p.17), uncertainty or sensitivity information can already be a burden for some end-users, especially novice users. Simple interpretation tasks, which do not involve complex decision making can be carried out with adjacent representation. However, for complex multi-location comparisons, an adjacent map comparison may introduce a cognitive overload (Harrower 2003; Viard et al. 2011). Hence, there is need to create an effective design of coincident representation, different than the one used in this study and cognitively easier for novice users.
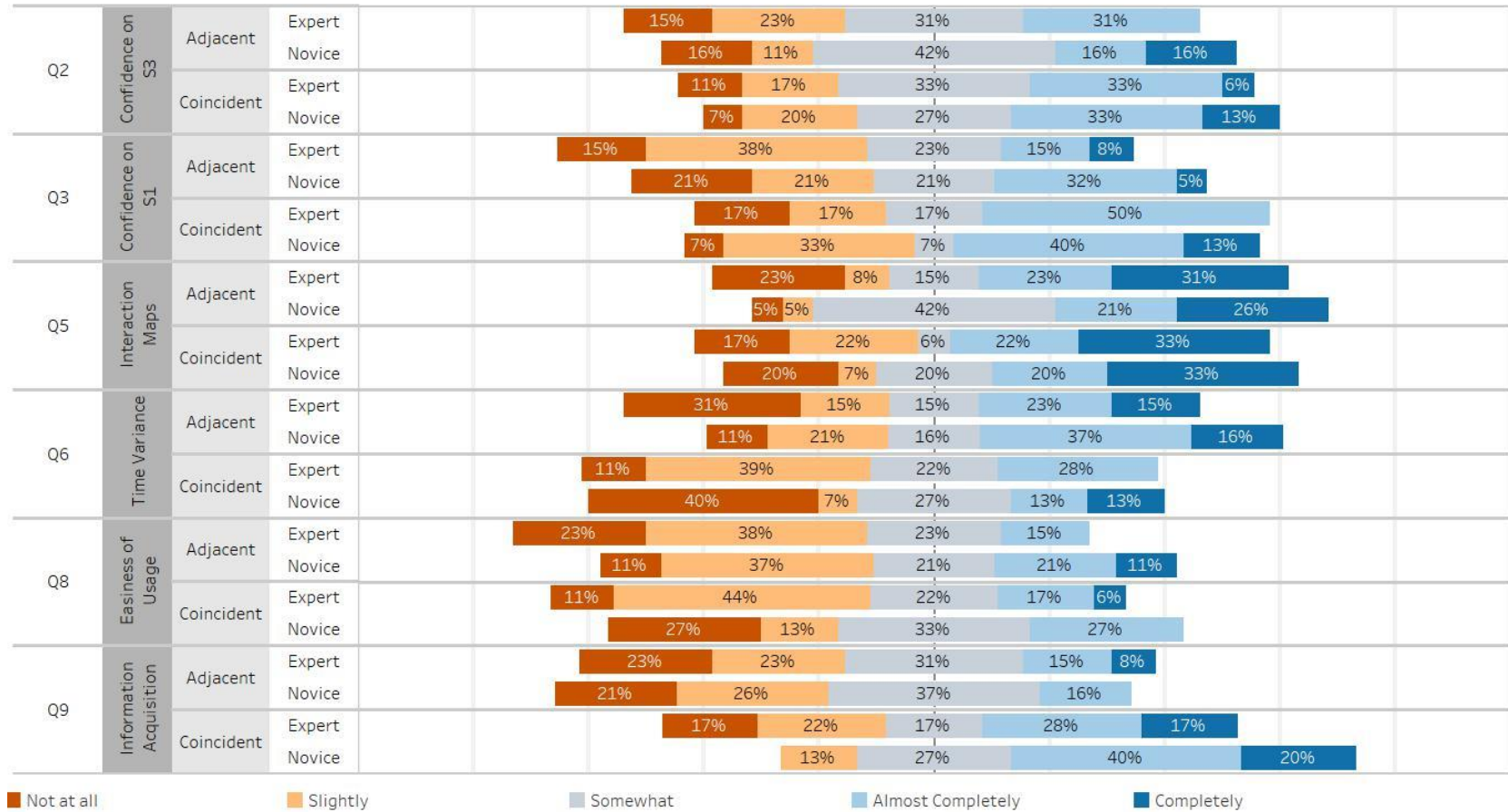
Figure IV-15 Confidence Level Frequencies for the Level of Agreement Questions for Each Group and the Level of Expertise

Analyzing the interaction effect of expertise level and the choice of preferred visualization on the confidence in SA map interpretation (Table IV-7), only the responses to Q9 showed a significant difference between experts and novices in the visualization choice. Since the combination of adjacent/novice was selected as the base line for the regression, depending on the odds ratio, it can be said that the odds of novice user, who chose the coincident representation, achieving a high level of agreement for Q9 are approximately 6 times the odds of novice users who selected the adjacent representation. This means that a novice user is expected to deem a coincident representation as more difficult for SA visualization than an adjacent representation. Considering the skills of novice users, their preference for adjacent representation might be predictable since the adjacent map representation is still most widely used form of spatial visualization in case of several parameters/spatial variables.

In regard to the third research question, it was hypothesized that participants would be using the interaction maps in their interpretation of model output. While for the majority of the survey questions there was no one correct answer, there was an expected correct answer for the first question. Participants who opted for using the interaction maps were also expected to give different answers from the participants who decided not to use interaction maps. The usage and the understanding of interaction maps, which depict the results of global sensitivity analysis, can be inferred from analysing the responses to Q1. When the responses are compared across the groups, the highest rate of correct answers came from experts who used coincident representations. For the adjacent visualization, the expertise level does not seem to affect the rate of correct answers, however, the difference between the correct answer under the use of

coincident versus the use of adjacent representation becomes 10 times more with the higher level of expertise.

46 out of 65 participants stated that they used interaction maps in their interpretation. For the participants who selected S_1 as the most influential factor and stated the use of interaction maps (19 out of 65), the interaction maps proved to be helpful in interpreting the results of SA. However, the majority of the participants who used the interaction maps, could not interpret the SA results correctly. This may be due to interpreting the main effects and interactions of model input factors separately and the difficulty of combining these two sources of information on model sensitivity in the final decision making. One future solution to this problem could be integrating the main and interaction effects, S_1 and S_T , into a single representation.

J.   Future Works and Conclusion

Comprehending land-use practices and their dynamics is quintessential for sustainable use of environment – and this learning process can be assisted by land-use modeling. However, many process representations in land-use models are subject to uncertainty, which imposes a limit on the confidence of the model output. As a solution to this problem, land-use models' reliability can be assessed by quantifying and graphically representing model output uncertainty. Understanding uncertainty sources and how they affect the model outcome is beneficial for: (1) understanding model behavior due to perturbations in input parameters; (2) improving the existing model, and (3) allocating modelling resources by prioritizing model input factors according to the results of sensitivity analysis.

In spatially explicit land-use models (i.e., models with spatially distributed outputs), sensitivity visualization is pursued to enhance the understanding of uncertainty variability, which can enhance model output investigation and eventually lead to a robust decision making.

In most of the decision-making problems, the end-users do not always have to know nor do they care about the details of model output variability due to input factor uncertainties. Yet, they might be open to learning about model output reliability through visualizing maps. Therefore, the maps depicting information about model uncertainty and sensitivity should be simple but informative. Consequently, simplifying visualization forms and making them interactive can be the next step in improving the proposed visual representations for SA mapping.

V.   Conclusion

A.   Summary

Because of the persistent nature of uncertainty and the difficulty of separating the error from the source; models cannot be proven true (Goodchild, 2008). Therefore, it is necessary to be as accurate as possible when assessing the robustness of model inference. The quality of the model is largely a function of its fitness for purpose.

In the first part of the study (Chapter II) concerning a land-use evaluation practice, first a spatially explicit U-SA was introduced for LMCE, particularly for criteria weights, and then the implemented methodology was extended to examine the criteria weights along with scale sensitivity. The findings of the first part show that LMCE provides more heterogeneity compared to global approach, however, raising the question of scale dependency. This question has been addressed in the second part, which showed that both scale and weights play an important role in the results and in the ranking of the decision alternatives. Moreover, the probability distributions for the sample criteria weights have been updated with re-considering the posterior information about EBI factors. This chapter concludes with a number of arguments for why the characterization and treatment of uncertainty is considered to be important in quantitative policy analysis.

Chapter III addressed a framework for meta-modeling and illustrates it with the implementation that uses the capabilities of surrogate modeling for analyzing model uncertainty and sensitivity. Using the example of an urban growth model, the meta-modeling approach significantly reduces computational effort required to carry out spatially explicit U-

SA. This study also brings to light a lot of future work possibilities discussed in the subsequent dissertation sections.

The overarching rationale of this dissertation to develop methods in support of better decision making. Therefore, in the final step (Chapter IV), the effectiveness of the different visualization techniques for SA outputs is examined as a communication tool for decision making. The visualization of SA and user confidence dependency has been examined based on an empirical study of a web-designed survey applied for participants coming from different level of expertise. Although the results did not show a statistically significant difference between compared visual representations, the coincident representation in the form of dominant maps improved the correct answer rate for the expert user group. Also, the survey results showed that the interaction maps do not make a significant improvement in the interpretation of land-use model SA results. The findings of this chapter provide a road map for the future efforts in improving the proposed representation for GSA visualization.

B.   Contribution

1.   Theoretical Knowledge Contribution

The investigation of iU-SA in local MCE for land-use suitability focuses on the effects of parameter uncertainty and scale on model output sensitivity. Unlike global MCE, local MCE explicitly accounts for spatial variability in evaluation criteria within defined neighborhoods (subregions). Moreover, criteria weights in local MCE are also assumed non-stationary and are standardized based on the local extreme values within the neighborhoods. In the implementation of local MCE, the watershed was selected as the spatial analysis unit comprising the neighborhoods. To understand the scale effect of the analysis unit on model

output, a local MCE model for prioritizing candidate land parcels for a conservation program was run at two different watershed levels. The sensitivity of evaluation results to watershed level was investigated in concert with uncertainty of criteria weights using an integrated approach to uncertainty and sensitivity analysis.

The results of this work showed that the iU-SA approach goes beyond the conventional practice of one-at-a-time (OAT) sensitivity analysis by providing spatial uncertainty and sensitivity maps. Moreover, the use of two different granularity levels of neighborhoods used to calculate land parcel suitability showed that it is insightful to examine the effect of scale on the stability of MCE model output. A potential practical value of the presented approach is the improved analytical support for land suitability evaluation requiring an explicit consideration of sub-optimal land units (high suitability/high uncertainty). The research results showed that spatially explicit iU-SA can be successfully applied to test the sensitivity of model output not only to various model input factors but also to various scale representations. The implication of the latter use of sensitivity analysis is our ability to determine whether or not the uncertainty of model output is subject to scaling effects.

The proposed methodology of PCE-based Sobol decomposition is an attractive alternative to conducting computationally expensive GSA based on a full sampling scheme. The implementation proposed in the research is also valuable in terms of applicability to any spatio-temporal model due to its model-independent algorithm. Especially, for high dimensional models with many input factors that can interact and contribute to the overall model variability, PCE can be used as an initial screening approach to find the most influential variables and guide further experiments with a smaller subset of model parameters.

Last but not least, the empirical study on testing the effectiveness of visualization of U-SA made an improvement in the explanatory power of land-use modeling by revealing the user confidence and the limitations of the selected visual representations for different level of expertise.

2. Practical Implications

The main practical implication of an extensive spatial U-SA are for decision makers who need to make decision based on model outputs. The results of spatial U-SA may not only increase the robustness of land-use model, but also help to allocate or direct the resources in case of a need for an expansion beyond the robust areas. Moreover, the output of U-SA can be used for factor prioritization during data collection stage since the influential model input factors are revealed after as the result of analysis.

During this study, the predominant development platforms have been open source Python and R. Additionally, some commercially licensed package programs were used during the visualization or simulation stages (i.e. ArcGIS, MATLAB, SPSS, tableau). Therefore, the implemented scripts can be used by urban planners and distributed freely. In the next step following the dissertation research, I plan to upload the source code to github once the general programmer-readable explanations and annotations in the source code are finished.

C. *Limitations*

Variance decomposition is a powerful approach to gain confidence in model results, as well as a method to analyze partial and interactive effects of model input parameters where uncertainty is expected to occur.

However, the major drawback of variance decomposition-based methods is that a model must be run multiple times for each uncertain input parameter. Moreover, the number of model runs necessary to obtain the satisfactory level of confidence exponentially increases with the number of parameters. For complex spatial models with large input datasets, which are computationally expensive to evaluate even for a single run, the total computational cost increases drastically. As discussed in Chapter III, a meta-modeling approach can significantly reduce computational cost while delivering stable sensitivity estimates and helping to account for the dependence between model output variability and its inputs. Yet, the model simulation is still the most time-consuming computation that can be accelerated with a parallel execution solution.

As the result of Chapter IV shows, the visualization of the multi-attribute sensitivity information is still challenging especially for a novice user. Trying to summarize the several sensitivity index values for a single cell and plotting them in a cartesian space is the most challenging part. In order to solve this issue, multi-attribute information is summarized into a representative statistics (mean) to represent the importance of parameter for the selected location. However, simplicity (or more explicitly dimension reduction) comes at a price because while reducing the dimensionality in order to manage the visualization, the information detail is also lost. Bearing in mind this simplification, the amount of information, which will be depicted can be expanded when desired.

D. *Future Research*

Studies showed that there is a tendency to prefer a certain but possibly less desirable outcome over an uncertain potential of more favorable outcome, which is symptomatic of risk aversion in decision making (Boyle et al. 2012). Therefore, a future research can focus on the

question of how the analysis of uncertainties should account for attitudes towards risk in decision making. A follow-up question might pertain to investigating possible risk/loss of accepting uncertain outcomes – as identified by analysis. In order to illustrate this question, an investigation of land-use evaluation decision making can focus on determining what the financial outcomes might accrue for the decision maker as a result of selecting highly suitable but uncertain land areas. Incorporating in the analysis risk-attitudes towards potential losses can clarify the overall picture for the final decision making. A possible approach can involve estimating risk by considering model output probabilities along with the possible consequences by changing the threshold values, which are used to define suitable areas.

In the near to midterm future, I would also like to extend my meta-modelling approach by experimenting with different design sets to test the efficiency of different design parameters and to see how they affect the accuracy of the sensitivity analysis results. Comparing the output of two different sensitivity analysis approaches (meta-modeling versus full-order analytical solution) to examine the convergence of analysis results is also a necessary step forward to put model predictions in perspective and improve decision making. The applied methodology is based on pixel-level calculation, namely, every sensitivity index is calculated per pixel. A possible next step may include considering the location of a pixel (i.e. neighboring pixels) and including information on spatial heterogeneity in the sensitivity analysis. Following this, other input parameters (i.e. input layers) could be spatially distributed when the simulation is performed in order to observe how the randomness is distributed.

Another future area that I would like to engage in is high-performance computing. A meta-modeling approach reduces the necessary number of model simulations needed for

implementing a spatially explicit approach to uncertainty and sensitivity analysis, however, the framework is still based on simulating model evaluations in response to variability in model parameter values. Especially, if the model under investigation has complex characteristics and is computationally expensive, the overall simulation time will increase rapidly even for a small number of simulations. Therefore, a solution based on parallel executions of the model will decrease the computational time for even complex models. With the increase in complexity and size of the data, the evaluation process for iU-SA becomes more and more computationally expensive due to increasing number of simulations. Therefore, as a future work, I would like to continue to investigate further computational acceleration techniques such as high-performance computing. This approach offers an opportunity to test large datasets and intractable models. I have already conducted a collaborative work on graphical processing units (GPU) implementation as a side projects (Erlacher et al. 2016). In my future research, I would like to continue developing my already established conceptual framework. Distributing the model simulations on different units/cores is possible through various high-performance architectures. High-performance architectures can be achieved with multiple central processing units (CPU), multi-core graphical processing units (GPU), clustered computing using a network of workstations, cloud & grid computing or general-purpose computing. All of these methods have promising performance advantages. GPU, when compared to closed computing architecture counterparts (supercomputers or other parallel computing resources) has the advantages of higher operating performance, higher main memory (off-chip) bandwidth, and efficiency of cost, energy and physical size (Zecena et al. 2013). Therefore, I will first test if General Purpose Graphical Processing Unit (GPGPU) cards provide sufficient speed-ups to reduce

the computational time during MC simulations for iU-SA in spatially explicit simulation models. Then, I will also compare the multi-CPU approach, which offers scalability and elasticity and can be implemented with a cluster of several machines. This is particularly advantageous for starting small and growing whenever the need occurs.

Last, I would also like to improve the already developed visualization technique (i.e., by experimenting with more user-friendly representations for dominance maps). A new method is needed to yield a satisfactory compression of the most important information in the high volumes data streaming from a iU-SA simulation. Along with this new technique, I will plan to develop an introductory level explanation of iU-SA in the form of an animation video in order to make the method more approachable for the end-user.

I expect my research agenda will be helpful to promote model transparency, inform the decision-making in land-use problems, and offer a systematic approach to tracing uncertainty in spatio-temporal models simulating different human-environment systems.

E.   Closure

While Orrell (2007) listed some scenarios about the world of 2100 in his book "The Future of Everything", he said the future forecasts represent only a sample of the known unknowns which are consistent with the forecast models and intergovernmental projections under different economic scenarios. The question to be answered about the future of environment is about the unknown unknowns. In order to demystify the crystal ball, we need to acknowledge that the models we are using are typically sensitive to errors in parameterization, so that our next step towards tomorrow becomes more solid. As stated by

Couclelis (2003), " *…accepting that uncertainty is an intrinsic property of complex knowledge and not just a flaw that needs to be excised*".

For policy making, especially when there is a limited budget, running complex model -even once- will not be feasible nor useful for decision making. Therefore, simplified response surfaces and sensitivity maps with outputs summarized are easier to inform the decision maker than other, complex and hard to understand output representations. To that effect, spatially explicit iU-SA helps to conceptualize some kinds of ignorance by characterizing our degree of uncertainty.

References

Abily M, Bertrand N, Delestre O, et al (2016) Spatial Global Sensitivity Analysis of High Resolution classified topographic data use in 2D urban flood modelling. Environ Model Softw 77:183–195. doi: 10.1016/j.envsoft.2015.12.002

Aerts JCJH, Clarke KC, Keuper AD (2003) Testing popular visualization techniques for representing model uncertainty. Cartogr Geogr Inf Sci 30:249–261. doi: 10.1559/152304003100011180

Alexander ER (1989) Sensitivity Analysis in Complex Decision Models. J Am Plan Assoc 55:323–333. doi: 10.1080/01944368908975419

Andrienko G, Andrienko N (2001a) Exploring spatial data with dominant attribute map and parallel coordinates. Comput Environ Urban Syst 25:5–15. doi: 10.1016/S0198-9715(00)00037-5

Andrienko G, Andrienko N (2001b) Constructing Parallel Coordinates Plot for Problem Solving. Proc Symp Smart Graph 9–14.

Armstrong M, Matheron G (1986) Isofactorial models for granulodensimetric data. Math Geol 18:743–757. doi: 10.1007/BF00899741

Babcock BA, Lakshminarayan PG, Wu J (1997) Targeting Tools for the Purchase of Environmental Amenities. Land Econ 73:325–339.

Berg J (2018) Tomorrow ' s Earth. Science (80-). doi: 10.1126/science.aau5515

Bertin J (1983) Semiology of Graphics: Diagrams, Networks, Maps. University of Wisconsin Press

Bilotta G, Cappello A, Hérault A, et al (2012) Sensitivity analysis of the MAGFLOW Cellular Automaton model for lava flow simulation. Environ Model Softw 35:122–131. doi: 10.1016/j.envsoft.2012.02.015

Bisantz AM, Cao D, Jenkins M, et al (2011) Comparing Uncertainty Visualizations for a Dynamic Decision-Making Task. J Cogn Eng Decis Mak 5:277–293. doi: 10.1177/1555343411415793

Boyle PA, Yu L, Buchman AS, Bennett DA (2012) Risk aversion is associated with decision making among community-based older persons. Front Psychol 3:1–6. doi: 10.3389/fpsyg.2012.00205

Brodlie K, Osorio RA, Lopes A (2012) A Review of Uncertainty in Data Visualization. In:

Expanding the Frontiers of Visual Analytics and Visualization. Springer London, London, pp 81–109

Burnaev E, Panin I, Sudret B (2017) Efficient design of experiments for sensitivity analysis based on polynomial chaos expansions. Ann Math Artif Intell 81:187–207. doi: 10.1007/s10472-017-9542-1

Butler J, Jia J, Dyer J (1997) Theory and Methodology Simulation techniques for the sensitivity analysis of multi-criteria decision models.

Butler J, Olson DL (1999) Comparison of Centroid and Simulation Approaches for Selection. J Multi-Criteria Decis Anal 161:146–161.

Byron L, Wattenberg M (2008) Stacked graphs - Geometry & aesthetics. IEEE Trans Vis Comput Graph 14:1245–1252. doi: 10.1109/TVCG.2008.166

Candau J, Rasmussen S, Clarke KC (2000) A coupled cellular automaton model for land use/land cover dynamics. In: 4th International Conference on Integrating GIS and Environmental Modeling. Banff, Alberta,Canada,

Carter B, Rinner C (2014) Locally weighted linear combination in a vector geographic information system. J Geogr Syst 16:343–361.

Chadwick G (1971) A Systems View of Planning : Towards a Theory of the Urban and Regional Planning Process. Pergamon, London, UK

Chaudhuri G, Clarke KC (2013) The SLEUTH land use change model: A review. Int J Environ Resour Res 1:88–104.

Chen Q, Mynett AE (2003) Effects of cell size and configuration in cellular automata based prey-predator modelling. Simul Model Pract Theory 11:609–625. doi: 10.1016/j.simpat.2003.08.006

Chen Y, Yu J, Khan S (2010) Spatial sensitivity analysis of multi-criteria weights in GIS-based land suitability evaluation. Environ Model Softw 25:1582–1591. doi: 10.1016/j.envsoft.2010.06.001

Chen Y, Yu J, Khan S (2013) The spatial framework for weight sensitivity analysis in AHP-based multi-criteria decision making. Environ Model Softw 48:129–140. doi: 10.1016/j.envsoft.2013.06.010

Chiles JP, Delfiner P (1999) Geostatistics: Modeling Spatial Uncertainty. Wiley, New York

Chu-Agor ML, Muñoz-Carpena R, Kiker G, et al (2011) Exploring vulnerability of coastal

habitats to sea level rise through global sensitivity and uncertainty analyses. Environ Model Softw 26:593–604. doi: 10.1016/j.envsoft.2010.12.003

Claessens L, Schoorl JM, Verburg PH, et al (2009) Modelling interactions and feedback mechanisms between land use change and landscape processes. Agric Ecosyst Environ 129:157–170. doi: 10.1016/j.agee.2008.08.008

Clarke KC (2004) The limits of simplicity: toward geocomputational honesty in urban modeling. Geodynamics 215–232.

Clarke KC (2008) A Decade of Cellular Urban Modeling with SLEUTH: Unresolved Issues and Problems. Plan Support Syst Cities Reg 47–60.

Clarke KC, Gaydos L, Hoppen S (1997) A Self-modifying Cellular Automaton model of historical urbanization in the San Francisco Bay Area. Environ Plan B 24:247–261.

Clarke KC, Gazulis N, Dietzel C, Goldstein NC (2007) A decade of SLEUTHing: lessons learned from applications of a cellular automaton land use change model. Class IJGIS Twenty years Int J Geogr Inf Sci Syst 413–425.

Cleveland WS (1993) Visualizing Data. Hobart Press

Çöltekin A, Heil B, Garlandini S, Fabrikant SI (2009) Evaluating the Effectiveness of Interactive Map Interface Designs: A Case Study Integrating Usability Metrics with Eye-Movement Analysis. Cartogr Geogr Inf Sci 36:5–17. doi: 10.1559/152304009787340197

Couclelis H (1985) Cellular worlds: a framework for modeling micro - macro dynamics. Environ Plan A 17:585–596. doi: 10.1068/a170585

Couclelis H (2003) The Certainty of Uncertainty: GIS and the Limits of Geographic Knowledge. Trans GIS 7:165–175. doi: 10.1111/1467-9671.00138

Crestaux T, Le Maître O, Martinez JM (2009) Polynomial chaos expansion for sensitivity analysis. Reliab Eng Syst Saf 94:1161–1172. doi: 10.1016/j.ress.2008.10.008

Crosetto M, Tarantola S (2001) Uncertainty and sensitivity analysis : tools for GIS-based model implementation. Int J Geogr Inf Sci 15:415–437.

Crosetto M, Tarantola S, Saltelli A (2000) Sensitivity and uncertainty analysis in spatial modelling based on GIS. Agric Ecosyst Environ 81:71–79. doi: 10.1016/S0167-8809(00)00169-9

Cukier RI, Fortuin CM, Shuler K., et al (1973) Study of the sensitivity of coupled reaction

systems to uncertainties in rate coefficients: I Theory. J Chem Phys 59:3873–3878.

Dahal KR, Chow TE (2015) Characterization of neighborhood sensitivity of an irregular cellular automata model of urban growth. Int J Geogr Inf Sci 29:475–497. doi: 10.1080/13658816.2014.987779

de Almeida CM, Batty M, Monteiro AMV, et al (2003) Stochastic cellular automata modeling of urban land use dynamics: Empirical development and estimation. Comput Environ Urban Syst 27:481–509. doi: 10.1016/S0198-9715(02)00042-X

Deman G, Konakli K, Sudret B, et al (2016) Using sparse polynomial chaos expansions for the global sensitivity analysis of groundwater lifetime expectancy in a multi-layered hydrogeological model. Reliab Eng Syst Saf 147:156–169. doi: 10.1016/j.ress.2015.11.005

DiBiase D (1990) Visualization in the Earth Sciences. Earth Miner Sci Bull Coll Earth Miner Sci Pennsylvania State Univ 59:13–18.

Erlacher C, Jankowski P, Blaschke T, et al (2017) A GPU-based parallelization approach to conduct spatially-explicit uncertainty and sensitivity analysis in the application domain of landscape assessment. GI_Forum 44–58. doi: 10.1553/giscience2017

Erlacher C, Şalap-Ayça S, Jankowski P, et al (2016) A GPU-based solution for accelerating spatially-explicit uncertainty- and sensitivity analysis in multi-criteria decision making. In: Proceedings of Spatial Accuracy 2016.

European Commission - IPSC (2008) SimLab 2.2 Reference Manual.

Feick R, Hall B (2004) A method for examining the spatial dimension of multi-criteria weight sensitivity. Int J Geogr Inf Sci 18:815–840. doi: 10.1080/13658810412331280185

Feizizadeh B, Jankowski P, Blaschke T (2014) A GIS based spatially-explicit sensitivity and uncertainty analysis approach for multi-criteria decision analysis. Comput Geosci 64:81–95. doi: 10.1016/j.cageo.2013.11.009

Fischer GW (1995) Range sensitivity of attribute weights in multiattribute value models. Organ Behav Hum Decis Process 62:252–266. doi: 10.1006/obhd.1995.1048

Fisher P (1999) Models of uncertainty in spatial data. In: Longley PA, Goodchild MF, Maguire DJ, Rhind DW (eds) Geographical information systems: Principles and Applications. John Wiley & Sons, Inc, pp 191–205

Foley J a, Defries R, Asner GP, et al (2005) Global consequences of land use. Science 309:570–4. doi: 10.1126/science.1111772

Fotheringham a S, Wong DWS (1991) The modifiable areal unit problem in multivariate statistical analysis. Environ Plan A 23:1025–1044. doi: 10.1068/a231025

Gatelli D, Kucherenko S, Ratto M, Tarantola S (2009) Calculating first-order sensitivity measures: A benchmark of some recent methodologies. Reliab Eng Syst Saf 94:1212–1219. doi: 10.1016/j.ress.2008.03.028

Gómez-Delgado M, Bosque-Sendra J (2004) Sensitivity Analysis in Multicriteria Spatial Decision-Making: A Review. Hum Ecol Risk Assess An Int J 10:1173–1187. doi: 10.1080/10807030490887221

Gómez-Delgado M, Tarantola S (2006) GLOBAL sensitivity analysis, GIS and multi-criteria evaluation for a sustainable planning of a hazardous waste disposal site in Spain. Int J Geogr Inf Sci 20:449–466. doi: 10.1080/13658810600607709

Goodchild M (2008) Imprecision and spatial uncertainty.

Guo J, Trinidad G, Smith N (2000) MOZART: A Multi-Objective Zoning and AggRegation Tool. Proc Philipp Comput Sci Congr 2000 197–201.

Halls JN (2002) A spatial sensitivity analysis of land use characteristics and phosphorus levels in Small Tidal Creek estuaries of North Carolina, USA. J Coast Res 340–351.

Harrower M (2003) Representing uncertainty: Does it help people make better decisions? UCGIS Work Geospatial vVsualization Knoweldge Discov Work 18–20.

Helton JC (1993) Uncertainty and sensitivity analysis techniques for use in performance assessment for radioactive waste disposal. Reliab Eng Syst Saf 42:327–367. doi: 10.1016/0951-8320(93)90097-I

Helton JC, Davis FJ (2002) Illustration of sampling based methods for uncertainty and sensitivity analysis. Risk Anal 22:591–622.

Helton JC, Davis FJ (2003) Latin hypercube sampling and the propagation of uncertainty in analyses of complex systems. Reliab Eng Syst Saf 81:23–69. doi: 10.1016/S0951-8320(03)00058-9

Helton JC, Johnson JD, Sallaberry CJ, Storlie CB (2006) Survey of sampling-based methods for uncertainty and sensitivity analysis. Reliab Eng Syst Saf 91:1175–1209. doi: 10.1016/j.ress.2005.11.017

Herman JD, Kollat JB, Reed PM, Wagener T (2013) From maps to movies: High-resolution time-varying sensitivity analysis for spatially distributed watershed models. Hydrol Earth Syst Sci 17:5109–5125. doi: 10.5194/hess-17-5109-2013

Heuvelink GBM (1989) Propagation of errors in spatial modelling with GIS. Int J Geogr Inf Syst 3:303–322. doi: 10.1080/02693798908941518

Heuvelink GBM (2003) Analysis Uncertainty Propagation in GIS: Why is it not that simple? In: Foody GM, Atkinson PM (eds) Uncertainty in Remote Sensing and GIS. John Wiley & Sons, Ltd, West Sussex, England, pp 155–165

Heuvelink GBM (1998) Uncertainty analysis in environmental modelling under a change of spatial scale. Nutr Cycl Agroecosystems 50:255–264. doi: 10.1023/A:1009700614041

Heuvelink GBM, Burrough PA (2002) Developments in statistical approaches to spatial uncertainty and its propagation. Int J Geogr Inf Sci 16:111–113. doi: 10.1080/13658810110099071

Heuvelink GBM, Burrough PA (1993) Error propagation in cartographic modelling using Boolean logic and continuous classification. Int J Geogr Inf Syst 7:231–246. doi: 10.1080/02693799308901954

Holland J (1999) Emergence : From Chaos to Order. Perseus Book

Homma T, Saltelli A (1996) Importance measures in global sensitivity analysis of nonlinear models. Reliab Eng Syst Saf 52:1–17. doi: 10.1016/0951-8320(96)00002-6

Hu Y, Garcia-Cabrejo O, Cai X, et al (2015) Global sensitivity analysis for large-scale socio-hydrological models using Hadoop. Environ Model Softw 73:231–243. doi: 10.1016/j.envsoft.2015.08.015

Hwang C., Yoon K (1981) Multiple attribute decision making : methods and applications a state-of-art survey. Springer-Verlag, New York

Inselberg A (1985) The plane with parallel coordinates. Vis Comput 1:69–91. doi: 10.1007/BF01898350

Jankowski P (1995) Integrating geographical information systems and multiple criteria decision-making methods. Int J Geogr Inf Syst 9:251–273. doi: 10.1080/02693799508902036

Jankowski P, Andrienko N, Andrienko G (2001) Map-centred exploratory approach to multiple criteria spatial decision making. Int J Geogr Inf Sci 15:101–127. doi:

10.1080/13658810010005525

Jankowski P, Nyerges TL, Smith A, et al (1997) Spatial group choice : a SDSS tool for collaborative spatial decision- making. 11:577–602.

Jantz CA, Goetz SJ (2005) Analysis of scale dependencies in an urban land-use-change model. Int J Geogr Inf Sci 19:217–241. doi: 10.1080/13658810410001713425

Jantz CA, Goetz SJ, Shelley MK (2003) Using the SLEUTH urban growth model to simulate the impacts of future policy scenarios on urban land use in the Baltimore-Washington metropolitan area. Environ Plan B Plan Des 31:251–271. doi: 10.1068/b2983

Jessop A (1999) Entropy in Multiattribute Problems. J Multi-Criteria Decis Anal 70:61–70.

Joerin F, Thériault M, Musy A (2001) Using GIS and outranking multicriteria analysis for land-use suitability assessment. Int J Geogr Inf Sci 15:153–174.

Jolliffe IT (2002) Principal Component Analysis, 2nd edn. Springer-Verlag, New York

Keeney RL (1992) Value-focused thinking: A path to creative decisionmaking. Harvard University Press, Cambridge

Kim JH (2013) Spatiotemporal scale dependency and other sensitivities in dynamic land-use change simulations. Int J Geogr Inf Sci 27:1782–1803. doi: 10.1080/13658816.2013.787145

Kinkeldey C, MacEachren AM, Riveiro M, Schiewe J (2015) Evaluating the effect of visually represented geodata uncertainty on decision-making: systematic review, lessons learned, and recommendations. Cartogr Geogr Inf Sci online fir:1–21. doi: 10.1080/15230406.2015.1089792

Kocabas V, Dragićević S (2006) Assessing cellular automata model behaviour using a sensitivity analysis approach. Comput Environ Urban Syst 30:921–953. doi: 10.1016/j.compenvurbsys.2006.01.001

Krosnick JA, Presser S (2010) Handbook of Survey Research, Second Edition. In: Marsden P V., Wright JD (eds) Second Edi. Emerald Group Publishing Limited, pp 263–314

Kucherenko S, Feil B, Shah N, Mauntz W (2011) The identification of model effective dimensions using global sensitivity analysis. Reliab Eng Syst Saf 96:440–449. doi: 10.1016/j.ress.2010.11.003

Kyriakidis PC, Goodchild MF (2006) On the prediction error variance of three common spatial interpolation schemes. Int J Geogr Inf Sci 20:823–855. doi:

10.1080/13658810600711279

Lamboni M, Makowski D, Lehuger S, et al (2009) Multivariate global sensitivity analysis for dynamic crop models. F Crop Res 113:312–320. doi: 10.1016/j.fcr.2009.06.007

Leitner M, Buttenfield BP (1997) Cartographic Guidelines on the Visualization of Attribute Accuracy. Proc AUTO-CARTO 13 184–194.

Leitner M, Buttenfield BP (2000) Guidelines for the display of attribute certainty. Cartogr Geogr Inf Sci 27:3–14. doi: 10.1559/152304000783548037

Li X, Liu X, Yu L (2014a) A systematic sensitivity analysis of constrained cellular automata model for urban growth simulation based on different transition rules. Int J Geogr Inf Sci 28:1317–1335. doi: 10.1080/13658816.2014.883079

Li X, Liu X, Yu L (2014b) A systematic sensitivity analysis of constrained cellular automata model for urban growth simulation based on different transition rules. Int J Geogr Inf Sci 28:1317–1335. doi: 10.1080/13658816.2014.883079

Ligmann-Zielinska A (2013) Spatially-explicit sensitivity analysis of an agent-based model of land use change. Int J Geogr Inf Sci 27:1764–1781. doi: 10.1080/13658816.2013.782613

Ligmann-zielinska A, Jankowski P (2014) Environmental Modelling & Software Spatially-explicit integrated uncertainty and sensitivity analysis of criteria weights in multicriteria land suitability evaluation. Environ Model Softw 57:235–247. doi: 10.1016/j.envsoft.2014.03.007

Ligmann-Zielinska A, Jankowski P (2008) A Framework for Sensitivity Analysis in Spatial Multiple Criteria Evaluation. In: Cova T, Miller H, Beard K, et al. (eds) Geographic Information Science SE - 14. Springer Berlin Heidelberg, pp 217–233

Ligmann-Zielinska A, Jankowski P (2012) Impact of proximity-adjusted preferences on rank-order stability in geographical multicriteria decision analysis. J Geogr Syst 14:167–187. doi: 10.1007/s10109-010-0140-6

Ligmann-Zielinska A, Jankowski P (2014) Spatially-explicit integrated uncertainty and sensitivity analysis of criteria weights in multicriteria land suitability evaluation. Environ Model Softw 57:235–247. doi: 10.1016/j.envsoft.2014.03.007

Ligmann-Zielinska A, Jankowski P, Watkins J (2012) Spatial Uncertainty and Sensitivity Analysis for Multiple Criteria Land Suitability Evaluation. In: GIScience 2012 : 7th

International Conference on Geographic Information Science. pp 2–5

Ligmann-Zielinska A, Sun L (2010) Applying time-dependent variance-based global sensitivity analysis to represent the dynamics of an agent-based model of land use change. Int J Geogr Inf Sci 24:1829–1850. doi: 10.1080/13658816.2010.490533

Lilburne L, Tarantola S (2009) Sensitivity analysis of spatial models. Int J Geogr Inf Sci 23:151–168. doi: 10.1080/13658810802094995

MacEachren AM (1992) Visualizing uncertain information. Cartogr Perspect 13:10–19. doi: 10.1.1.62.285

MacEachren AM, Brewer CA, Pickle LW (1998) Visualizing georeferenced data: representing reliability of health statistics. Environ Plan A 30:1547–1561. doi: 10.1068/a301547

MacEachren AM, Kraak M-J (2001) Research Challenges in Geovisualization. Cartogr Geogr Inf Sci 28:3–12. doi: 10.1559/152304001782173970

MacEachren AM, Kraak MJ (1997) Exploratory Cartographic Visualisation: Advancing the Agenda. Comput Geosci 23:335–343. doi: 10.1002/9780470979587.ch11

MacEachren AM, Robinson A, Hopper S, et al (2005) Visualizing geospatial information uncertainty: What we know and what we need to know. Cartogr Geogr Inf Sci 32:139–160. doi: 10.1559/1523040054738936

MacEachren AM, Taylor D (eds) (1994) Visualization in Modern Cartography, 1st edn. Pergamon, London, UK

Malczewski J (2000) On the use of weighted liner combination method in raster GIS: common and best practice approaches. Trans GIS 1:5–22.

Malczewski J (2004) GIS-based land-use suitability analysis: a critical overview. Prog Plann 62:3–65. doi: 10.1016/j.progress.2003.09.002

Malczewski J (2011) Local Weighted Linear Combination. Trans GIS 15:439–455. doi: 10.1111/j.1467-9671.2011.01275.x

Malczewski J (2006) GIS-based multicriteria decision analysis: a survey of the literature. Int J Geogr Inf Sci 20:703–726. doi: 10.1080/13658810600661508

Malczewski J, Liu X (2014) Local ordered weighted averaging in GIS-based multicriteria analysis. Ann GIS 20:117–129. doi: 10.1080/19475683.2014.904439

Malczewski J, Rinner C (2005) Exploring multicriteria decision strategies in GIS with

linguistic quantifiers: A case study of residential quality evaluation. J Geogr Syst 7:249–268. doi: 10.1007/s10109-005-0159-2

Malczewski J, Rinner C (2015) Multicriteria Decision Analysis in Geographic Information Science. Springer Berlin Heidelberg

Marrel A, Iooss B, Jullien M, et al (2011) Global sensitivity analysis for models with spatially dependent outputs. Environmetrics 22:383–397. doi: 10.1002/env.1071

Ménard A, Marceau DJ (2005) Exploration of spatial scale sensitivity in geographic cellular automata. Environ Plan B Plan Des 32:693–714. doi: 10.1068/b31163

Metropolis N, Ulam S (1949) The Monte Carlo Method. J Am Stat Assoc 44:335–341.

Monat J (2009) The benefits of global scaling in multi-criteria decision analysis. Judgm Decis Mak 4:492–508.

Montello DR, Golledge R (1998) Scale and Detail in the Cognition of Geographic Information : Report of a Specialist Meeting held under the auspices of the Varenius Project. Santa Barbara, California

Moreau P, Viaud V, Parnaudeau V, et al (2013a) An approach for global sensitivity analysis of a complex environmental model to spatial inputs and parameters: A case study of an agro-hydrological model. Environ Model Softw 47:74–87. doi: 10.1016/j.envsoft.2013.04.006

Moreau P, Viaud V, Parnaudeau V, et al (2013b) An approach for global sensitivity analysis of a complex environmental model to spatial inputs and parameters: A case study of an agro-hydrological model. Environ Model Softw 47:74–87. doi: 10.1016/j.envsoft.2013.04.006

Moreno N, Wang F, Marceau D (2008) An object-based land-use cellular automata model to overcome cell size and neighborhood sensitivity. In: Proceedings of GEOBIA 2008– Pixels, Objects, Intelligence GEOgraphic Object Based Image Analysis for the 21st Century.

Morgan MG, Henrion M (1990) Uncertainty : a guide to dealing with uncertainty in quantitative risk and policy analysis. Cambridge University Press

Najm HN (2009) Uncertainty quantification and polynomial chaos techniques in computational fluid dynamics. Annu Rev Fluid Mech 41:35–52. doi: 10.1146/annurev.fluid.010908.165248

NCGIA SLEUTH - Project Gigapolis. http://www.ncgia.ucsb.edu/projects/gig/. Accessed 2 Sep 2016

Nitzsch R Von, Weber M (1993) The Effect of Attribute Ranges on Weights in Utility Multiattribute Measurements. Manage Sci 39:937–943.

NRCS (2016) Natural Resources Conservation Service. http://www.nrcs.usda.gov/wps/portal/nrcs/main/national/programs/. Accessed 11 Feb 2016

O'Hagan A (2011) Polynomial Chaos: A tutorial and critique from a statistician's perspective. SIAM/ASA J Uncertain Quantif 20:1–20.

Oakley J, Hagan AO (2000) Bayesian Inference for the uncertainty distribution of computer model outputs. Biometrika 89:769–784.

Openshaw S (1978) An optimal zoning approach to the study of spatially aggregated data. In: Masser I, Brown PJB (eds) Spatial representation and spatial interaction. Springer US, Boston, MA, pp 95–113

Openshaw S, Rao L (1995) Algorithms for reengineering 1991 Census geography. Environ Plan 27:425–446. doi: 10.1068/a270425

Pan Y, Roth A, Yu Z, Doluschitz R (2010) The impact of variation in scale on the behavior of a cellular automata used for land use change modeling. Comput Environ Urban Syst 34:400–408. doi: 10.1016/j.compenvurbsys.2010.03.003

Perez KL (2008) The Allocation of Conservation Reserve Program Acreage: A Political Economy Perspective. North Carolina State University

Pontius RG, Neeti N (2010) Uncertainty in the difference between maps of future land change scenarios. Sustain Sci 5:39–50. doi: 10.1007/s11625-009-0095-z

Potter K, Rosen P, Johnson CR (2012) From quantification to visualization: A taxonomy of uncertainty visualization approaches. In: IFIP Advances in Information and Communication Technology. Springer Berlin Heidelberg, pp 226–247

Qin X (2013) Local Ideal Point Method for GIS-based Multicriteria Analysis : A Case Study in London , Ontario.

Rajabi MM, Ataie-Ashtiani B, Simmons CT (2015) Polynomial chaos expansions for uncertainty propagation and moment independent sensitivity analysis of seawater intrusion simulations. J Hydrol 520:101–122. doi: 10.1016/j.jhydrol.2014.11.020

172

Ratto M, Pagano A (2012) State Dependent Regressions : From Sensitivity Analysis to Meta-modeling. In: Environmental Modeling, and Control System Design. London, pp 171–190

Reichelderfer K, Boggess W (1988) Government decision making and program performance: the case of the conservation reserve program. Am J Agric Econ Agric Appl Econ Assoc 70:1–11.

Ribaudo MO, Hoag DL, Smith ME, Heimlich R (2001) Environmental indices and the politics of the Conservation\rReserve Program. Ecol Indic 1:11–20.

Rinner C, Heppleston A (2006) The Spatial Dimesions of Multi-Criteria Evaluation- Case study of a home Buyer's spatial decision support system. In: Raubal M, Miller HJ, Frank AU, Goodchild MF (eds). Springer Berlin Heidelberg, pp 338–352

Roura-Pascual N, Krug RM, Richardson DM, Hui C (2010) Spatially-explicit sensitivity analysis for conservation management: Exploring the influence of decisions in invasive alien plant management. Divers Distrib 16:426–438. doi: 10.1111/j.1472-4642.2010.00659.x

Roy B (1996) Multicriteria methodology for decision aiding. Kluwer, Dordrecht

Rutherford MJ, Crowther MJ, Lambert PC (2015) The use of restricted cubic splines to approximate complex hazard functions in the analysis of time-to-event data: a simulation study. J Stat Comput Simul 85:777–793. doi: Doi 10.1080/00949655.2013.845890

Saaty TL (1980) The analytic hierarcy process: planning,priority setting,resource allocation. McGraw-Hill,Inc., New York

Saint-Geours N, Bailly J-S, Grelot F, Lavergne C (2014) Multi-scale spatial sensitivity analysis of a model for economic appraisal of flood risk management policies. Environ Model Softw 60:153–166. doi: 10.1016/j.envsoft.2014.06.012

Saisana M, Saltelli A, Tarantola S (2005) Uncertainty and sensitivity analysis techniques as tools for the quality assessment of composite indicators. J R Stat Soc Ser A (Statistics Soc 168:307–323. doi: 10.1111/j.1467-985X.2005.00350.x

Şalap-Ayça S, Jankowski P (2016) Integrating local multi-criteria evaluation with spatially explicit uncertainty-sensitivity analysis. Spat Cogn Comput 16:106–132. doi: 10.1080/13875868.2015.1137578

Şalap-Ayça S, Jankowski P, Clarke KC, et al (2018) A meta-modeling approach for spatio-temporal uncertainty and sensitivity analysis: an application for a cellular automata-based Urban growth and land-use change model. Int J Geogr Inf Sci 32:1–26. doi: 10.1080/13658816.2017.1406944

Saltelli A, Annoni P, Azzini I, et al (2010) Variance based sensitivity analysis of model output. Design and estimator for the total sensitivity index. Comput Phys Commun 181:259–270. doi: 10.1016/j.cpc.2009.09.018

Saltelli A, Chan K, Scott EM (2000) Sensitivity Analysis. Wiley, New York

Saltelli A, Ratto M, Andres T, et al (2008) Global Sensitivity Analysis. The Primer. John Wiley & Sons, Ltd, Chichester, UK

Saltelli A, Ratto M, Tarantola S, Campolongo F (2006) Sensitivity analysis practices: Strategies for model-based inference. Reliab Eng Syst Saf 91:1109–1125. doi: 10.1016/j.ress.2005.11.014

Saltelli A, Tarantola S, Chan K (1999a) A Role for Sensitivity Analysis in Presenting the Results from MCDA Studies to Decision Makers. J Multi-Criteria Decis Anal 145:139–145.

Saltelli A, Tarantola S, Chan KPS (1999b) A quantitative model-independent method for global sensitivity analysis of model output. Technometrics 41:39–56.

Saltelli A, Tarantola S, Chan KPS (1999c) A Quantiative Model-Independent Method for Global Sensitivity Analysis of Model Output. Techniques 41:39–56.

Samat N (2006) Characterizing the scale sensitivity of the cellular automata simulated urban growth: A case study of the Seberang Perai Region, Penang State, Malaysia. Comput Environ Urban Syst 30:905–920. doi: 10.1016/j.compenvurbsys.2005.11.002

Sanyal J, Member S, Zhang S, et al (2009) A User Study to Compare Four Uncertainty Visualization Methods for 1D and 2D Datasets.

Seaber PR, Kapinos FP, Knapp GL (1987) Hydrologic Unit Maps, United States Geological Survey Water-Supply Paper 2294. USGS, Denver, CO

Slocum TA, Cliburn DC, Feddema JJ, Miller JR (2003) Evaluating the Usability of a Tool for Visualizing the Uncertainty of the Future Global Water Balance. Cartogr Geogr Inf Sci 30:299–317. doi: 10.1559/152304003322606210

Sobol' IM (2001) Global sensitivity indices for nonlinear mathematical models and their

Monte Carlo estimates. Math Comput Simul 55:271–280. doi: 10.1016/S0378-4754(00)00270-6

Sobol' IM (1993) Sensitivity analysis for non-linear mathematical models. Math Model Comput Exp 1:407–414.

Sobol' IM, Asotsky D, Kreinin A, Kucherenko S (2011) Construction and Comparison of High-Dimensional Sobol' Generators. Wilmott 64–79. doi: 10.1002/wilm.10056

Sobol' IM, Turchaninov VI, Levitan YL, Shukhman BV (1992) Quasirandom sequence generators. Keldysh Institute of Applied Mathematics, Russian Academic of Sciences, Moscow

Spense R (2014) Information Visualization, 3rd edn. Springer International Publishing

Stewart T, Ely D Range sensitivity: A necessary condition and a test for the validity of weights. In: Multiple Criteria Decision Making Conference. Cleveland,Ohio, USA,

Store R, Kangas J (2001) Integrating spatial multi-criteria evaluation and expert knowledge for GIS-based habitat suitability modelling. Landsc Urban Plan 55:79–93. doi: 10.1016/S0169-2046(01)00120-7

Sudret B (2008) Global sensitivity analysis using polynomial chaos expansions. Reliab Eng Syst Saf 93:964–979. doi: 10.1016/j.ress.2007.04.002

Sudret B (2014) Polynomial chaos expansions and stochastic finite element methods. In: Phoon, K K, Ching J (eds) Risk and Reliability in Geotechnical Engineering. CRC Press, pp 265–300

Syphard AD, Clarke KC, Franklin J, et al (2011) Forecasts of habitat loss and fragmentation due to urban growth are sensitive to source of input data. J Environ Manage 92:1882–1893. doi: 10.1016/j.jenvman.2011.03.014

Tang W, Jia M (2014) Global sensitivity analysis of a large agent-based model of spatial opinion exchange: A heterogeneous multi-GPU acceleration approach. Ann Assoc Am Geogr 104:485–509. doi: 10.1080/00045608.2014.892342

Tarantola S, Giglioli N, Jesinghaus J, Saltelli A (2002) Can global sensitivity analysis steer the implementation of models for environmental assessments and decision-making? Stoch Environ Res Risk Assess 16:63–76. doi: 10.1007/s00477-001-0085-x

The Demographia (2015) Demographia World Urban Areas.

Tobler WR (1979) Cellular geography. Philos Geogr 379–386. doi: 10.1007/978-94-009-

9394-5

Torrens PM, Nara A (2007) Modeling gentrification dynamics: A hybrid approach. Comput Environ Urban Syst 31:337–361. doi: 10.1016/j.compenvurbsys.2006.07.004

Torrens PM, O'Sullivan D (2000) Cities, cells, and complexity: developing a research agenda for urban geocomputation. In: 5th international conference on GeoComputation. University of Greenwich, UK, pp 1–14

Ulam S (1952) Random processes and transformations. Proc Int Congr Math Vol 2 264–275.

USDA (2011) Fact sheet - Conservation Reserve Program Sign-Up 41 Environmental Benefit Index (EBI).

van Vliet J, Bregt AK, Brown DG, et al (2016) A review of current calibration and validation practises in land-change modeling. Environ Model Softw 174–182. doi: 10.1016/j.envsoft.2016.04.017

Viard T, Caumon G, Levy B (2011) Adjacent versus coincident representations of geospatial uncertainty: Which promote better decisions? Comput Geosci 37:511–520. doi: 10.1016/j.cageo.2010.08.004

Villa-Vialaneix N, Follador M, Ratto M, Leip A (2012) A comparison of eight metamodeling techniques for the simulation of N 2O fluxes and N leaching from corn crops. Environ Model Softw 34:51–66. doi: 10.1016/j.envsoft.2011.05.003

von Neumann J (1966) Theory of Self-Reproducing Automata. University of Illinois Press, Champaign, IL, USA

Voogd H (1983) Multicriteria Evaluation for Urban and Regional Planning. Pion, London

Wackernagel H (2003) Multivariate Geostatistics: an Introduction with Applications. Springer Berlin Heidelberg, New York

Wei P, Lu Z, Song J (2015) Variable importance analysis: A comprehensive review. Reliab Eng Syst Saf 142:399–432. doi: 10.1016/j.ress.2015.05.018

White R, Engelen G (1994) Urban systems dynamics and cellular automata: Fractal structures between order and chaos. Chaos, Solitons and Fractals 4:563–583. doi: 10.1016/0960-0779(94)90066-3

White R, Engelen G (1993) Cellular automata and fractal urban form: a cellular modelling approach to the evolution of urban land-use patterns. Environ Plan A 25:1175–1199. doi: 10.1068/a251175

White R, Engelen G, Uljee I (1997) The use of constrained cellular automata for high-resolution modelling of urban land-use dynamics. Environ Plan B Urban Anal City Sci 24:323–343. doi: 10.1068/b240323

WHO (2016) World Health Organization. http://www.who.int/gho/urban_health/situation_trends/urban_population_growth_text/en/. Accessed 2 Sep 2016

Wiener N (1938) The Homogenous chaos. Am J Math 60:897–936.

Womach J (2005) CRS Report for Congress: Agriculture: A Glossary of Terms, Programs, and Laws, 2005 Edition.

Wong DWS (2009) The Modifiable Areal Unit Problem (MAUP). In: Fotheringham AS, Rogerson PA (eds) The SAGE Handbook of Spatial Analysis. pp 105–124

Xiu D, Karniadakis GE (2002) The Wiener-Askey polynomial chaos for stochastic differential equations. Soc Ind Appl Math J Sci Comput 24:619–644.

Xiu D, Lucor D, Su CH, Karniadakis GE (2002) Stochastic modeling of flow-structure interactions using generalized polynomial chaos. J Fluids Eng 124:51. doi: 10.1115/1.1436089

Xu E, Zhang H (2013) Spatially-explicit sensitivity analysis for land suitability evaluation. Appl Geogr 45:1–9. doi: 10.1016/j.apgeog.2013.08.005

Yeh AG-O, Li X (2006) Error propagation and model uncertainties of cellular automata in urban simulation with GIS. Comput Environ Urban Syst 30:10–28.

Zecena I, Burtscher M, Jin T, Zong Z (2013) Evaluating the Performance and Energy Efficiency of N -Body Codes on Multi-Core CPUs and GPUs. 1–8.

Zhang J, Goodchild MF (2002) Uncertainty in geographical information. CRC Press

Zhang J, You S (2012) CudaGIS: report on the design and realization of a massive data parallel GIS on GPUs. In: Proceedings of the Third ACM SIGSPATIAL IWGS Workshop. pp 102–108

Survey Sample for Instrument Group A

Visualizing Urban Growth Future Forecast

Imagine you are a city planner for San Diego County and you have been asked to forecast a geographical boundary of the city by 2050. To make your forecast you are using an urban growth model (UGM), which has been used by over 90 cities. However, you have a meticulous boss who wants detailed information about the city's geographical extent forecast. In particular, your boss is interested in the reliability of the forecast and the uncertainty of predicted future urban expansion.

In order to provide your boss with information about the uncertainty of future growth, you have decided to use sensitivity maps compiled by your office colleague. Sensitivity maps can tell you how the model output changes when the model input parameters are changed. The change in the model output can be interpreted as the forecast uncertainty. This means that if the model is more sensitive to an input parameter, any small change in that parameter can alter the model results.

Below you see the example of UGM result map for 2050 (Figure 1). This map shows the probability of a cell to become urbanized in the future (i.e. the pixels in red have 100 to 90% probability to become urbanized in 2050). In order to analyze the sensitivity of input parameters, the model was run for 252 times with randomly generated input parameters to calculate the variation in the outputs. The maps in the next section (Section 2) have been compiled based on these output maps for the selected region inside the black rectangle.

Please select the best possible choice in the upcoming questions. In answering your questions, full confidence is neither a requirement nor expected.
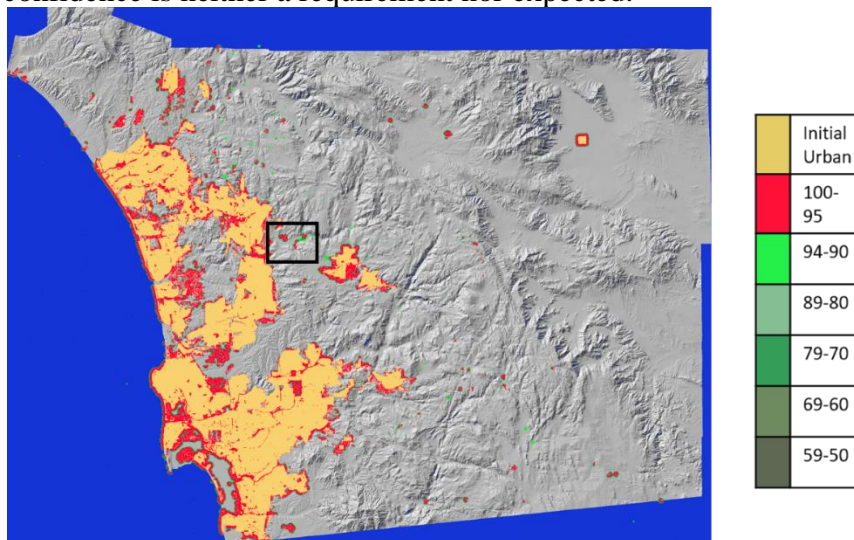

Figure 1. Probability Map of Urban Development for San Diego for year 2050 – **Colors**

indicate the probability of a cell to become urbanized

178

Test Group 1: Adjacent Representation: Static Graph Representation

SECTION 2

The maps below show sensitivity analysis results of the urban growth model (UGM) (from 2001 to 2050) for a selected sub-region (the black rectangle area in Figure 1) in San Diego County. There are five input parameters (S1-S5) being investigated for the UGM.

The background color (gray) indicates no data values and the color bar shows how the sensitivity values for each parameter change. The color selection was intentionally made in order to increase the contrast to help visualize changes in small pixel clusters.
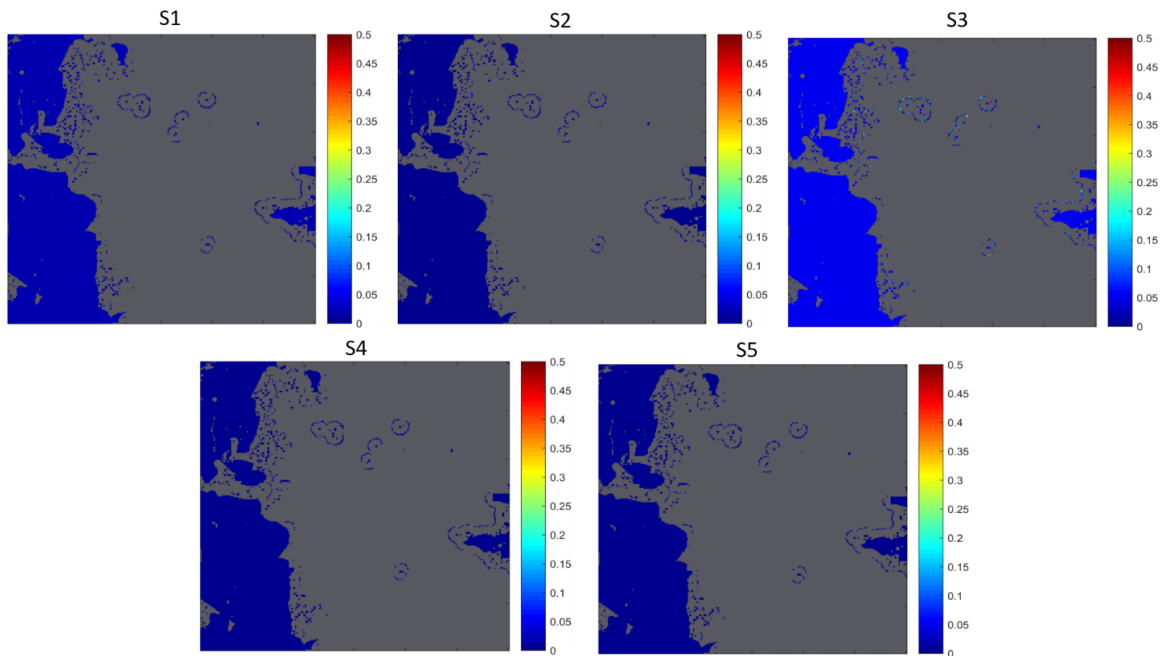
MAIN EFFECT SENSITIVITY MAPS

Figure 2 Main Effect Sensitivity Maps

The first five sensitivity maps (Figure 2) are the **MAIN EFFECT SENSITIVITY MAPS** which show the SELECTED SINGLE VARIABLE'S PORTION of the overall variance.

They depict how a small variation in a single input parameter will affect the model output (the greater the value at the given map location, the greater the sensitivity of the model to that parameter).

For example, the value of sensitivity index S1 equal to 0.7 means that the influence of S1 (first parameter) on the overall urban growth variance is 70%.

INTERACTION MAPS

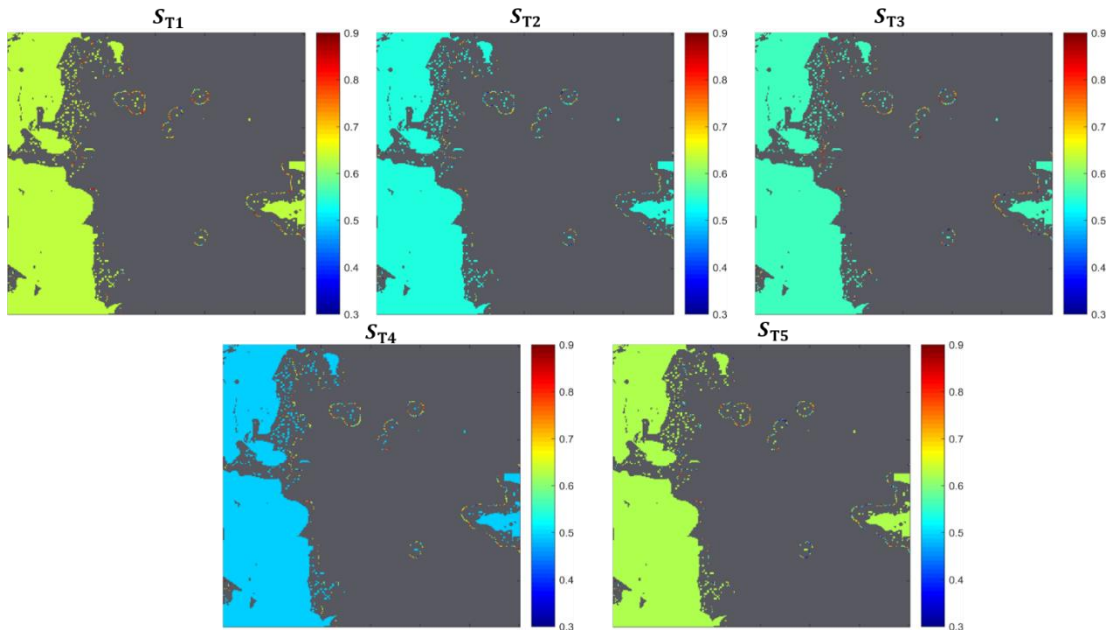

Figure 3 Interaction Maps

The second set of sensitivity maps (Figure 3) are **INTERACTION MAPS** which show the TOTAL CONTRIBUTION OF PAIRS OF PARAMETERS expressed by total sensitivity index ST. For example, the sensitivity index ST1 represents the total contribution of 1 st parameter to the model variance resulting from the parameter's interactions with other model parameters. A low S1 and high ST1 means, variability of 1st parameter is more influential during parameter interactions rather than singly treated.

Therefore, a high value of the interaction index ST1 means that the interactions between the 1st input parameter and the other parameters result in high model output variability.

1. According to the presented maps, which model input parameter do you think is more influential than the others for the selected area?
   - 1st Parameter
   - 2nd Parameter
   - 3rd Parameter
   - 4th Parameter
   - 5th Parameter
2. How confident are you in making simple approximations (50%, 75 %, etc.) about the level of SENSITIVITY associated with S3 for the forecasted area?
   - Not at all
   - Slightly
   - Somewhat
   - Almost completely

- Completely

3. How confident are you in making simple approximations (50%, 75 %, etc.) about the level of SENSITIVITY associated with S1 for the forecasted area?
   - Not at all
   - Slightly
   - Somewhat
   - Almost completely
   - Completely
4. Did you use INTERACTION MAPS (Figure 3) while answering any of the above questions?
   - Yes
   - No
5. How important was using INTERACTION MAPS (Figure 3) to answer any of the above questions?
   - Not at all
   - Slightly
   - Somewhat
   - Almost extremely
   - Extremely
6. In the below charts, the mean of main effect (first-order) sensitivity values change over the forecast period.
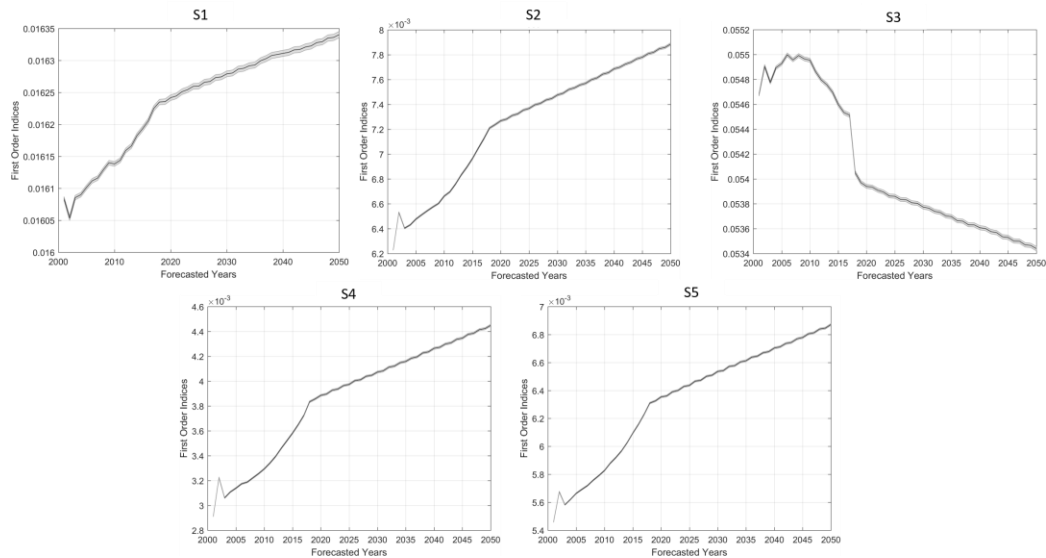
Using the value change representation in the chart, how confident are you in making simple comparisons (50%,75%, etc.) between the level of SENSITIVITY associated with parameters for 2020?

- Not at all
- Slightly
- Somewhat
- Almost completely
- Completely

7. If you had to explain SENSITIVITY in this urban growth model to other people, how confident would you feel to use this type of visualization??
    - Yes
    - No
    - Not sure

8. The idea of visualizing sensitivity as presented in the questionnaire was easy to comprehend
    - Not at all
    - Slightly
    - Somewhat
    - Almost completely
    - Completely

9. Sensitivity visualization makes the interpretation of the model output too difficult and complex to use
    - Not at all
    - Slightly
    - Somewhat
    - Almost completely
    - Completely

10. Sensitivity visualization (Figure 2 and 3) helps in interpreting the urban growth model output.
    a. Yes
    b. No
    c. Not sure

Additional Details about your level of expertise

SECTION 3

11. What is the highest level of education you have completed?
    1. Some high school
    2. High school graduate
    3. Some college
    4. Trade/technical/vocational training
    5. College graduate
    6. Some postgraduate work
    7. Postgraduate degree

12. Your primary work expertise in: (select all that apply)

- Urban planning
- Map visualization
- Decision support
- GIS
- Environmental Management/ Environmental Sciences
- Statistics/ Data Analytics
- Engineering
- None of the above